

Touch comes of Age - Maturational Plasticity in Somatosensory Mechanosensation

Dissertation
for the award of the degree
"Doctor rerum naturalium"
at the Georg-August-Universität Göttingen

within the doctoral programme Sensory and Motor Neuroscience
of the Georg-August University School of Science (GAUSS)

submitted by
M. Sc.
Niklas Michel
born in Pirna, Germany

Göttingen, 2019

Thesis advisory committee

Prof. Dr. Manuela Schmidt, Somatosensory Signaling and Systems Biology Group, Max Planck Institute of Experimental Medicine

Prof. Dr. Martin Göpfert, Dept. of Cellular Neurobiology, Schwann-Schleiden Research Centre

Prof. Dr. Luis Pardo, Dept. of Molecular Biology of Neuronal Signals, Max Planck Institute of Experimental Medicine

Members of the examination board

Referee: Prof. Dr. Manuela Schmidt, Somatosensory Signaling and Systems Biology Group, Max Planck Institute of Experimental Medicine

Co-referee: Prof. Dr. Martin Göpfert, Dept. of Cellular Neurobiology, Schwann-Schleiden Research Centre

Other members of the Examination Board

Prof. Dr. Luis Pardo, Dept. of Molecular Biology of Neuronal Signals, Max Planck Institute of Experimental Medicine

Prof. Dr. Jochen Staiger, Dept. of Neuroanatomy, Center of Anatomy of the Göttingen University

Prof. Dr. Ralf Heinrich, Dept. of Cellular Neurobiology, Schwann-Schleiden Research Centre

Dr. Christian Vogl, Vogl Group, Institute for Auditory Neuroscience & InnerEarLab

Day of the oral examination: 14th of June 2019

"Question everything."

Maria Mitchell

Acknowledgements

Dear Manuela and David, I will be forever grateful you gave me this chance to research, fail, learn, grow, never stop questioning, thrive and flourish. Manuela, I have learned so much from you. Your thoughtful care and supervision has brought out the best in me. You are one impressive scientist!

Thank you Martin for your time, input and support. Thank you Luis for your wide-open door and your kind and valuable advise and support. I thank Ralf, Jochen and Christian for their straightforward agreement to attack my thesis on the 14th of June. I am thankful to my institute, my university, the GGNB, the SFB889, the DFG and the Max Planck Society.

Thanks to all members of the Schmidt group for the team spirit, collaboration and the most pleasant collegueship. Meike, our paths aligned in a beautiful way. I wish you all the best, my dear companion. Thank you Pratibha, my mechano-clamp hero. Your determination is awe-inspiring. Thank you Julia for all your help, valuable input and delight. Thank you Christin, your strength and openness are most refreshing. Thank you Tanja for all the help, it is so enjoyable to work with you. Thank you Sergej for your efforts and camaraderie.

Swati, my love, you are my best friend and partner. I thank you with all my heart for your support, care and affection. You can always count on me.

Ich danke meinen Eltern und meiner Familie für Rückhalt, Rat, Humor, Wohlwollen und Auf-den-Teppich-Holen! Besonders danke ich Dir, Karin. Mama ist die Beste.

Thank you Santhi for believing in me and letting me know I'll never walk alone.

Ich danke meinen FreundInnen, denn ohne Freundschaft geht gar nichts; besonders meinen Kumpels Hanne, Valentin, Jannik, Kauz, Hauke, Markus, Philipp, Georg, Philipp, Torsten, Linus, Robin und Daniel.

Michael, dir habe ich viel zu verdanken! Danke für dein Vorbild und deinen Glauben an mich!

Danke auch an Annabel!

Finally, I thank the PhDnet and the doctoral researchers who made my time worthwhile, especially Maria!

Abstract

Somatosensory mechanosensation remains to be the least understood sensory system in vertebrates. It requires the activation of specialised neurons which innervate the skin and internal organs. A subset of these dorsal root ganglion neurons express Piezo2, which has recently been found to be the key player in the senses of touch and proprioception. This ion channel accomplishes mechanotransduction - the conversion of mechanical stimuli into electrical signals. Tactile sensitivity in humans is subject to regulation and ageing processes. Moreover, it is altered in diverse pain conditions and autism spectrum disorders. In this line, this thesis sets out to investigate whether tactile sensitivity changes with maturation and ageing in healthy mice. Strikingly, a significant and specific decrease of Piezo2-mediated mechanically-activated currents in dorsal root ganglion neurons of four- to twelve-week-old wild-type mice was found. Moreover, both glabrous and hairy skin mechanosensitivity were also found to decrease in these maturing mice by longitudinal testings. This plasticity in somatosensory mechanosensation has previously been unreported. It challenges the fields assumptions about mature physiology and poses an optimal model for studying the molecular underpinnings of age-dependent regulation of somatosensory mechanotransduction. In that regard, significant changes in the transcriptome of DRG neurons between four and twelve weeks of age were found. Piezo2 mRNA was found to contain a decreasing amount of exon 33. This alternative splicing was shown to decrease Ca^{2+} permeability and might partly explain the phenotype. Furthermore, by means of patch-seq - the combination of electrophysiology and single-cell RNA-seq - promising candidate genes were found to be maturationally regulated in a sensory neuron subtype-specific manner. The findings are discussed and put into perspective with regard to ageing, sensory restriction and the somatosensory research field.

Table of Contents

List of Figures	xi
List of Tables	xiii
1 Introduction	1
1.1 Somatosensation and sensory neurons	1
1.1.1 Somatosensory mechanosensation	2
1.2 Piezo2	4
1.3 State of the art and aim of this study	6
2 Materials and Methods	7
2.1 Animals	7
2.2 DRG dissection and primary culture	8
2.3 Electrophysiology	8
2.3.1 Setup and solutions	8
2.3.2 Mechano-clamp	9
2.3.2.1 Data processing	10
2.3.3 Sodium currents	12
2.3.4 Current-clamp	12
2.4 Behavioural testing	13
2.4.1 Mechanical sensitivity	13
2.4.1.1 Glabrous skin - Dynamic Plantar Aesthesiometer	13
2.4.1.2 Hairy skin - tape response assay	14
2.4.2 Thermal sensitivity - Hargreaves test	15
2.4.3 Statistical analysis	15
2.5 Molecular Biology	16
2.5.1 Quantitative PCR	16
2.5.2 Patch-seq: single-cell harvest	17
2.5.3 Single-cell RNA sequencing	18
2.5.3.1 Library preparation and sequencing	18
2.5.3.2 Bioinformatics	18
3 Results	21
3.1 Chronicle of declining touch	21

TABLE OF CONTENTS

3.1.1	Maturation decreases Piezo2 currents	22
3.1.2	Ageing does not affect other electrophysiological parameters	24
3.1.3	Age-dependent decrease in somatosensory mechanosensation	26
3.1.3.1	Hind paw sensitivity decreases with maturation	26
3.1.3.2	Hairy skin mechanosensitivity decreases with maturation	27
3.1.4	Summary of the descriptive part	29
3.2	Exploring the plasticity	30
3.2.1	Piezo2 transcription	30
3.2.2	Single-cell transcriptomics	31
3.2.2.1	Electrophysiological characterisation of single-cell samples	32
3.2.2.2	RNA sequencing of single-cell samples	36
3.2.3	Summary of the mechanistic part	40
3.3	Summary of the experimental findings	42
4	Discussion	43
4.1	Questioning the methods	43
4.1.1	Draw backs in electrophysiology	43
4.1.1.1	Contrasting ionic recording conditions	45
4.1.2	DIVs	46
4.1.3	Limitations of behavioural paradigms	46
4.1.3.1	Dynamic Plantar Aesthesiometer	46
4.1.3.2	Hargreaves test	47
4.1.3.3	Tape response assay	47
4.1.4	Patch-seq	48
4.2	Questioning the findings	49
4.2.1	Comparison to sensory decline in high age	49
4.2.2	Timeline of the decline	50
4.2.3	Reasons for the decline	50
4.2.4	Mechanism	52
4.2.5	Relevance	53
	References	55
	Appendix A	67
A.1	Declaration	67
A.2	Curriculum Vitae	67

List of Figures

1.1	"Demócrito" by Dosso Dossi, 1540	1
1.2	Skin somatosensation	3
1.3	Soma size and functional marker profile of DRG sensory neuron subtypes	4
1.4	Human Piezo protein function	5
1.5	Life phases of the house mouse	6
2.1	Mechano-clamp setup	10
2.2	Classification of sensory neurons	12
2.3	Timeline of longitudinal behavioural testing of age cohorts	13
3.1	Exemplary comparison of days <i>in vitro</i>	22
3.2	Maturation attenuates RA-MA currents in DRG neurons	23
3.3	IA-MA currents and MA responder type populations do not change with age in medium- and large-diameter cultured DRG neurons	24
3.4	Voltage-gated sodium currents do not change with age in medium- and large-diameter cultured DRG neurons	25
3.5	Hind paw sensitivity decreases with maturation	27
3.6	Hairy skin mechanosensitivity decreases with maturation	28
3.7	Whole DRG qPCR hints at age-dependent splicing	30
3.8	Detailed current-clamp-based classification of sensory neurons	32
3.9	Action potential categorisation in DRG neurons	33
3.10	Mechano-clamp characterisation of sensory neuron subtypes	35
3.11	Patch-seq of single mechanoinensitive sensory DRG neurons	37
3.12	Patch-seq of single mechanosensitive sensory DRG neurons	39

List of Tables

2.1	Composition of measuring solutions for electrophysiological experiments	9
2.2	Electrophysiological parameters of 128 analysed RA-MA cells	11
2.3	Sequences of primers used for quantitative real-time PCR	16
3.1	Gene Ontology annotation verifies categorisation of nociceptors	38
3.2	Age-dependently differentially transcribed genes in electrophysiologically defined sensory neuron subtypes	41

1

Introduction



Figure 1.1: "Demócrito"
by Dosso Dossi, 1540

For Democritus, a philosopher born around 460 BC in ancient Greece, touch was the universal sense and all senses were a derivative of it (English, 1915). Aristotle put the sense of touch on top of the hierarchy of the senses together with taste, a variant of touch according to him, followed by smelling, hearing and finally seeing (Massie, 2013). Simple lifeforms incapable of locomotion can survive on touch and taste only, he found, illustrating the absoluteness of these elemental senses.

Sensory research has come a long way ever since: From the study of the peripheral structures establishing the first contact with stimuli to the conduction and processing of gathered data to the percept and qualia of sensation, or even to the modulation of lifespan by the senses (e.g. Linford et al., 2011).

Today, we differentiate between the special senses that have specialised organs devoted to them (eyes, ears, nose and tongue) and the somatic senses, from greek $\sigma\omega\mu\alpha$, *soma*, meaning body or one's entity in the physical world. Somatosensation arises from all over the body, i.e. from the skin and internal organs, and comprises touch (pressure, vibration, proprioception), pain (nociception) and temperature (thermoception).

1.1 Somatosensation and sensory neurons

The somatic senses are in charge of transducing aspects of reality arising from outside and within the body. For instance, humans sense the kinetic energy of fermions, the constituent particles of matter in motion on the smallest scales as temperature. After all, the homeostasis of body temperature is crucial to the survival of such homoiotherm animals. On larger scales, we sense the electromagnetic repulsion of atoms in close vicinity as mechanical force, taking the forms of pressure and vibration or indentation and stretch. If the magnitude of the force acting on sensory structures is of relevance to our survival,

1. INTRODUCTION

we are mostly able to sense and process it due to evolutionary specialisation. Forces at the lower end of that perceivable range stemming from outside the body are felt as vibration, light touch or itch. A force strong enough to destroy biological tissue, be it mechanical, chemical, heat or cold, elicits painful sensations when acting on our body.

From within the body, plentiful stimuli are being made sense of by our nervous system as well. Thermosensors monitor temperature. Chemo- and osmosensors sense nutrients, CO₂ concentration or blood oxygenation levels. Baroreceptors track blood pressure or renal flow rates. Stretch sensors oversee the state of the bladder, the lung or the gastrointestinal tract. Proprioceptors receive input from joints and muscles about the position and exertion of body parts and the list goes on further. Generally, sensory nerve cells have evolved to detect such signals and relay them to the spinal chord and the brain, where they can be processed and integrated centrally.

In vertebrates the cell bodies of somatosensory neurons are clustered in the dorsal roots of spinal nerves forming the dorsal root ganglia (DRG). From there these pseudounipolar neurons extend their axons in two branches: one towards the periphery, e.g. to the skin, for stimulus detection, the other towards the central nervous system, see figure 1.2. For cranial innervation, sensory neuron cell bodies reside in the trigeminal ganglia. In that way the DRG house the cell bodies or somata of all sorts of different sensory neurons the distal processes of which innervate a respective dermatome according to the spinal level.

Historically, the DRG neurons were categorised according to the diameter of their soma. First, using light microscopy two types were discerned: large light and small dark cells (Andres, 1961). Later, the discovery of molecular markers allowed more precise discrimination. For example, the soma size of *Ntrk1/TRKA*⁺ nociceptors was shown to be small, medium for *Ntrk2/TRKB*⁺ mechanoreceptors and large for *Ntrk3/TRKC*⁺ muscle afferents (McMahon et al., 1994). Thanks to advances in science and technological innovation the transcriptome of single DRG neurons, i.e. the entirety of messenger RNA (mRNA) molecules expressed from genes, can be mapped and correlated with the cells phenotype, such as soma size or electrophysiology. Comprehensively analysing the transcriptomes of 622 single mouse DRG neurons, Usoskin et al., (2015) confirmed the anticipated major neuronal types. Furthermore, they provided in-depth marker profiles of several distinct classes of sensory neuron subtypes, see figure 1.3.

1.1.1 Somatosensory mechanosensation

Most DRG neurons (e.g. 82% in rats; Viatchenko-Karpinski and Gu, 2016) are capable of mechanotransduction - the conversion of mechanical stimuli into biological, electrically encoded signals. Primary afferent fibres transduce noxious, i.e. painful, and innocuous mechanical stimuli. They can be distinguished by their innervation targets, axon diameters, myelination status, conduction velocities and firing kinetics, i.e. adaptation of nerve impulses to an ongoing stimulus (see figure 1.2). The high-threshold mechanoreceptors transduce noxious signals. Their unmyelinated fibres have low conduction velocities (C-fibres) and terminate as free nerve endings in the epidermal layer of the skin. Nociceptive DRG neurons are the most numerous, probably due to their evolutionarily critical role in warning the organism of harm. Innocuous mechanical stimuli are detected by the low-threshold mechanoreceptors (LTMRs). Their neurites are myelinated, show high conduction velocities (A β and A δ) and innervate specialised structures. Some mechanoreceptors form palisade, circumferential and lanceolate endings around the shafts of hairs and detect hair pull and deflection (Chalfie, 2009; Moehring

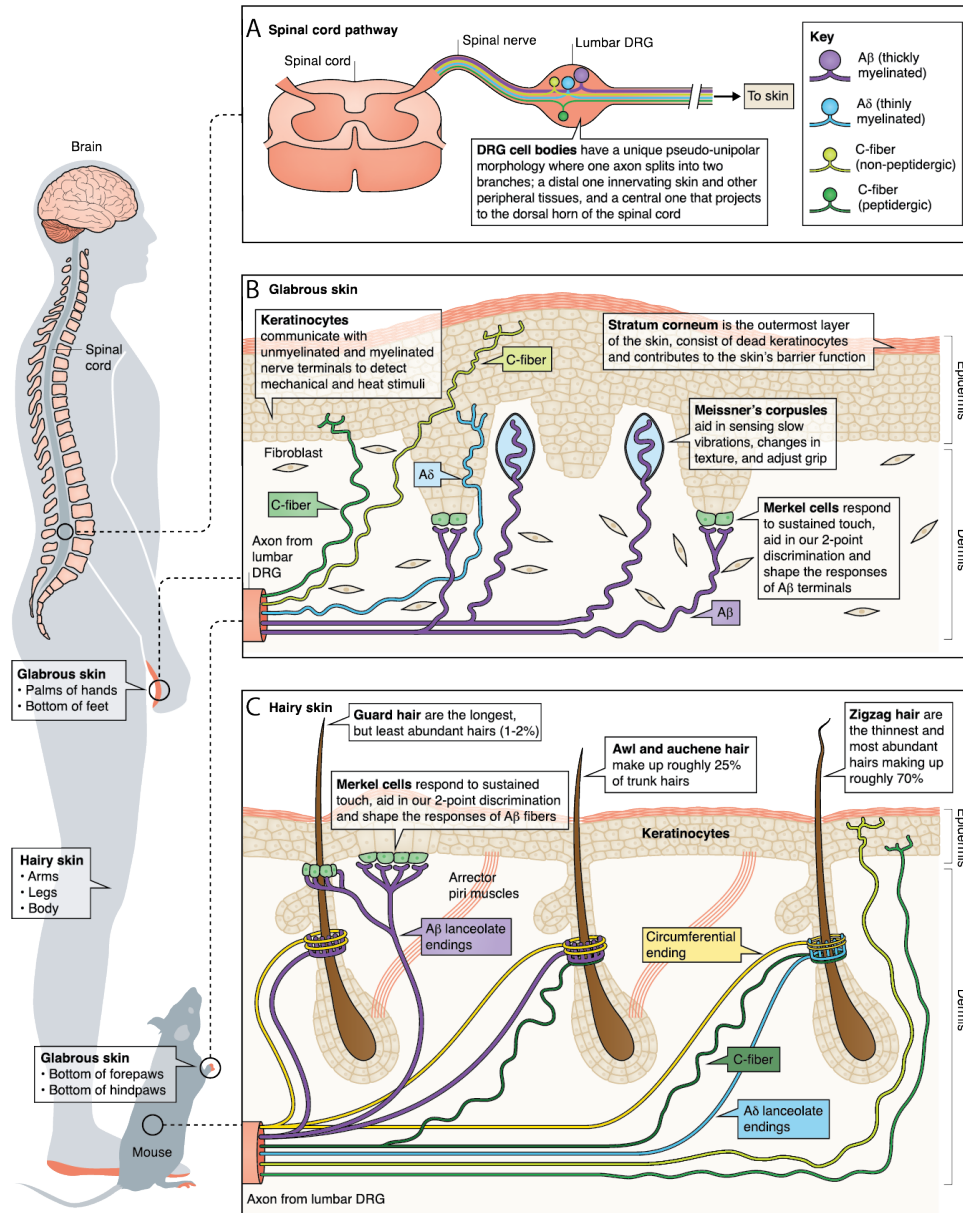


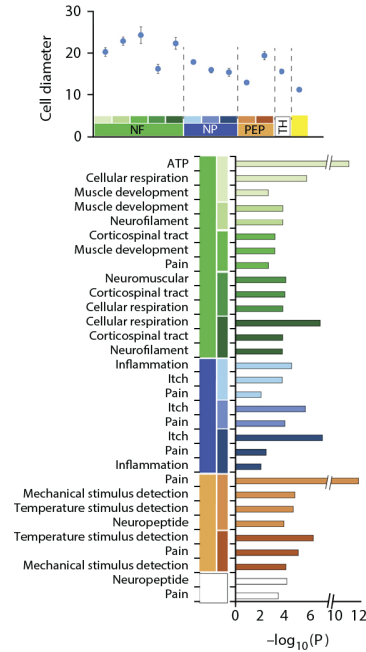
Figure 1.2: Skin somatosensation

"(A) Cell bodies of the dorsal root ganglia (DRG) neurons are found near the spinal cord, where they extend a centrally projecting axon to the dorsal horn and a distal projecting, longer axon to the hairy and glabrous skin (or deeper muscle, bone, or tendon tissue; not shown). A β -fibres are thickly myelinated, fast conducting, and generally have large-diameter cell bodies; A δ -fibres are thinly myelinated, conduct at medium speed, and generally have medium-diameter cell bodies; non-myelinated C-fibres conduct much more slowly and generally have smaller cell bodies. (B) Glabrous skin innervation shows the diversity of somatosensory neurons that terminate within the thick layer of the epidermis (between keratinocytes) and the underlying dermis. Keratinocytes can communicate with the distal terminals of noxious-detecting peptidergic (deeper) and non-peptidergic C-fibres (more superficial), as well as with the terminals of A δ -fibres and A β -fibres. A β -fibre endings innervate Merkel cell complexes and aid in touch sensation by helping shape our detection of two-point discrimination. (C) The mammalian hairy skin is comprised of a thinner layer of the epidermis and contains three different type of hairs, where each afferent type can be identified by its innervation pattern of the hair follicle as well as its morphology. For example, Guard hairs are the least abundant and longest hair and are innervated by A β -fibres, which have circumferential endings. Zigzag hairs, on the other hand, are the most abundant, have a distinct zigzag shape, and are innervated by C-fibres or A δ -fibres that have circumferential endings. All mammals except humans are equipped with these highly differentiated touch organs." Figure and text from Moehring et al., (2018).

1. INTRODUCTION

Figure 1.3: Soma size and functional marker profile of DRG sensory neuron subtypes

Sensory neuron types are clustered according to their mRNA expression profile and their soma size in μm (mean \pm SEM) is plotted at the top. Figure and the following text were modified from Usoskin et al., (2015). "Examining the expression of known markers in the four neuronal clusters, we identified the first, the NF cluster, as expressing neurofilament heavy chain (*Nefh*) and parvalbumin (*Pvalb*), previously associated with myelinated DRG neurons. The second, the PEP cluster, showed expression of substance P (*Tac1*), TRKA (*Ntrk1*) and calcitonin gene-related peptide (CGRP, also known as *Calca*), previously associated with peptidergic nociceptors. The third, the NP cluster, showed expression of *Mrgprd* and *P2rx3*, previously associated with nonpeptidergic nociceptors. The fourth, the TH cluster, showed distinct expression of tyrosine hydroxylase (*Th*), which has been described in a distinct subclass of unmyelinated neurons".



et al., 2018). Others form direct synaptic contact with sensory end organs, such as (see figure 1.2, reviewed by Olson et al., (2016) and Moehring et al., (2018))

- Merkel cells, forming Merkel cell-neurite complexes, sensing sustained touch and pressure
- Meissner's corpuscles, sensing changes in texture and slow vibrations
- Pacinian corpuscles, sensing deep pressure and fast vibrations
- Ruffini's corpuscles, sensing skin stretch

Mechanosensitive DRG neurons as well as the end organs produce proteins capable of mechanotransduction. These proteins form pores in the plasma membrane of the cells and the action of mechanical force increases their open probability (Chalfie, 2009; Martinac and Poole, 2018). Due to passive diffusion down an electrochemical gradient open pores conduct currents of charged particles, i.e. salt ions. Ionic currents across the plasma membrane can change its potential in terms of voltage or even exert downstream effects on their own in the case of calcium ions. A depolarisation of the membrane potential of a mechanically activated (MA) sensory neuron, a so-called receptor potential, may eventually lead to the opening of voltage-gated pores, culminating in the generation of an action potential (AP), i.e. a nerve impulse. These APs travel along the axon towards the central nervous system, where they are made use of as sensory information (see also top left panel in figure 1.4).

It has not been long since we learned of the molecular identity of the perhaps most important MA ion channel in mammalian somatosensory mechanosensation: Piezo2.

1.2 Piezo2

The Piezo family of proteins consists of two members, Piezo1 and Piezo2, and was first described by Coste et al., (2010). The name is derived from the Greek word $\pi\acute{\iota}\epsilon\sigma\eta$, *piesi*, meaning pressure. This family is evolutionarily highly conserved as its members share no homology to any known ion channel

and do not contain known protein domains (Coste et al., 2010). Furthermore, orthologs can be found in numerous species ranging from the rice plant *Oryza sativa* to the fruitfly *Drosophila melanogaster* to several mammals (Coste et al., 2010), highlighting their elemental importance in biological function.

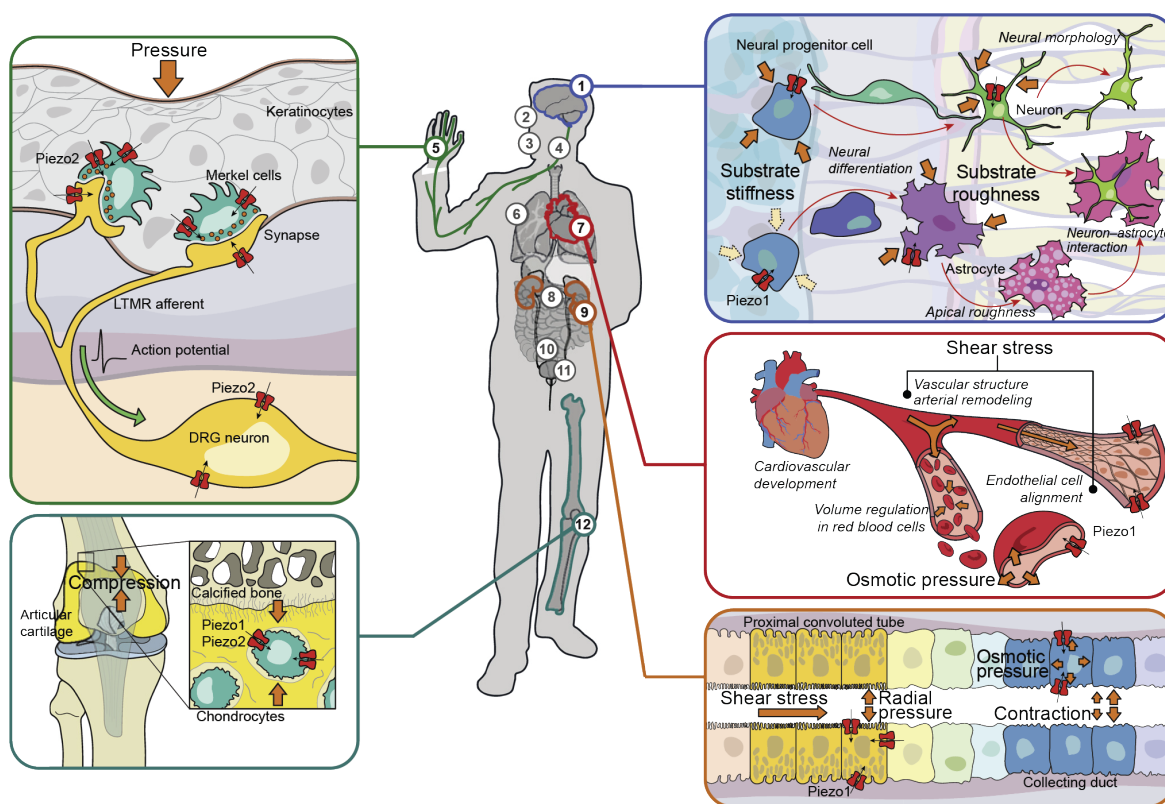


Figure 1.4: Human Piezo protein function

"Numbered tissues are as follows: 1, brain; 2, optic nerve head; 3, periodontal ligament; 4, trigeminal ganglion; 5, dorsal root ganglion and skin; 6, lungs; 7, cardiovascular system and red blood cells; 8, gastrointestinal system; 9, kidney; 10, colon; 11, bladder; and 12, articular cartilage. Tissues in which Piezo function has been extensively studied are expanded to show detail. Top left inset illustrates Piezo2 expressed in Merkel cells of the skin, where mechanical activation of Piezo mediates depolarization and activation of dorsal root ganglion cell afferents, which also express Piezo2. Together, these cells are involved in sensing light touch and proprioception (DRG, dorsal root ganglion; LTMR, Low-threshold mechanoreceptor). Bottom left inset highlights the expression of both Piezo1 and Piezo2 in chondrocytes of articular cartilage, where they activate under compressive force. Top right inset illustrates the role of Piezo1 in sensing mechanical properties of the environment of neural progenitor cells, thereby initiating signaling pathways that lead to neuronal differentiation and subsequent development of neurite morphology, neuron–glia interactions, and nanoroughness of glial membranes. Middle right inset depicts the role of Piezo1 in regulating volume of red blood cells as well as sensing shear stress to regulate vascular branching and alignment of endothelial cells. Bottom right inset shows the role of Piezo1 in sensing fluid flow throughout the nephron of the kidney. Deficits in Piezo1 function in the kidney may lead to downstream effects on urinary osmolarity and renal pathologies ." Figure and text from Wu et al., (2017)

The number of tissues in which Piezos are found to be expressed and the number of physiological roles they are being implicated in is constantly growing as a result of ongoing research (see figure 1.4). Piezo2 was so far shown to be the main *bona fide* mechanotransducer in light touch (Ranade et al., 2014) and proprioception (Ranade et al., 2014; Woo et al., 2015; Florez-Paz et al., 2016). It was also found to be required for human stem cell-derived touch receptor mechanotransduction (Schrenk-Siemens et al., 2015). Additionally its function in mechanically-induced pain is emerging (Dubin et al., 2012; Eijkelkamp et al., 2013; Ferrari et al., 2015; Murthy et al., 2018; Zhang et al., 2019). The fact that

1. INTRODUCTION

conventional knockout of the *Piezo2* gene in mice is perinatally lethal (Dubin et al., 2012; Ranade et al., 2014) has been assumed to be due to a crucial role in lung development or function (Nonomura et al., 2017).

Not surprisingly, mutations of the human *PIEZO2* gene can be associated to diseases. Distal arthrogyriposis 3/Gordon Syndrome and distal arthrogyriposis 5/Marden-Walker Syndrome are amongst those (McMillin et al., 2014; Delle Vedove et al., 2016; Mahmud et al., 2017; Haliloglu et al., 2017; Alishch et al., 2017; Dai et al., 2018; Matías-Pérez et al., 2018; Yamaguchi et al., 2019; Zapata-Aldana et al., 2019). Affected patients show joint and muscle contractures, selective loss of discriminative touch perception and profoundly decreased proprioception (Chesler et al., 2016).

1.3 State of the art and aim of this study

In somatosensory research the house mouse is the model system of choice. Most groups consider mice to be of optimal age for behavioural and *in vitro* experiments at six to eight postnatal weeks (Minett et al., 2011; Eijkelkamp et al., 2013; Ranade et al., 2014; Schrenk-Siemens et al., 2015). Some impactful data in the *Piezo2* research field was generated using mice of four to eight weeks of age (Poole et al., 2014; Murthy et al., 2018; Zhang et al., 2019). In these studies, mice were often loosely described as being adult (e.g. Heidenreich et al., 2012; Eijkelkamp et al., 2013). However, Pratibha Narayanan, Ph.D. (formerly Schmidt group, Max Planck Institute of Experimental Medicine, Germany) noticed high variability in the data gathered from such young mice. She was investigating the native *Piezo2* interactome (Narayanan et al., 2016, 2018) when she noticed an age-dependent difference in *Piezo2*-mediated currents. When separating the data of her wild-type (WT) control group by age, DRG neurons of six-week-old C57Bl/6J mice produced considerably higher *Piezo2*-mediated MA currents than eight-week-old ones.

According to the Jackson Laboratory research institute (also known as JAX, USA) C57Bl/6J mice are considered to be of mature adult physiology only at an age of three to six months (see figure 1.5). They state that for most biological processes and structures, rapid maturational growth continues beyond the age of sexual maturity (five weeks) until about twelve weeks.

We hypothesised that the observed age-difference in *Piezo2*-mediated MA currents might be the harbinger of maturational plasticity neglected by the field. The aim of this thesis is to test this hypothesis by investigating possible age differences in murine *Piezo2*-mediated function both *in vitro* and *in vivo*.

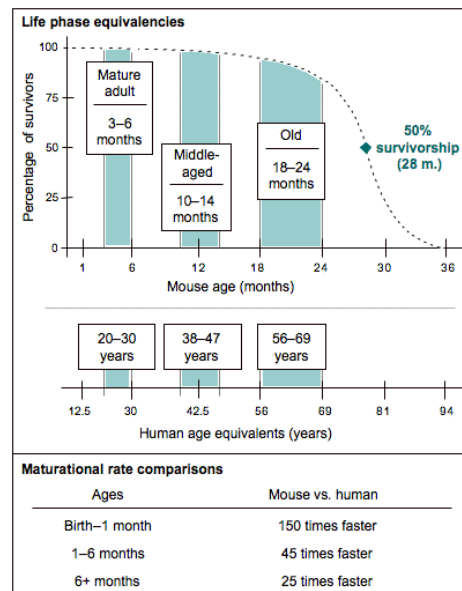


Figure 1.5: Life phases of the house mouse

"Representative age ranges for mature life history stages in C57BL/6J mice; comparison to human beings. (Adapted from Figure 20-3: Flurkey K, Curren JM, Harrison DE. 2007. The Mouse in Aging Research. In The Mouse in Biomedical Research 2nd Edition. Fox JG, et al, editors. American College Laboratory Animal Medicine (Elsevier), Burlington, MA, pp. 637-672.)" Figure and text from The Harrison Lab, (2007)

2

Materials and Methods

Questioning our assumptions about mature physiology with regard to Piezo2-mediated currents, we intended to resolve the function of this principal mechanotransducer at an extended range of postnatal life phases. In order to not investigate unspecific and multifaceted changes brought about by senescence (e.g. García-Piqueras et al., 2019), the following carefully chosen and strictly monitored age groups are what this thesis revolves around:

- 4 weeks old, "juvenile"
- 8 weeks old, "adolescent"
- 12 weeks old, "adult"
- 10 - 15 months old, "middle-aged"

The following pages are dedicated to spelling out the technical and methodological details of our experimental and empirical investigations.

2.1 Animals

Wild-type C57Bl/6J mice were group-housed in individually-ventilated cages in a 12 h light/dark cycle in the animal facility of the Max Planck Institute of Experimental Medicine with water and food *ad libitum*. During the light phase, experiments were performed according to the guidelines of the aforementioned institute and with permission of the *Niedersächsisches Landesamt für Verbraucherschutz und Lebensmittelsicherheit*. Only male animals were included in this study in order to reduce possible behavioural variation during the estrous cycle and to circumvent sex differences in gene regulation and expression (Yang et al., 2006). Animal welfare and housing was taken care of by the staff of the aforementioned animal facility.

2.2 DRG dissection and primary culture

For culturing murine DRG cells, a protocol was adopted from Coste et al., (2010) and Avenali et al., (2014). In order to harvest DRGs, mice were sacrificed by CO₂ inhalation according to the animal welfare law. After decapitation and subsequent removal of the back skin, the backbone was excised. The dorsal, superficial muscle layers were cut open and the now accessible vertebrae were bisected longitudinally, caudal along the coronal plane to reveal the spinal cord and the DRGs resting in the intervertebral foramina. Having abscised the dorsal and ventral roots, all DRGs were collected in serum-free DMEM/F12 with Glutamax. The tissue was shook manually and briefly every 15 minutes while digesting in collagenase for 60 minutes at 37 °C. This was followed by short trituration with a P1000 pipette and 30 minutes of digestion by papain at 37 °C. Then, cells were spun down for 1 minute by centrifuging them at 200 relative centrifugal force (1000 rpm in Centrifuge 5702, Eppendorf AG, Germany). Afterwards, the tissue was thoroughly triturated in 2 ml of serum-free medium. For separating cells from debris, a layer of bovine serum albumin solution (0.15 $\frac{\text{g}}{\text{ml}}$) was pipetted carefully beneath these digested cells and this column was centrifuged for 10 minutes at 200 relative centrifugal force.

While making sure the separated debris does not get close to the formed cell pellet, as much supernatant as possible was removed using a Pasteur pipette. Now the pelleted cells were resuspended in a small amount of medium supplemented with 10 % horse serum and 100 $\frac{\text{ng}}{\text{ml}}$ nerve growth factor, 50 $\frac{\text{ng}}{\text{ml}}$ glial cell line-derived neurotrophic factor, 50 $\frac{\text{ng}}{\text{ml}}$ neurotrophin 3 and 50 $\frac{\text{ng}}{\text{ml}}$ neurotrophin 4. Coverslips were mounted to a custom plastic recording chamber (toolshop, MPI of Experimental Medicine, Germany). First, they were coated with 1 $\frac{\text{mg}}{\text{ml}}$ poly-D-lysine for 90 minutes. Second, they were coated with 20 $\frac{\mu\text{g}}{\text{ml}}$ laminin for 30 minutes before plating the cells. They were kept at 37 °C and 5 % CO₂ and 20 minutes after plating, the chambers were filled up to 500 μl with the supplemented medium. Experiments started ~ 24 h after culturing to ensure reliable adhesion to the coated surface before mechanical stimulation. For *in situ* qPCR (see 2.5.1), the undigested DRGs were rid of most of the medium they were collected in and flash frozen using liquid nitrogen before storage at -80 °C until experimental usage. In the majority of cases, culturing was done by Sergej Zeiter (University Medical Center Göttingen, Germany).

2.3 Electrophysiology

2.3.1 Setup and solutions

Whole-cell voltage and current-clamp recordings of cultured DRG neurons were performed at room temperature under an inverted light microscope (Axiovert 135 with LD-Achroplan 40x/0.6 Korr Ph2 and EC Plan-Neofluar 100x/1.3 Oil Pol M27 objectives, Carl Zeiss AG, Germany) resting on an anti-vibration table inside a Faraday cage. An EPC 10 USB single amplifier (HEKA Elektronik Dr. Schulze GmbH, Germany) connected to a computer running the PatchMaster (HEKA) software was used for voltage-clamping, current injection and recording of electrophysiological data. For manoeuvring the preamplifier with the attached recording pipette a PatchStar Micromanipulator (Scientifica Ltd, United Kingdom) was used. An MPCU-3 (Lorenz Meßgerätebau, Germany) controlled the pressure inside the patch pipette. Mechanical stimulation of cells was achieved by using a piezoelectrically driven

micromanipulator (Physik Instrumente GmbH & Co.KG, Germany). A constant flow of bath solution (see table 2.1) was ensured throughout experiments via a gravity driven, self-built application system and suctioning by a pump for continuous exchange of solution, while keeping the bath volume low and stable. Bath and pipette solutions are both listed in table 2.1. Using a PIP 6 Vertical Pipette Puller (HEKA) borosilicate glass capillaries (PG10165-4, P. Clamp Glass 0010, World Precision Instruments, Germany) were pulled into patch pipettes, showing 1.5 - 4.5 M Ω of resistance in patch-clamp experiments. Some of these pipettes were melted shut under a microscope to yield smooth blunt probes with a tip diameter of $\sim 4 \mu\text{m}$ for mechanical stimulation.

Table 2.1: Composition of measuring solutions for electrophysiological experiments

Values for the components are concentrations in mM. Mg-ATP and Na-GTP were added freshly on the day of the experiment. The pH of the different solutions was adjusted (before the addition of the aforementioned salts) with, from left to right: NaOH, CsOH, NaOH, KOH. The osmolarity was determined after pH titration and values are listed as mOsm. AP = action potential; ECS = extracellular solution, bath solution; ICS = intracellular solution, pipette solution

Experiment Component	Mechano-clamp		AP recording	
	ECS	ICS	ECS	ICS
NaCl	127		140	10
KCl	3		4	110
MgCl ₂	1	1	1	1
CaCl ₂	2.5	1	2	
HEPES	10	10	10	10
D-Glucose	10		4	
EGTA		5		1
CsCl		133		
Mg-ATP		4		4
Na-GTP		0.4		0.4
pH	7.3	7.6	7.4	7.3
Osmolarity	285	280	300	290
Reference	Coste et al., 2010		Poole et al., 2014	

2.3.2 Mechano-clamp

MA currents, notably the ones mediated by the Piezo2 ion channels, were studied by combining whole-cell voltage-clamp and mechanical stimulation of DRG neurons, i.e. indenting the somata with a blunt probe as described above. This method is referred to as mechano-clamp and depicted in figure 2.1. Medium- and large-diameter neurons with few or no attachments to neighbouring cells were clamped at -70 mV. Series resistance compensation was done at more than 60 % (see table 2.2) and cells were only considered for analysis if their series resistance was lower than 10 M Ω . For mechanical stimulation the probe was positioned 3 μm away from the cell membrane before the start of the protocol. With a velocity of $0.8 \frac{\mu\text{m}}{\text{ms}}$ during the ramp phase the probe delivered 500 ms long stimuli every 5 s in 1 μm increments. Visually, it was made sure the probe touched the cell membrane only upon the third stimulus and the fourth was then considered as producing 1 μm of soma indentation. Recorded currents were low-pass filtered at 10 kHz.

2. MATERIALS AND METHODS

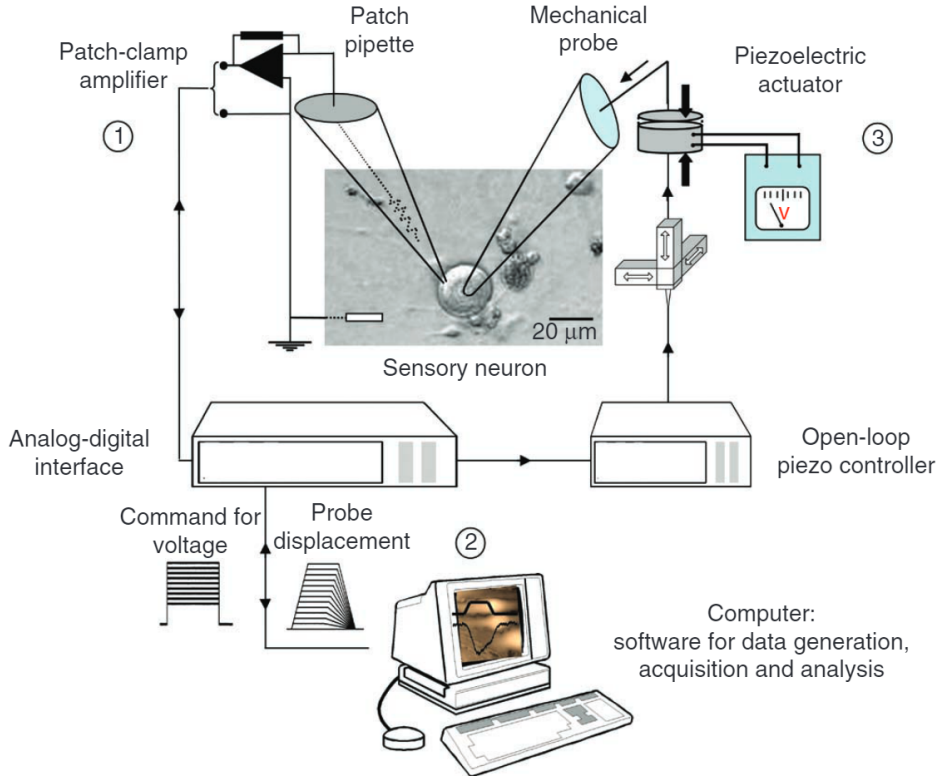


Figure 2.1: Mechano-clamp setup

"Schematic representation of the mechano-clamp circuit. (1) Cultured sensory neurons are recorded using the patch-clamp technique; a glass pipette is filled with a pipette solution, and an Ag/AgCl wire connects the cell to the patch-clamp headstage, which is a sensitive current-to-voltage converter. (2) The patch-clamp amplifier is connected to a computer through an analog-digital interface, allowing data generation, acquisition and analysis. (3) The mechanical probe is connected to a piezoelectric actuator, which is ideal for applications requiring high-resolution movements for micro- and nanopositioning. Piezoceramic actuators make use of the deformation of the piezoelectric material when an electric field is applied. The piezoelectric actuator is connected to a linear amplifier driver, and stimulus parameters are set through the PatchMaster software." Figure and text from Hao and Delmas, (2011).

2.3.2.1 Data processing

The protocol for processing and analysing mechano-clamp data was adopted from Coste et al., (2010) and Eijkelkamp et al., (2013) and Narayanan et al., (2018). The mean baseline current and its standard deviation were determined using the online analysis parameters of the FitMaster software (HEKA) and cells displaying more than 750 pA of leak current at the -70 mV holding potential were excluded from analysis. By subtracting the baseline current from the extremum of the elicited current during mechanical stimulation, the response amplitude was calculated. To discern noise from signal, MA currents were only considered signals when this amplitude exceeded the noise threshold, see equation 2.1. Amplitudes below it were categorised as non-responsive (NRs).

$$\text{noise threshold} = \overline{\text{baseline}} \pm 6 * SD_{\text{baseline}} \quad (2.1)$$

Furthermore, since the deactivation of MA currents could only be properly judged and fitted when signals were of a certain magnitude, a response threshold was applied to reliably categorise adaptation types above it, see equation 2.2. The stimulus intensity needed to evoke MA currents beyond this

threshold is called displacement threshold (Narayanan et al., 2018). Cells showing signals between these two mentioned thresholds were categorised as weak-responders (WRs).

$$response\ threshold = \overline{baseline} \pm 26 * SD_{baseline} \quad (2.2)$$

Contrary to hitherto published absolute thresholds (Jia et al., 2016; Narayanan et al., 2016, 2018), these relative thresholds account for recording conditions and signal-to-noise differences between cells and recordings.

Next, MA currents classifying as responses were fit to a mono-exponential curve using the built-in trace fit function of the FitMaster software (HEKA). Rapidly-adapting (RA), intermediately-adapting (IA) and slowly-adapting (SA) current types were determined using the resulting inactivation time constant τ according to equation 2.3. Currents were also considered SA when they lacked inactivation throughout the stimulus.

$$\tau_{RA} < 10ms < \tau_{IA} < 30ms < \tau_{SA} \quad (2.3)$$

With soma diameters of up to 40 μm (for average value, see table 2.2) and very long processes *in vivo* the studied mouse DRG sensory neurons are relatively huge cells for patch-clamp recordings. Though their processes are not as long *in vitro*, they are still plentiful and make for enormous capacitance values. Compared to somatic regions close to the recording pipette, such cellular plasma membrane compartments can have significantly higher access resistance. This results in poor space clamp and erroneous recordings (Williams and Mitchell, 2008; Bar-Yehuda and Korngreen, 2008; Cummins et al., 2009) that cannot be further compensated for. Reliable space clamping of the membrane potential was difficult despite having avoided to record from cells attached to neighbouring cells and having used pipettes with low resistances, thereby having achieved low series resistance and high compensation of the same (see table 2.2). When mechanically-evoked currents were of big magnitude, they were sometimes accompanied by another current type. This other current was negative as well, implying to be an inward cationic current. It activated within milliseconds in some cells, displaying a big MA current and inactivated quickly as well. Judging from these observations, the second current had to be mediated by fast voltage-gated sodium channels, see 2.3.3 and 3.1.2. Since these channels are half-maximally active at a membrane potential of $\sim -40\text{ mV}$ (see figure 3.4), the observations imply that hefty MA currents can depolarise an imperfectly clamped cell considerably. In order to avoid substantial depolarisation and subsequent variation of voltage-dependent Piezo2 currents (Coste et al., 2010; Moroni et al., 2018), cells producing enormous MA currents had to be excluded from the statistical

Table 2.2: Electrophysiological parameters of 128 analysed RA-MA cells

See section 2.3 and equations 2.2 and 2.3 for details. C-slow = cancellation of slow capacitive transients \sim cell capacitance

Analysed RA-MAs	Mean	SD	SEM
Series resistance ($\text{M}\Omega$)	5.80	1.32	0.12
Series resistance compensation (%)	77.11	13.82	1.22
Baseline current (pA)	-266.19	173.89	15.37
Responder threshold (pA)	± 266.81	172.93	15.29
Soma diameter (μm)	28.92	3.60	0.32
C-slow (pF)	65.07	21.93	1.94

2. MATERIALS AND METHODS

analysis of the current amplitude and τ , but not from counting response types qualitatively. Since the described sodium artefacts could be recorded following MA current amplitudes of ≈ 15 nA, quantitative parameters of cells showing more than 10 nA were not included.

2.3.3 Sodium currents

Whole-cell voltage-gated sodium currents were recorded using a standard voltage jump protocol. From a holding potential of -70 mV, 50 ms long voltage jumps were performed every 2 s in 5 mV increments from -80 to +35 mV. After plotting the maximal, leak-subtracted amplitude versus the respective voltage, the Boltzmann distribution and the Goldman-Hodgkin-Katz equation were used to fit the data (current-voltage fit type of the series fit window of the FitMaster software; see FitMaster Manual 2.40, HEKA). The following parameters were analysed:

- V_{half} = half-activating voltage
- E_{rev} = reversal potential
- I_{max} = peak current density amplitude

2.3.4 Current-clamp

Established from research done in DRG neurons of cats (Koerber et al., 1988), guinea-pigs (Djouhri et al., 1998; Djouhri and Lawson, 2001), rats (Fang et al., 2005; Viatchenko-Karpinski and Gu, 2016) and mice (Lechner et al., 2009; Poole et al., 2014; Wetzel et al., 2017), sensory neuron types can be classified by the shape of their action potential. To that end, cultured DRG neurons were subjected to stepwise injections of current pulses in whole-cell current-clamp-mode in standard physiological salt solutions (Poole et al., 2014, see table 2.1). The current pulses were 1 s long, their magnitude was individually adjusted to each cell, varying between 50 and 2000 pA, as DRG size and excitability varies greatly. With the FitMaster software (HEKA), the resting membrane potential was determined. The amplitude of recorded action potentials, the rise and decay times as well as the full width at half maximum of recorded spikes were measured using the Igor Pro software (WaveMetrics, Inc., USA) with the NeuroMatic package installed (Jason Rothman, thinkrandom.com). The presence of a bump (two instead of one inflection point) in the falling phase of an action potential was checked for by calculation of the derivative of the voltage trace $\frac{\Delta V}{\Delta T}$ and counting minima in that phase. Adapted from Poole et al., (2014) and Wetzel et al., (2017), sensory neurons were then classified as depicted in figure 2.2.

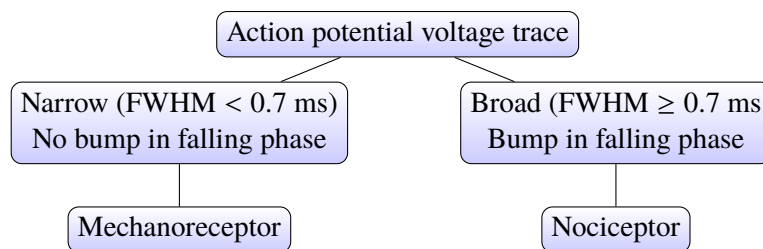


Figure 2.2: Classification of sensory neurons

Poole et al., (2014) used the shape of recorded action potentials in the depicted way to classify sensory neurons as mechanoreceptors or nociceptors. FWHM = full width at half maximum of evoked spike in voltage trace.

2.4 Behavioural testing

In order to test the effect of maturation and ageing on *in vivo* somatosensation in mice, two cohorts of six young mice each and a cohort of eight middle-aged mice were tested for mechanosensitivity in glabrous (see 2.4.1.1) and hairy skin (see 2.4.1.2) and thermal sensitivity in glabrous skin (see 2.4.2). Due to time restrictions, the project could not wait for young mice to come of old age. A second cohort of four middle-aged mice was introduced to gather more tape response assay (TRA) data (test plan summarised in figure 2.3). All mice were introduced to the setup and acclimated in the testing boxes three and two days before their first testing round, as well as for two hours before every experiment in order for them to be calm and not engaging in exploratory and major grooming behaviour upon test start.

Starting at an age of four weeks, the young mice were tested every two weeks five times in a row until the adult age of twelve weeks. Middle-aged mice were tested twice with two weeks between tests as well. The different tests were performed separately on consecutive days, starting with the Dynamic Plantar Aesthesiometer, then Hargreaves test on day two and finally the TRA on day three.

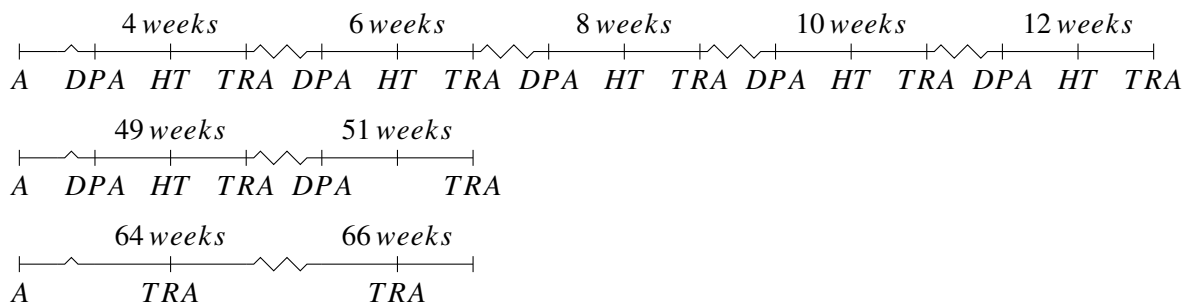


Figure 2.3: Timeline of longitudinal behavioural testing

This scheme represents the testing schedule of different age cohorts of WT mice; see text for details. Their postnatal age is labelled above, the performed tests are labelled below the time bar. Top row: Maturing mice were tested every two weeks. Middle and bottom row: Two cohorts of middle-aged mice were tested separately. A = acclimation; DPA = Dynamic Plantar Aesthesiometer; HT = Hargreaves test; TRA = tape response assay.

2.4.1 Mechanical sensitivity

2.4.1.1 Glabrous skin - Dynamic Plantar Aesthesiometer

For investigating non-noxious mechanosensitivity of the glabrous skin of the hind paws of WT mice, the animals were set down in transparent plastic boxes on an elevated grid, beneath which the Dynamic Plantar Aesthesiometer (Ugo Basile SRL, Italy) equipped with an upright filament was placed. After positioning the tip of the filament right beneath the centre of the plantar surface of the hind paw of interest, the testing protocol was started: the filament was projected upwards gently touching the skin with continuously increasing force of up to 10 g within 40 s (Minett et al., 2011; Avenali et al., 2014; Sondermann et al., 2019). This force ramping was discontinued automatically upon withdrawal of the hind paw and the latency and the respective force value were noted down. This protocol was repeated five times per paw with at least two minutes between any stimulus on the same mouse.

2. MATERIALS AND METHODS

2.4.1.2 Hairy skin - tape response assay

In the past, adhesive removal tests or TRAs have been used to test for sensorimotor deficits following spinal cord (E.J. et al., 2002) or brain injury (Bouet et al., 2009), such as middle cerebral artery occlusion (Freret et al., 2009; Ogle et al., 2012). Adhesive tape was applied to the front paws and the delay until notice and removal was measured. In more recent studies, adhesive dots applied to the hind paw were used by Roberson et al., (2013) to test plantar tactile sensitivity. Finally, Ranade et al., (2014) used a TRA to show defects in innocuous touch sensation by affixing a 3 cm piece of adhesive tape to the back of a mouse and count the number of bouts in response to it. (Note that a tape assay can also be used to quantify hair follicle weakness and loss in a hair-pull test; Lay et al., 2016).

Here, a TRA is used to quantify sensory-driven behaviour for hairy skin mechanosensation. To that end, mice acclimated in the mentioned plastic boxes on a glass plate (see 2.4.2) were taken out and red 12.7 mm circular adhesives (Microtube Tough Spots[®], Diversified Biotech, Inc., USA; Ogle et al., 2012; Roberson et al., 2013) were adhered to their upper back as the tape stimulus. When the tape was applied to lower back areas in pilot experiments, the mice got it off too easily. Therefore this harder-to-reach area was chosen to record response time courses over several minutes. The mice were then set back into their cleaned box (freed of droppings etc. to reduce distraction) and their tape-directed responses monitored as follows:

- "wet-dog shake" = 1 bout
- trying to reach tape with snout = 1 bout
- burst of directed scratching with hind leg = 1 bout
- neck grooming with front paw = 1 bout
- grooming of head, lower back, paws, legs, ventral areas or tail = no bout

These responses were time-tracked and counted using the Android app Counter and Timer (version 1.4, risinier, available at <https://play.google.com/>). Data was exported as a text file and converted to an analysable data frame format using Python (version 3.6.1, Python Software Foundation, available at <http://www.python.org>). Recording was stopped when the mouse managed to get the tape off or after a trial time of five minutes.

Though this assay was adapted from Ranade et al., (2014), my implementation of bout tracking poses a considerable upgrade to its sensitivity, see section 4.1.3.3. The following parameters were analysed:

- tape riddance (success/time-out)
- total number of bouts, total trial time
 - bouts per minute
- no response time = sum of time throughout which no bout occurred for 15 seconds or more
- time course of bouts
 - area under the curve of the time course plot (cumulative bouts vs. time)

The quantification of the latter, as well as the statistical analysis of all parameters will be explained in section 2.4.3.

2.4.2 Thermal sensitivity - Hargreaves test

Sensitivity of hind paws to heat was assessed with the Hargreaves test, as described by Minett et al., (2011) and Sondermann et al., (2019) and by using the IITC Plantar Analgesia Meter (IITC Life Science Inc., USA). The mice were placed on a glass plate inside the boxes mentioned before and left to acclimatise. Then, a weak, visible light beam was focused onto the centre of the plantar surface of a hind paw and then intensified to provide thermal stimulation. The stimulus intensity had been set to a value that lead to an average paw withdrawal latency of ~ 10 s. It was kept constant for all tests performed in this study. Upon behavioural response to the stimulus, stimulation was stopped and the latency of paw withdrawal was noted down. For each paw, five values were acquired with at least two minutes between any stimulation of the same mouse.

2.4.3 Statistical analysis

Statistical testing was done with the GraphPad Prism software (version 8.0.2, GraphPad Software, USA). For hind paw sensitivity measurements (2.4.1.1 and 2.4.2), data points from individual mice at a given time point were excluded, in case less than five trials for any paw were recorded. The study design (see figure 2.3) requires testing across cohorts of young and middle-aged mice, which does not allow matching of observations per mouse. Therefore, mice with missing values were not excluded from analysis entirely, so that complete sets of trials were still analysed for respective time points. In this sense, two young mice missing data from one time point, respectively, were still analysed for the sake of including as many data points as possible. The body of single latency values per mouse, time point and paw was tested for normality using the D'Agostino and Pearson test (D'Agostino and Belanger, 1990), and for outliers using the ROUT test (Motulsky and Brown, 2006). Since no outliers were found, interindividual differences were disregarded in the following analysis, as marked variation in behavioural data can be expected, even in age-matched, inbred, isogenic mice (Loos et al., 2015). Each set of five values (per mouse, age and paw) was averaged, the arithmetic means of which were then averaged per paw and age. The standard deviations were pooled in a weighted manner using the following formula by Cohen, (1989):

$$SD_{pooled} = \sqrt{\frac{(SD_1^2 + SD_2^2 + SD_n^2)}{n}} \quad (2.4)$$

The yielded grand means with pooled SDs per paw and time point were analysed using two-way analysis of variance (ANOVA) with Tukey's Honest Significant Difference (HSD) test (Tukey, 1949).

For the analysis of the TRA data, it was required to statistically test across cohorts of different mice as well. Therefore, one mouse that could not be tested at four weeks of age was not excluded from the following testings.

The χ^2 test was used to test whether the rate of mice managing to get the tape off in time changes with age. Time courses of bouts were plotted per second and then averaged for each time point. The area under these averaged time course curves (baseline at 0 bouts) was calculated with the trapezoid rule

2. MATERIALS AND METHODS

(Gagnon and Peterson, 1998) for every $\Delta X = 1$ s. Since the averaged time courses were plotted over five minutes with such temporal resolution, the quantification of the total areas under the curve is expected to yield values in the orders of magnitude of 10^3 to 10^4 total bouts * s. The yielded averages \pm SEM of the different age groups, as well as the averages of the total bouts and total bouts per minute were each analysed using one-way ANOVA with Tukey's HSD test.

2.5 Molecular Biology

2.5.1 Quantitative PCR

Total ribonucleic acid (RNA) was isolated and purified from primary cultures of DRG neurons or snap-frozen DRG tissue (see 2.2) using the NucleoSpin RNA XS kit (MACHEREY-NAGEL GmbH & Co. KG, Germany) according to the manufacturer's instructions. Utilising the QuantiTect reverse transcription kit (QIAGEN GmbH, Germany), genomic deoxyribonucleic acid (DNA) was digested and first-strand complementary DNA was synthesised. For assessing gene expression of different exons of Piezo2 (see ??), quantitative real-time polymerase chain reaction (qPCR) was employed using the Power SYBR Green system. Sample cDNA ($\approx 1 - 100$ ng or H_2O as negative control) together with 100 mM forward and reverse primers (see table 2.3) and SYBR Green Master Mix were pipetted into 386 well plates in triplicates (technical replicates) and analysed in a LightCycler 480 (F. Hoffmann-La Roche AG, Switzerland).

The melting curves of the amplicates were analysed to ensure primer specificity. Then, the second derivative maximum method (Rasmussen, 2011; Luu-The et al., 2005) of the LightCycler was used to determine the threshold cycle (C_T) values, i.e. the respective PCR cycle number at which SYBR green fluorescence rises above background. The reference gene for relative quantifications was GAPDH for expression, and Piezo2, exon 25 for relative exon expression or splice analysis. The calibration group was the juvenile one. The $2^{-\Delta\Delta C_T}$ method (Livak and Schmittgen, 2001) was used for calibrations, normalisations and quantifications, where

$$\Delta\Delta C_T = (C_{T, target gene} - C_{T, reference gene}) - (C_{T, calibrator} - C_{T, reference gene}) \quad (2.5)$$

Statistical testing was done using one-way ANOVAs with Tukey's HSD test (GraphPad Prism 8.0.2).

Table 2.3: Sequences of primers used for quantitative real-time PCR

Target	Sense	Sequence
GAPDH	sense	CAATGAATACGGCTACAGCAAC
GAPDH	antisense	TTACTCCTTGGAGGCCATGT
Piezo2, exon 25	sense	AAAAGCCATTGCCGAGGTCT
Piezo2, exon 25	antisense	GATGCCGATGCAGACGAAGT
Piezo2, exon 33	sense	CAGACAAACAGAAAGCCAAGGG
Piezo2, exon 33	antisense	GGAAGCATGATCAACCCAAGG
Piezo2, exon 35	sense	CTCAGCCATTTTAGCCTTGC
Piezo2, exon 35	antisense	CAGATCCTTTGCGTCTCTCC

2.5.2 Patch-seq: single-cell harvest

Electrophysiologically characterised DRG neurons (MA currents and action potentials, see 2.3) were harvested using the patch pipette after recordings and their RNA subjected to sequencing. To that end, some alterations to the patch-clamp technique had to be put in place (Cadwell et al., 2017b,a):

- wide pipettes of 1 - 2.5 M Ω
- very low volume of pipette solution
- KCl-based pipette solution (instead of CsCl-based; in order to record proper action potentials)
- RNase-free setup, materials, solutions; careful RNase-free working style

After voltage- and current-clamp experiments, negative pressure was applied to the patch pipette in whole-cell-mode to aspirate cytosolic contents, as suggested by Cadwell et al., (2017b) and Fuzik et al., (2016). The content of the patch pipette was transferred, by applying positive pressure to it with a syringe, to a 1.5 ml centrifuge tube filled with 100 μ l of cool lysis buffer containing TCEP from the Nucleospin RNA purification kit (Macherey-Nagel, see 2.5.1). Often, pipettes were broken inside the tube to ensure full transfer of cellular material to the buffer. These tubes were shortly kept on ice, if necessary, and flash frozen in liquid nitrogen and stored at -80 °C as soon as possible. RNA purification was done the same way, as for acute and cultured DRGs, described in the previous section, shortly before downstream experiments to avoid long-term storing of purified RNA.

For establishing this workflow, I tested such aspirates via qPCR, including serial dilutions of RNA of known concentration and cell-free aspirates as controls. Single-cell RNA samples from whole-cell-mode aspiration of the cytosol of cultured DRG neurons could not be reliably and consistently amplified. This is most likely due to the fact that not enough material could be gathered with this technique, even when using the widest possible patch pipettes and aspirating for dozens of minutes. Therefore, I implemented another way of harvesting the soma of DRG neurons that pays tribute to the enormous soma sizes of the particular cells of interest and termed it "OBST":

- Off the cell
 - retract the recording pipette carefully from whole-cell-mode to enable closing of the membrane patch
- Break the pipette
 - widen the opening of the pipette gingerly by breaking the glass by lowering it onto the coverslip away from the cell
 - apply positive pressure throughout this process to avoid aspiration of unwanted particles
- Suck in the soma and sever the processes
 - position the widened opening centrally to aspirate the soma by applying negative pressure to the point, where it can be pulled out of the bath solution reliably
 - use the stimulation probe to sever the cells processes and to get rid of attached cells and debris

2. MATERIALS AND METHODS

- Transfer
 - manoeuvre the pipette holding the aspirate delicately through the surface of the bath solution, but be quick and clean from there on
 - swiftly take out the pipette from the holder, connect a syringe filled with air via a tube to the back-end of the pipette, lower the front-end into the prepared cool lysis buffer in a centrifuge tube
 - transfer all contents by applying pressure until a bubble is produced
 - break the front-end glass on the tube wall below the buffer level to be sure to have transferred attached material as well

The samples collected this way could consistently be amplified in qPCR pilot experiments, yielding ~ 20 pg of RNA per sample, as estimated by comparison of the mentioned spike-in controls (serial dilution of RNA of known concentration). Since estimations of the average RNA yield of single-cells range from ~ 10 pg for mammalian cells (Lambolez et al., 1995; Cadwell et al., 2017b,a; Huang et al., 2018) to ~ 50 pg for vertebrate neurons (Sucher et al., 2000), the achieved yield was considered satisfactory.

2.5.3 Single-cell RNA sequencing

Reverse transcription, library preparation, sequencing, raw read and quality check, mapping and normalisation of reads as well as gene annotation was done by Gabriela Salinas, Ph.D., Orr Shromroni, Ph.D. and Fabian Ludewig from the Transcriptome and Genome Analysis Laboratory (TAL) Microarray and Deep-Sequencing Facility in Göttingen, Germany.

2.5.3.1 Library preparation and sequencing

For cDNA synthesis the SMART Ultra Low Input RNA kit for Illumina Sequencing (Clontech Laboratories, Inc., USA) was used in an MJ Thermocycler according to the supplier's protocol. Clean-up reactions were done with Ampure XP beads (Beckman Coulter Genomics, UK). For library preparation the Nextera DNA Sample Prep kit (Illumina, Inc., USA) was used in combination with Illumina-compatible adaptors and PCR primers from Integrated DNA Technologies, Inc., USA. Libraries were quantitated by a Fragment Analyzer using the High Sensitivity DNA analysis kit and Kapa Biosystems Illumina library Quantitation kit. Libraries were sequenced on the HiSeq4000 (Illumina, single-end 50 bp fragments; 20-30 Mio reads/sample).

2.5.3.2 Bioinformatics

Raw read and quality check Sequence images were transformed with Illumina software BaseCaller to BCL files, which was demultiplexed to fastq files with bcl2fastq (version 2.17.1.14; Illumina). The sequencing quality was asserted using FastQC (version 0.11.5; Andrews, 2014).

Mapping and Normalisation Sequences were aligned to the reference genome *Mus musculus* (mm10 version 84, https://www.ensembl.org/Mus_musculus/Info/Index) using the STAR aligner (Dobin et al., 2013; version 2.5.2a) allowing for 2 mismatches within 50 bases. Subsequently, read counting was

performed using featureCounts (version 1.4.5-p1; Liao et al., 2014). Read counts were analyzed in the R/Bioconductor environment (version 3.4.2; www.bioconductor.org) using the R package edgeR (version 3.22.5; Robinson et al., 2010). For differential gene expression analysis (DGE), results ($p < 0.05$) were filtered for $\log_2(\text{fold change})$ and false discovery rate ($|\log\text{FC}| > 1.5$ and $\text{FDR} < 0.05$). Gene annotation was performed using Mus Musculus entries via biomaRt R package (version 2.32.1.; Durinck et al., 2009). Functional annotation of results with Gene Ontology (GO, a major bioinformatic knowledge database) was done using the topGO R package (version 2.35.0; Alexa and Rahnenfuhrer, 2018. topGO: Enrichment Analysis for Gene Ontology).

3

Results

We have come to understand there is a yet unpublished age-dependent decrease in Piezo2 function *in vitro* as well as in the sense of touch in male WT C57Bl/6J mice. In the first part of this chapter I intend to prove that with descriptive data. I will then go on to dig deeper into the mechanism of this decrease.

For presentation of numeric data I will show individual values wherever possible. For sample sizes around and above $n = 20$, single values will be shown in the form of violin plots: similar to a box plot, the minimum, maximum, median and quartiles are shown. In addition, single values are represented as a kernel density plot, the width of which depicts the frequency of data points.

3.1 Chronicle of declining touch

Whilst investigating the native Piezo2 interactome, Pratibha Narayanan, Ph.D. noticed age-dependent differences in the Piezo2-mediated current data of her control groups. Following up on her preliminary findings, I started by investigating the function of Piezo2 proteins in male WT mice of different ages with electrophysiological experiments. Recording Piezo2 mediated RA-MA currents is the most direct method to quantify the function of this key player of somatosensory mechanosensation. By gently poking cultured DRG neurons with a blunt probe while whole-cell voltage clamping (see 2.2 and 2.3), different types of MA currents could be recorded. Note that the Piezo proteins were first described in such a DRG culture system as well (Coste et al., 2010).

Initially, patch-clamp and RNA isolation experiments were done on both the first and the second day after culturing. However, as shown in figure 3.1, observed differences between those time points hindered pooling of the data and urged me to disregard the second day *in vitro* (DIV 2) for my central line of argument. After all, culturing is known to change electrophysiological parameters (Song et al., 2018).

The presented data in the following subsections 3.1.1 and 3.1.2 were acquired with CsCl-based recording pipette solution in order to reduce contamination of recordings with unwanted potassium currents (Coste et al., 2010), such as currents mediated by numerous inwardly-rectifying potassium

3. RESULTS

channels (e.g. $K_{ir}2.1$, Abrams et al., 1996) and cyclic nucleotide-regulated channels (Stieber et al., 2005; see also section 2.3).

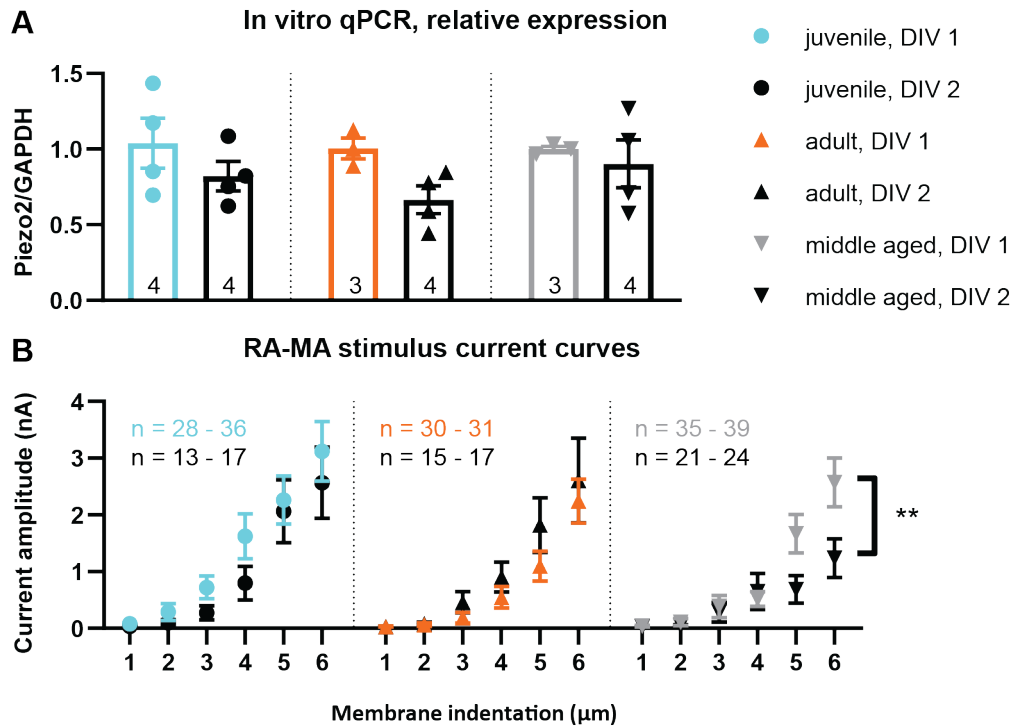


Figure 3.1: Exemplary comparison of days *in vitro*

A: Relative expression analysis of Piezo2 normalised to GAPDH and calibrated to the first day *in vitro* (DIV 1) reveals a slight trend for reduced mRNA expression on DIV 2 (not taking into account possible changes in GAPDH mRNA expression), $p=0.045$, two-way ANOVA. Value pairs of DIV 1 and 2 stem from the same animal; N = number of different animals is depicted in the bars. B: RA-MA amplitudes differ on DIV 2 in the middle-aged group, $** p \leq 0.01$, two-way ANOVA with Tukey's HSD test. $N_{juvenile} = 10$, $N_{adult} = 8$, $N_{middle-aged} = 7$.

3.1.1 Maturation decreases Piezo2 currents

The only mechanotransducer known so far to be responsible for the detection of light touch in vertebrate somatosensory neurons is Piezo2 (Ranade et al., 2014, 2015; Anderson et al., 2017; Martinac and Poole, 2018). In mice, this mechanically-gated ion channel facilitates fast MA currents, since these are selectively obliterated upon deletion of Piezo2 (Ranade et al., 2014). Representative RA-MA current traces are shown in figure 3.2A. Comparing such Piezo2-mediated RA-MA currents in medium- and large-diameter cultured DRG neurons of male WT C57Bl/6J mice of different ages, I found the following trends:

RA-MA currents are strongest early in murine life As depicted in figure 3.2A and B, the RA-MA currents of juveniles have a higher amplitude than those of adults; the difference reaches statistical significance already at relatively low stimulus intensities of 4 and 5 μ m membrane indentation. Juvenile current amplitudes at 4 μ m indentation are also significantly higher than those of middle-aged mice. The amplitudes of adolescents numerically lie between those of juveniles and adults at these stimulus intensities, while those of middle-aged mice are not smaller than those of adults. Taken together,

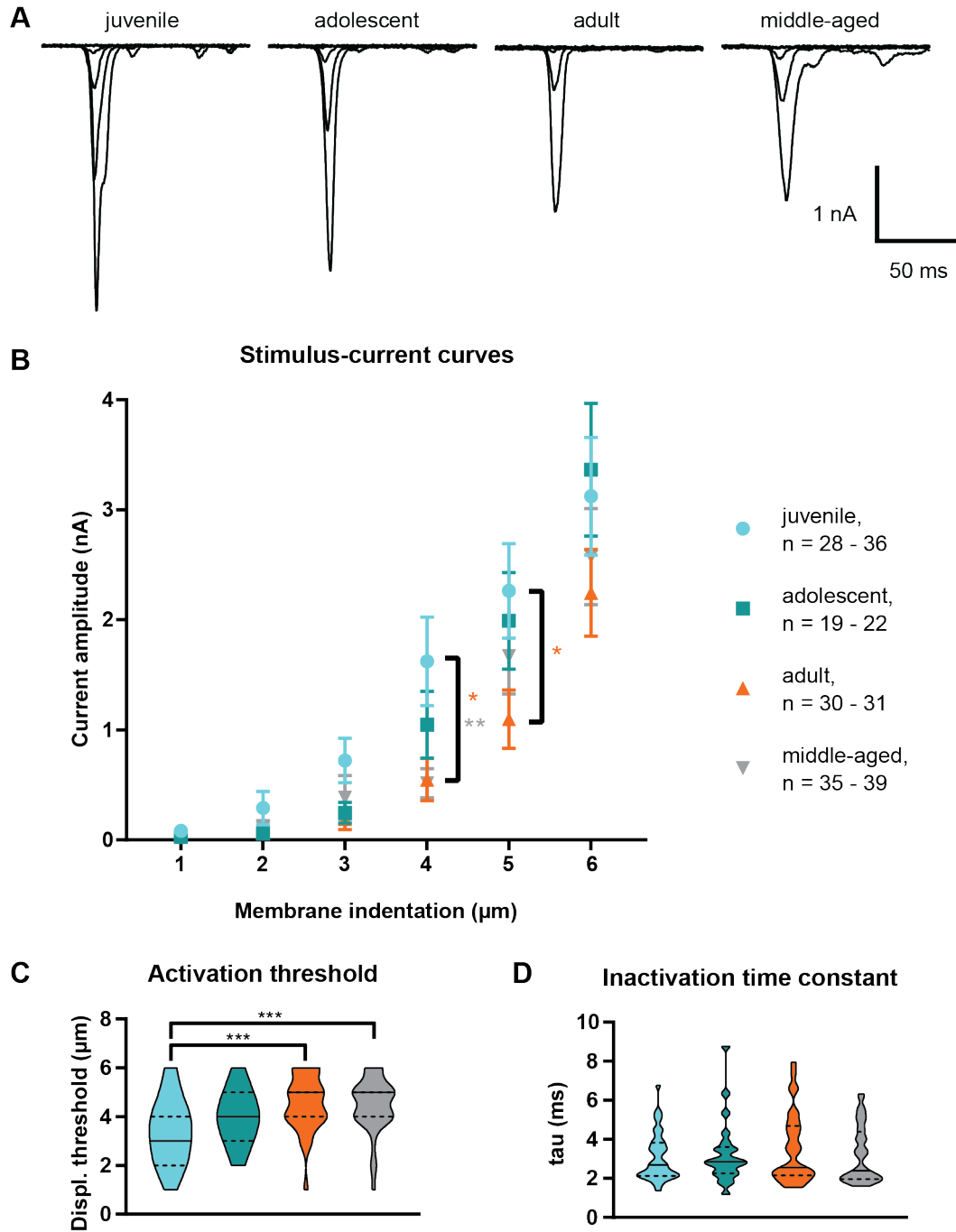


Figure 3.2: Maturation attenuates RA-MA currents in DRG neurons

A: Representative whole-cell current traces of rapidly-inactivating currents of cultured medium- and large-diameter DRG neurons of mice of different age groups, labelled above each trace, during mechanical stimulation of the soma with 1 to 6 μm membrane indentation in 1 μm steps. B: Quantification of peak RA-MA current amplitudes. Numbers of cells range, as not all recordings remained stable throughout all stimuli. * $p \leq 0.05$, ** $p \leq 0.01$, two-way ANOVA with Tukey's HSD test. C: Violin plot of minimal stimulus intensities that produced robust RA-MA signal; high smoothing to more comprehensibly depict the frequencies of the whole number values (1 μm steps). *** $p \leq 0.001$, one-way ANOVA with Tukey's HSD test. D: Inactivation time constants of maximal RA-MA signals; light smoothing to more accurately depict continuous values. ns, one-way ANOVA. Values in B are given as arithmetic mean \pm SEM, lines in C and D show median and quartiles (dashed). $N_{\text{juvenile}} = 10$, $N_{\text{adolescent}} = 4$, $N_{\text{adult}} = 8$, $N_{\text{middle-aged}} = 7$.

these data suggest that Piezo2-mediated current amplitudes in somatosensory neurons decline during maturation.

3. RESULTS

RA-MA currents are most sensitive early in murine life In cultured DRG neurons of juvenile mice, only relatively weak stimuli were needed to produce discernable RA-MA signals (see subsection 2.3.2.1. The displacement threshold, quantised in figure 3.2C, was significantly higher in neurons of adult and middle-aged mice. Again, the corresponding average of adolescents lies between juveniles and adults. The distributions of values of adult and middle-aged mice are highly similar. Altogether, these data suggest that sensitivity of Piezo2-mediated mechanotransduction in somatosensory neurons declines during maturation.

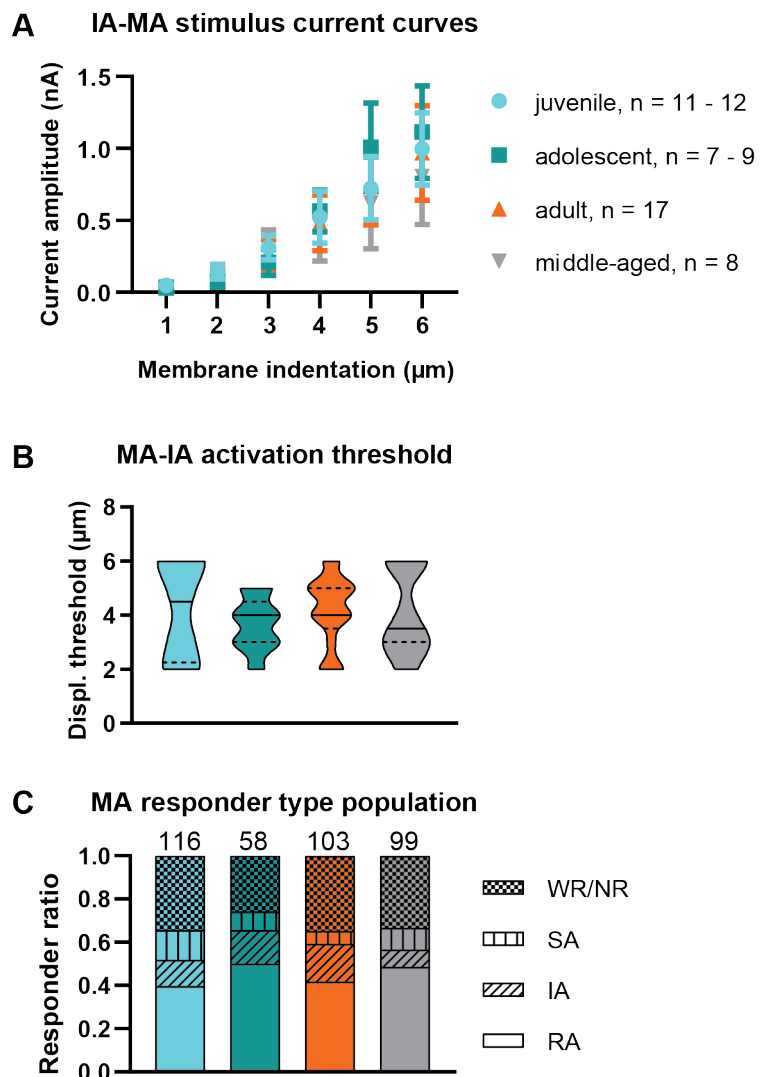
RA-MA adaptation unvaried Undeterred by these age-dependent differences in RA-MA currents, the inactivation kinetics remain unchanged, as represented by very similar τ values, see figure 3.2E. Despite the described attenuation of Piezo2-mediated RA-MA currents with maturation, the hallmark characteristic of these currents (i.e. the rapid adaptation) remains unaffected across all age groups.

3.1.2 Ageing does not affect other electrophysiological parameters

In order to put the observed decline in DRG RA-MA currents into the context of the highly complex model system and to elucidate the specificity of the impact of maturation and ageing on Piezo2 function, other parameters and current types were examined.

Figure 3.3: IA-MA currents and MA responder type populations do not change with age in medium- and large-diameter cultured DRG neurons

A: Quantification of peak IA-MA current amplitudes. Numbers of cells range, as not all recordings remained stable throughout all stimuli. ns, two-way ANOVA. Values in are given as arithmetic mean \pm SEM. B: Violin plot of minimal stimulus intensities that produced robust IA-MA signal. ns, one-way ANOVA. Lines show median and quartiles (dashed). A and B: $N_{juvenile} = 8$, $N_{adolescent} = 3$, $N_{adult} = 6$, $N_{middle-aged} = 5$. C: Ratio of recorded response types in medium- and large-diameter DRG neurons. Numbers of recorded cells per age group are given above the respective bar. ns, χ^2 test. Mind that these ratios do not represent the whole population of DRG neurons. $N_{juvenile} = 10$, $N_{adolescent} = 4$, $N_{adult} = 10$, $N_{middle-aged} = 7$.



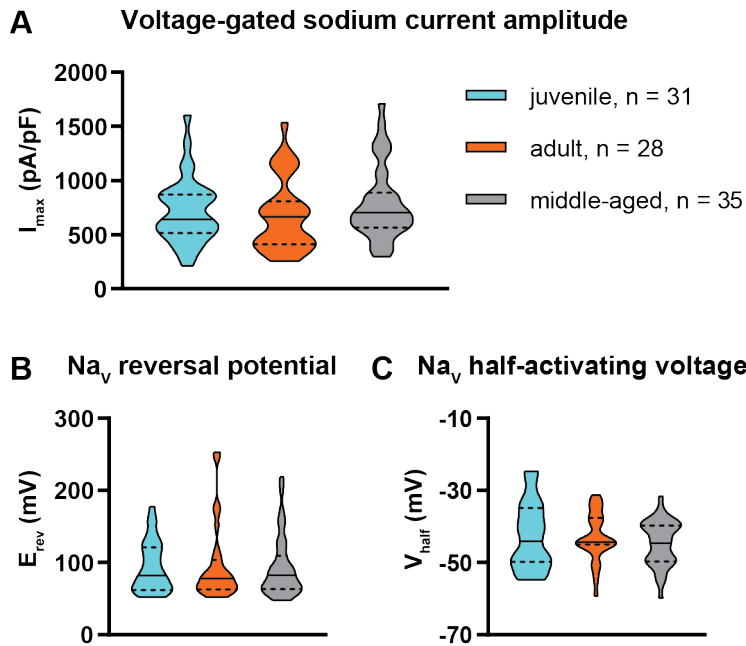


Figure 3.4: Voltage-gated sodium currents do not change with age in medium- and large-diameter cultured DRG neurons Sodium currents were recorded by applying a voltage jump protocol to cultured whole-cell voltage clamped medium- and large-diameter DRG neurons of mice of different ages. By using a common current-voltage fit (see 2.3.3), the plotted parameters were determined: the peak current density amplitude, I_{max} (A); the reversal potential, E_{rev} (B); the half-activating voltage, V_{half} (C). Values are given as arithmetic mean \pm SEM. ns, one-way ANOVA. $N_{juvenile} = 5$, $N_{adult} = 5$, $N_{middle-aged} = 6$.

IA-MA currents are unaffected by ageing As mentioned in chapter two (2.3.2.1), one can distinguish three types of MA currents in murine DRG neurons by means of their inactivation time constants τ (Coste et al., 2010). While RA-MA currents are mediated by Piezo2 predominantly (Coste et al., 2010; Dubin et al., 2012; Ranade et al., 2014), SA-MA currents have recently been shown to be mediated by Tentonin3/TMEM150c (Hong et al., 2016). They are the predominant current type in small-diameter DRG neurons. Since I particularly recorded from medium- and large-diameter neurons, I did not record enough SA-MA responders for proper statistical comparison. Little is known about the molecular correlates of IA-MA currents. Contrary to RA-MA currents, IA-MA currents are unaffected by siRNA-mediated knockdown of Piezo2 (Coste et al., 2010). Ageing did not effect the IA-MA currents recorded in this study. Statistical differences between the age groups were found for neither the stimulus-response quantification, nor the measured displacement thresholds; see figures 3.3A and B, respectively. This observed permanence of IA-MA currents hints at the specific impact of maturation on the Piezo2-mediated RA-MA currents.

MA current type ratios remain constant with age Figure 3.3C depicts the fractions of the different MA current types described before, as recorded in the studied cultured DRG neurons. It helps visualise that no significant changes of those ratios occurred with age (χ^2 test). The observed ratios are consistent with previously reported data (Coste et al., 2010).

Voltage-gated sodium currents are consistent across age groups In addition to mechanically stimulating the DRG neurons in whole-cell voltage clamp, I applied fast-paced voltage jump protocols to measure voltage-gated sodium currents, see section 2.3.3. Neither the half-activating voltage V_{half} , the reversal potential E_{rev} , nor the peak current density amplitude I_{max} of sodium currents were significantly different between the tested age groups of juvenile, adult and middle-aged mice, see figure 3.4.

3. RESULTS

In toto, the findings agree that maturation impacts Piezo2-mediated RA-MA currents, but neither their inactivation kinetics, IA-MA currents nor voltage-gated sodium currents. Mechanotransduction in cultured DRG neurons facilitated by the Piezo2 protein becomes less sensitive and the transduction currents decrease in amplitude. Meanwhile, the mechanosensitive fraction and the fraction of RA-MA responders amongst medium- and large-diameter DRG neurons remains constant.

3.1.3 Age-dependent decrease in somatosensory mechanosensation

Following in the wake of the electrophysiological findings that Piezo2-mediated currents decrease with maturation, I set out to investigate whether these changes have measurable consequences for the behaviour of the mouse coming of age. To this end, I performed behavioural assays to test glabrous and hairy skin somatosensation with a focus on non-noxious mechanosensation, as Piezo2 is the principle mechanotransducer in light touch (Ranade et al., 2014; Anderson et al., 2017). Tests were performed on twelve four-week-old male WT C57Bl/6J mice every two weeks, as well as on two cohorts of eight and four middle-aged mice respectively; see section 2.4.

3.1.3.1 Hind paw sensitivity decreases with maturation

At first, the Dynamic Plantar Aesthesiometer (see 2.4.1.1) was used to probe the mechanical sensitivity of the hind paw, as had been done before (Ranade et al., 2014; Woo et al., 2014; Avenali et al., 2014; Rouwette et al., 2016; Iftinca et al., 2016), in WT mice at different ages. I hypothesised that sensitivity declines with maturation, akin to the described decline in Piezo2 function (see 3.1.1). Expectably, higher forces should be required to elicit withdrawal responses with age, with the lowest threshold in the youngest mice tested and the highest in adult and middle-aged mice. Since the filament force ramps linearly (0 - 10 g in 40 s), required hind paw withdrawal forces are directly proportional to withdrawal latency values, which are plotted in figure 3.5A.

Mechanical sensitivity decreases abruptly before eight weeks of age Appreciably, the hypothesised maturational decline in mechanical hind paw sensitivity became evident. Four-week-old mice showed the lowest withdrawal response thresholds indeed with remarkably high statistical confidence, yet no significant differences were found between any of the older age groups. While the six-week-olds showed the second lowest threshold by median and arithmetic mean, the distribution of values at eight weeks of age is highly similar to that at the twelve-week time point. This data situation differs from the trends observed in RA-MA currents, where data of eight- and twelve-week-olds were not as congruent.

Thermal sensitivity decreases continuously between six and twelve weeks of age Next, I determined hind paw sensitivity to heat of the aforementioned WT mice of different ages using the Hargreaves radiant heat test (Hargreaves et al., 1988; Avenali et al., 2014; Iftinca et al., 2016); see section 2.4.2. As can be seen in the plot of the hind paw withdrawal latencies in figure 3.5B, thermal sensitivity in these mice decreased over the course of maturation as well. Notably though, this change in sensitivity follows a quite different temporal trend: the measured sensitivity stays rather constant between the testing ages of four and six weeks (no significant difference). Then, it decreases significantly and continuously so, until it remains constant in the here tested mice from the mature age of twelve weeks on (no difference to middle-aged group).

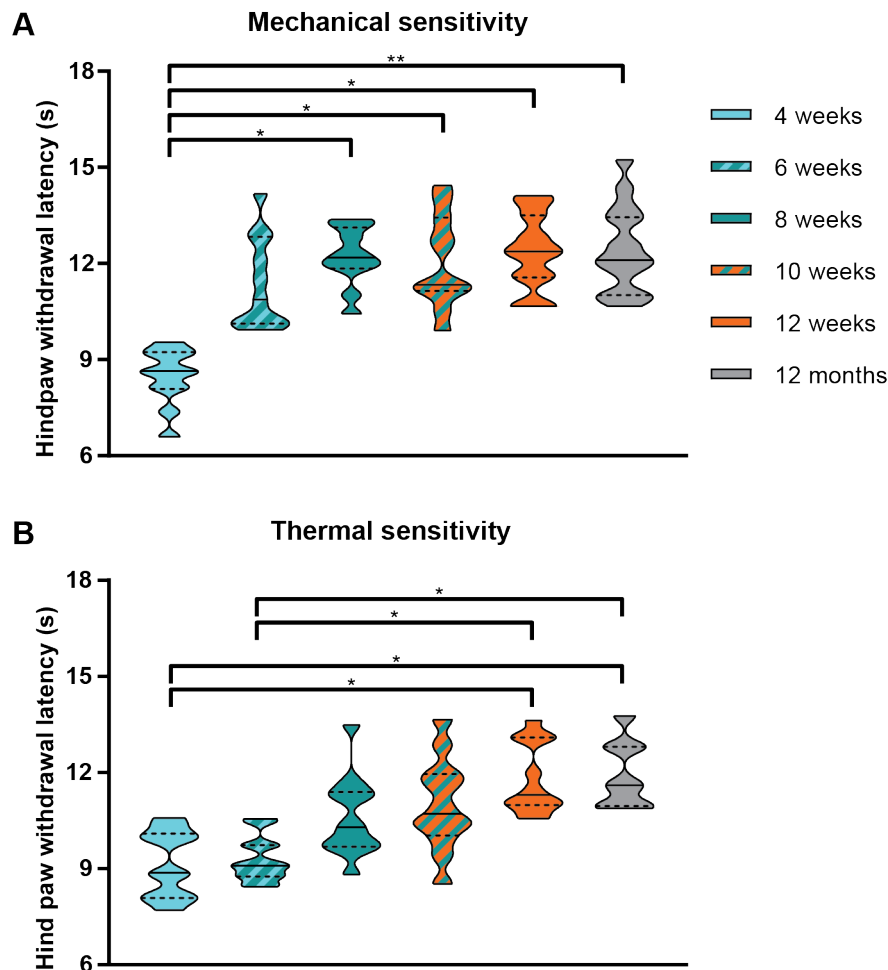


Figure 3.5: Hind paw sensitivity decreases with maturation

Twelve young and eight middle-aged male WT C57Bl/6J mice were tested using a Dynamic Plantar Aesthesiometer (A) and a Hargreaves Apparatus (B) on different days. Their hind paw withdrawal latencies to a ramping filament force (A) or a heat-inducing light ray (B) acting on the plantar surface are plotted in these violin plots: Areas represent frequency distributions of single trial outcomes between minimum and maximum, lines show the median, dashed lines mark the quartiles. * $p \leq 0.05$, ** $p \leq 0.01$, one-way ANOVA with Tukey's HSD test on grand means with pooled and weighted SEM of means per mouse and time point; no differences between paws, two-way ANOVA on grand means per paw and time point; differences between individual mice were neglected, since no outliers were detected, ROUT (Q = 1 %).

3.1.3.2 Hairy skin mechanosensitivity decreases with maturation

Finally, I aimed at examining hairy skin non-noxious mechanosensation, as Piezo2 was shown to be the main mechanotransducer in this modality as well (Ranade et al., 2014; Yamaguchi and Otsuguro, 2017). To that end, I adapted the tape response assay used by Ranade et al., (2014), as described under 2.4.1.2. In brief, young or middle-aged mice were acclimated in transparent plastic boxes until calm. Then, red 12.7 mm circular adhesives were taped to their superior-dorsal fur. Their behaviour was monitored closely until they managed to get the tape off, or until five minutes had passed.

Ranade et al., (2014) have shown that the total number of tape-directed bouts is vastly reduced in *Piezo2^{CKO}* mice. Here, in WT mice of different ages, this parameter is not significantly different, see figure 3.6E. However, by introducing time tracking of every single bout, significant differences in the tape response behaviour were found between the tested age groups. Juvenile mice at the age of four weeks were most sensitive to the attached tape, as they almost constantly tried to reach it and get it

3. RESULTS

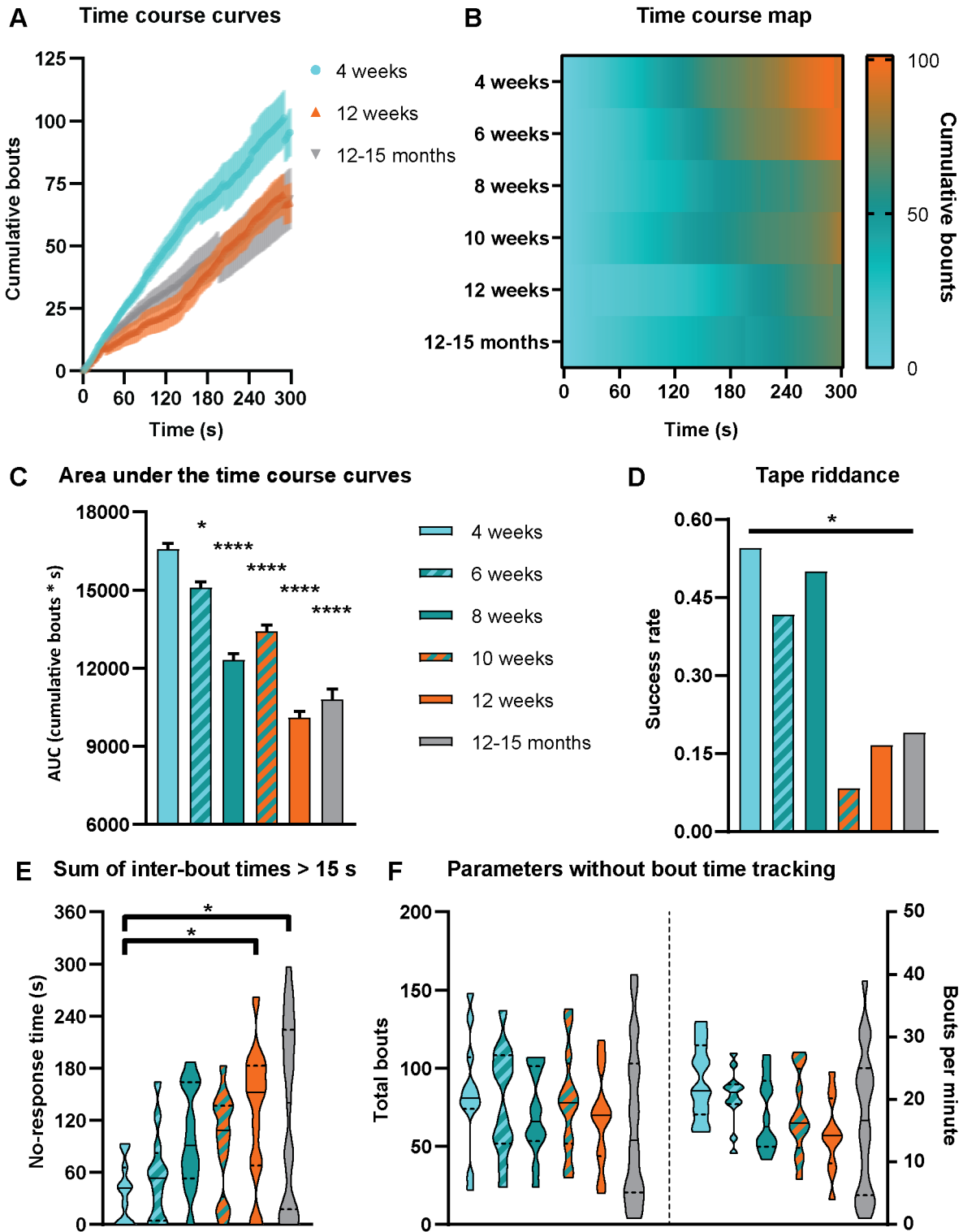


Figure 3.6: Hairy skin mechanosensitivity decreases with maturation

Twelve young and twelve middle-aged male WT C57Bl/6J mice were subjected to the tape response assay every two weeks: a 12.7 mm circular adhesive was affixed to their upper back and their behaviour was monitored for up to 5 min. A: XY plot of averaged time courses \pm SEM of tape-directed bouts of three key age groups, other age groups not shown here for clarity. B: Heat map of averaged bout time courses of all tested age groups, shown without SEM for clarity. C: Quantification of averaged bout time courses, error bars show SE; only significant differences to the 4 w group are indicated for clarity, no significant differences between 8 and 10 w, and 12 w and 12-15 months of age. D: Rate of mice that managed to get the tape off before the end of the 5 min trial time. E: Sums of times spent not responding to the tape for > 15 s. * $p \leq 0.05$, one-way ANOVA with Tukey's HSD test. F: Violin plots of total bout counts and total bouts per total trial time, lines indicate median and quartiles (dashed); note that there are no significant differences, one-way ANOVA.

off. This is represented by steep bout time course curves in figure 3.6A and B and large areas under these curves, figure 3.6C. As a consequence, they were also the most successful with detaching the tape before the trial time-out at five minutes, as depicted in figure 3.6D. Very much like the described decline in hind paw sensitivity (see 3.1.3.1) this decline in hairy skin mechanosensitivity was purely maturational, as there were no significant differences between adult twelve-week-old and middle-aged (12-15 months old) mice.

3.1.4 Summary of the descriptive part

The results shown so far agree that Piezo2 function decreases throughout maturation. This becomes evident, as not only the Piezo2-mediated currents in mouse DRG neurons decrease with particular specificity, but also Piezo2-mediated behaviours, such as light touch detection in glabrous and hairy skin, are declining between four and twelve weeks of age.

The following sections are dedicated to elucidating the mechanisms behind this maturational plasticity.

3. RESULTS

3.2 Exploring the plasticity

3.2.1 Piezo2 transcription

To explore possible changes in the transcription and expression of the mechanotransducer of interest, I performed qPCR experiments as described under 2.5.1. The results are summarised in figure 3.7. One might assume the distinct decline in Piezo2 function described above could arise from degressive expression in DRG neurons with age. Yet, the unchanged ratio of mechanosensitive neurons and RA responders across the observed age groups (figure 3.3C) suggests otherwise. Indeed, I found that expression of Piezo2 mRNA does not decrease between juvenile and middle-aged life phases (figure 3.7A), but it is worth noting that high intragroup variability impedes the confident detection of differences and trends in Piezo2 mRNA expression.

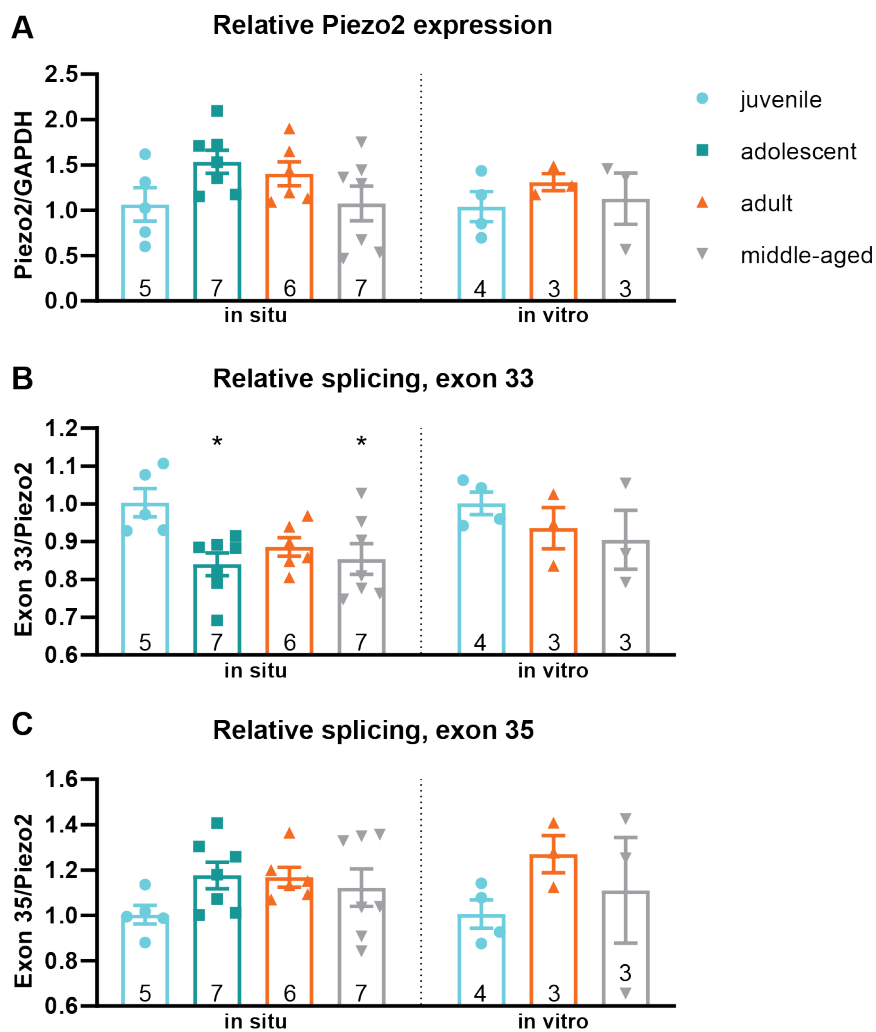


Figure 3.7: Whole DRG qPCR hints at age-dependent splicing

Purified RNA of acutely isolated DRGs (*in situ*) and cultured DRGs (DIV 1) was subjected to real-time quantitative PCR. A: Relative expression of Piezo2 (normalised to housekeeper GAPDH) compared to juvenile mice. Numbers indicate animal count. B, C: Expression of alternatively spliced Piezo2 exons 33 (B) and 35 (C) normalised to the constitutively expressed exon 25 calibrated to the juvenile group. Asterisks indicate significant differences to juvenile group. Bars show arithmetic mean \pm SEM.

A group of researchers around Alexander Chesler, Ph.D. (National Center for Complementary and Integrative Health, USA) and Mark Hoon, Ph.D. (National Institute of Dental and Craniofacial Research, USA) recently showed that multiple distinct Piezo2 isoforms are expressed in a tissue-specific manner. Especially in sensory neurons, the mechanotransducer undergoes extensive alternative splicing, yielding numerous variants with functional differences (Szczot et al., 2017). We hypothesised that age-dependent shifts in the Piezo2 isoform expression pattern of sensory neurons might contribute to the observed plasticity observed *in vitro* and *in vivo*, as described in the first part of this chapter. Therefore, I looked at the relative expression levels of mRNAs coding for Piezo2 exon 33 and the newly described exon 35, both of which were shown to be alternatively spliced. These two exons are both located close to the pore domain in a large intracellular C terminal loop (Coste et al., 2015; Ge et al., 2015; Szczot et al., 2017) and were shown to be implicated in regulating ion channel properties and function (Szczot et al., 2017). The authors reported that exon 35 influences the current inactivation kinetics, as Piezo2 variants containing the exon had two-fold faster inactivation rates than variants without it. In unison with constant inactivation time constants of Piezo2 currents across the studied age groups (figure 3.2E), relative expression levels of exon 35 mRNA were found to be unchanged with age (figure 3.7C).

Interestingly, the data show a maturational decrease in the mRNA expression of exon 33 in DRG cells, see figure 3.7B. Szczot et al., (2017) showed that the presence of this exon positively affects permeability for calcium. Calcium permeability is an influential factor for Piezo2 function, as the ion leads the selectivity sequence of this cation channel ($\text{Ca}^{2+} > \text{K}^+ > \text{Na}^+ > \text{Mg}^{2+}$; Coste et al., 2010). Strikingly, they found a profound decrease in the mechanical activation threshold in the presence of intracellular calcium in an exon 33-containing variant, which was absent in a variant lacking the exon. The maturational decrease in expression of exon 33 found here correlates with the increase of the activation threshold of Piezo2-mediated currents (see figure 3.2), as well as with the decrease in Piezo2-mediated somatosensory mechanosensitivity shown in section 3.1.3.

Unfortunately, the described findings are only partially reproduced in the data of cultured DRG, yet the low number of animals tested in these *in vitro* qPCRs does not allow high statistical confidence.

In summary, age-dependent splicing of Piezo2 mRNA and shifts in isoform expression patterns may very well contribute to the described decline in somatosensory mechanosensation. Yet, whole-cell DRG qPCR experiments lack the resolution to resolve changes of different classes of sensory neurons. The findings reported in this section can hardly be attributed to any specific sensory modality. To overcome this diffraction, we need to zoom in on the subclasses of DRG neurons.

3.2.2 Single-cell transcriptomics

So far, *in vitro* and *in situ* experiments to describe and scrutinise changes observed in Piezo2-mediated functions within the scope of this thesis were carried out on whole DRGs. Yet, as described in the introduction (section 1.1), these ganglia hold the somata of many, very different subclasses of sensory neurons as well as other cell types. Usoskin et al., (2015) have demonstrated in a comprehensive way that these subclasses vary not only in their function, but in their molecular fingerprint also. In their oft-cited study, they performed single-cell RNA sequencing on hundreds of sensory neurons from mouse lumbar DRGs and determined distinct clusters of eleven subtypes of neuronal cells by their RNA expression profiles (see also figure 1.3).

3. RESULTS

In order to narrow down the sensory types involved in the modalities of somatic sensation subject to this project, we decided to make use of the combination of electrophysiological and transcriptomic characterisation of single DRG neurons. We hope that by accessing the identificational power of this combination we can dissect and pinpoint maturational alterations of RNA expression profiles underlying the observed and described changes in Piezo2 function and somatosensation.

The patch-clamp method central to this project is of advantage in this endeavour. In current-clamp-mode with standard, physiological ionic conditions, recordings of evoked action potentials can be used to distinguish mechanoreceptors from nociceptors (Poole et al., 2014), see 2.3.4 and next section. In voltage clamp mode, mechano-clamp can be used to probe mechanoresponsiveness of sensory neurons, quantify MA currents and identify the low-threshold RA-MA population. Finally, the method allows for targeted harvesting of single somata, see 2.5.2. The isolated RNAs of those can be sequenced, and the turnout of transcriptomic analyses can be directly correlated to the documented electrophysiological profile and the soma size of the respective neuron, as well as to the age of the respective mouse (Sucher and Deitcher, 1995; Sucher et al., 2000; Fuzik et al., 2016; Cadwell et al., 2017b). Bringing together this amount and depth of information was hoped to grant us mechanistic insight into the age-dependent plasticity of Piezo2-mediated somatosensory mechanosensation.

3.2.2.1 Electrophysiological characterisation of single-cell samples

As described in section 2.3.4, the shape of action potentials of mouse DRG neurons recorded in whole-cell current-clamp experiments can be used to distinguish mechanoreceptors from nociceptors (Lechner et al., 2009; Poole et al., 2014; Wetzel et al., 2017). Taking into account the molecular marker profiles of single neurons as acquired by RNA-seq (see 3.2.2.2), I adapted the classification scheme described by Poole et al., (2014) with the slight change of setting the critical FWHM value from 0.7 to 0.8 ms. The detailed decision tree is depicted in figure 3.8. In short, narrow APs with a FWHM shorter than 0.8 ms lacking a bump in the falling phase were reliably confirmed to belong to the mechanoreceptor subclasses. Broad APs with a bump reliably turned out to show marker profiles of nociceptors indeed. The classes of spikes with mixed or ambiguous parameters could not be consistently predicted by electrophysiology and the respective neurons were excluded from the dataset underlying the figures 3.9 and 3.10.

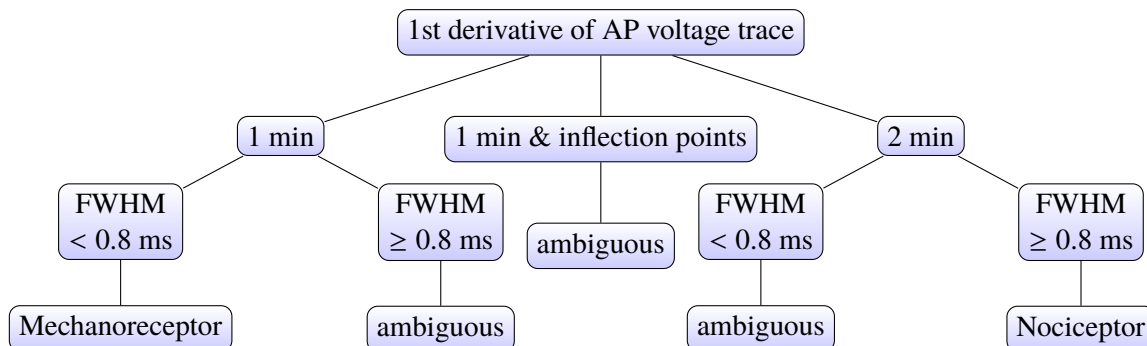


Figure 3.8: Detailed current-clamp-based classification of sensory neurons

Recordings of evoked action potentials (AP) are analysed to classify sensory neurons as mechanoreceptors or nociceptors. min = minimum/minima in $\frac{\Delta V}{\Delta T}$ of voltage recording in the falling phase of an AP; FWHM = full width at half maximum of evoked spike in voltage trace.

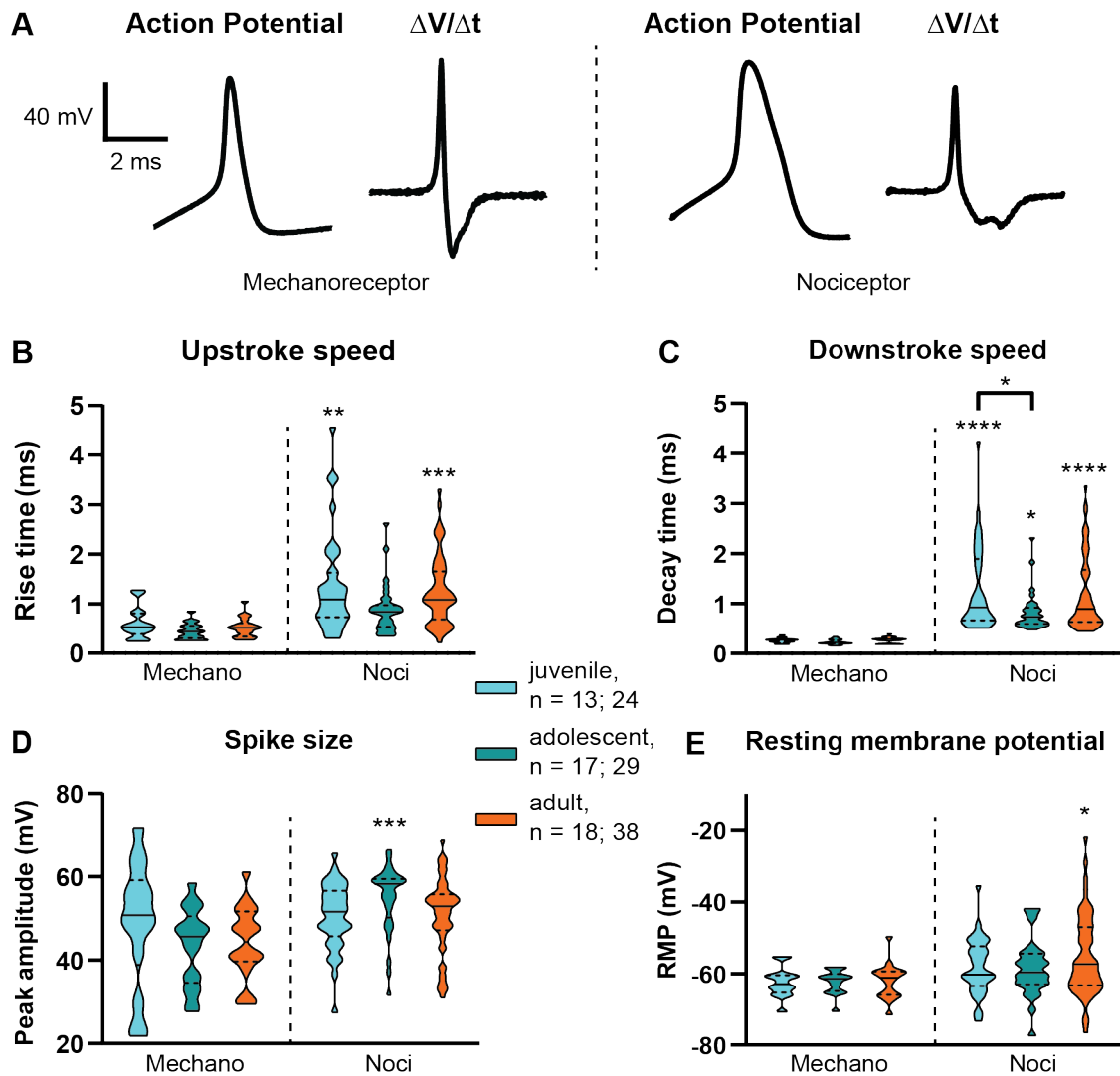


Figure 3.9: Action potential categorisation in DRG neurons

A: Representative whole-cell voltage recordings of action potentials from cultured DRG neurons and their first derivative. Spikes of sensory neurons differ in their duration and shape. Spikes of nociceptors show a hump in the falling phase and two minima in the first derivative. Numbers indicate number of studied mechanoreceptors and nociceptors, respectively. Shown parameters are the rise times from 20 to 90 % of the peak (B), decay times (63.2 % of peak, C), peak voltages (D) and resting membrane potentials (E). Asterisks indicate differences between mechanoreceptors (mechano) and nociceptors (noci) of the same age group, unless indicated otherwise; * $p \leq 0.05$, ** $p \leq 0.01$, *** $p \leq 0.001$, **** $p \leq 0.0001$, two-way ANOVA with Tukey's HSD test; lines mark median and quartiles (dashed). Despite a slight difference in the decay time between juvenile and adolescent nociceptors, no age differences were found. $N_{juvenile} = 12$, $N_{adolescent} = 6$, $N_{adult} = 14$.

Mechanoreceptors and nociceptors show different action potentials To electrophysiologically characterise cultured DRG neurons of male WT mice of different ages, whole-cell patch-clamp experiments were conducted with KCl-based pipette solution. By injecting increasing amounts of current in current-clamp-mode, evoked action potentials were recorded, categorised according to their shape as described above and compared quantitatively. Example traces of APs of the two distinguishable sensory neuron subtypes and their first derivatives are depicted in figure 3.9A. As expected and described before (Lechner et al., 2009; Poole et al., 2014; Wetzel et al., 2017), the spikes of the two types varied greatly in speed, as evident in the significant differences in rise and decay times, see figure 3.9B and C.

3. RESULTS

Additionally, nociceptors produced APs of slightly greater peak amplitude and their resting membrane potentials were slightly less polarised, see figure 3.9D and E, respectively. All these differences have been described in DRG neurons of multiple species, such as cats (Koerber et al., 1988), guinea-pigs (Djoughri et al., 1998; Djoughri and Lawson, 2001), rats (Fang et al., 2005; Viatchenko-Karpinski and Gu, 2016) and mice (Lechner et al., 2009; Poole et al., 2014; Wetzell et al., 2017). I therefore assume that these different characteristics are rather conserved hallmarks of sensory neuron types and essential to their function as such. Ergo, it is neither surprising nor conflicting that no age differences were found for these parameters.

Mechanoreceptors and nociceptors show differences in MA currents The same cells subjected to current-clamp before were mechanically stimulated in voltage clamp mode. This mechano-clamping was done in the same way as shown in the beginning of this chapter (see 3.1.1), the only difference being the ionic recording conditions; see table 2.1. In particular, the internal solution used here is potassium- rather than caesium-based. This leads to inwardly-rectifying potassium channels (e.g. $K_{ir}2.1$, Abrams et al., 1996) and cyclic nucleotide-regulated channels (Stieber et al., 2005) not being blocked by internal Cs^+ ions. More importantly, additional MA currents showed up in the recorded traces and interfered with the recordings of the MA currents of interest. Summation, subtraction and kinetic mismatch (see figure 3.10B) of the different currents distort the electrophysiology described in CsCl-based solution. In particular, currents resembling $I_{K_{mech}}$ (carried by Kv1.1-Kv1.2 heteromers, Hao et al., 2013, see also transcription of *Kcna1* and *2* genes in figure 3.12), as depicted in figure 3.10A, make for different amplitudes and inactivation times of the RA-MA currents of interest. Consequently, the age-dependent decrease in Piezo2 function observed with CsCl-based internal solution could not be reproduced in these experiments, see section 4.1.1.1.

Nevertheless, differences in the MA currents of mechanoreceptors and nociceptors were found. Neurons displaying narrow APs without a bump in the falling phase were slightly more likely to produce bigger RA-MA current amplitudes (figure 3.10D). However, the displacement thresholds were not found to differ between the sensory types, see figure 3.10E. While the observed inactivation kinetics of RA-MA currents were faster than those observed with CsCl-based internal solution (Poole et al., 2014), nociceptors showed slightly longer inactivation times, see figure 3.10F. Another difference to the electrophysiology of DRG neurons described in section 3.1 is that little to no IA- and SA-MA currents were observed, possibly as a result of the kinetic mismatch of overlaying MA currents described above. Still, a clear difference in the fraction of generally mechanosensitive neurons (RA-, IA- and SA-MA responders) versus weakly or non-responsive neurons (WRs and NRs) was found: cultured nociceptors are predominantly insensitive to mechanical stimulation of their soma, see figure 3.10G. All these observations have been described by others before (Viatchenko-Karpinski and Gu, 2016), except for the slight difference in τ . Though, Poole et al., (2014) had shown a slower channel gating latency in nociceptors versus mechanoreceptors similar to the difference described here.

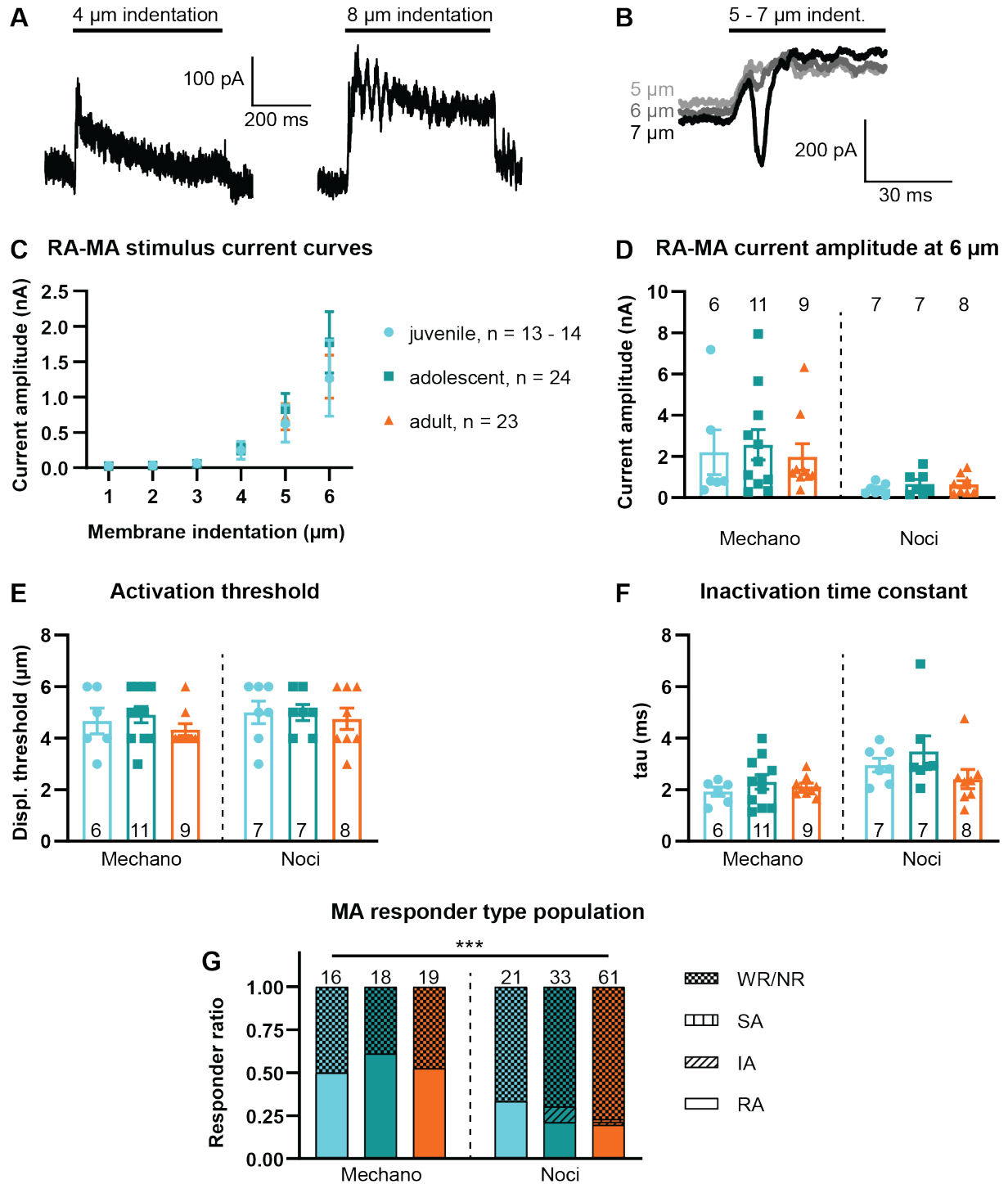


Figure 3.10: Mechano-clamp characterisation of sensory neuron subtypes

A: Representative whole-cell MA current traces at -70 mV holding potential, presumably showing $I_{K_{mech}}$. B: Interference of different MA currents. C: No difference in averaged RA-MA current amplitudes, two-way ANOVA. D: Nociceptors show lower maximal RA-MA amplitudes, $p = 0.0024$, two-way ANOVA, no differences between individual groups found by Tukey's HSD test. E: No difference in displacement thresholds. F: Nociceptors show slightly longer inactivation times, $p = 0.0043$, two-way ANOVA, no differences between individual groups found by Tukey's HSD test. G: Nociceptors show a lower share of mechanosensitive neurons, $*** p \leq 0.001$, χ^2 test with cell numbers of mechanosensitive cells irrespective of inactivation type versus WR/NRs. $N_{juvenile} = 12$, $N_{adolescent} = 6$, $N_{adult} = 14$.

3. RESULTS

3.2.2.2 RNA sequencing of single-cell samples

After characterising cultured DRG neurons by means of patch-clamp, many of those cells could be aspirated into the patch pipette using the so-termed OBST technique, see section 2.5.2. Since aspiration of the cytosol in whole-cell-mode did not yield reliable mRNA amplification in pilot single-cell qPCRs (not shown) and DRG somata are particularly big and well attached, the pipette was detached from the cell after recording and carefully broken to widen the opening while applying positive pressure to avoid aspiration of unwanted extracellular solution. Then, processes and other attached cells were severed and cleared away with the help of the stimulation probe, while the soma was aspirated or pulled out of the bath using suction. Swiftly, it was transferred into cool lysis buffer and stored at -80 °C until isolation of RNA shortly before cDNA synthesis and library preparation. Purified RNA of 74 single-cells was sent for sequencing in three batches:

1. 16 juvenile and adult NR nociceptors
2. 20 juvenile and adult RA-MA mechanoreceptors
3. 38 juvenile and adult mixed samples, including ambiguous types (see figure 3.8)

Unfortunately, the important second dataset is not shown in this thesis as its processing was not completed in time. The other two datasets were checked for quality and the sequences were aligned to the reference genome *Mus musculus* (mm10 version 84, https://www.ensembl.org/Mus_musculus/Info/Index). Mapped reads were normalised for library size (counts per million mapped reads, cpm) and gene length (reads per kilobase of transcript, per million mapped reads, RPKM). Differential gene expression (DGE) analysis was performed on the raw data using the R package edgeR (Robinson et al., 2010), results ($p < 0.05$) were filtered for $\log_2(\text{fold change})$ and false discovery rate ($|\log_{2}FC| > 1.5$ and $FDR < 0.05$).

scRNA-seq of non-responder nociceptors identifies heat sensors A subset of the first batch of NR nociceptors showed high expression levels of mRNA transcribed from the *Tac1* (tachykinin 1 or substance P) gene, see figure 3.11. Usoskin et al., (2015) reported that transcription of this gene marks thermosensitive (cold and heat) neurons. Since these samples showed transcription of the well-studied heat sensor *Trpv1* (Caterina et al., 1997) and virtually no transcription of the cold sensor *Trpm8* (McKemy et al., 2002; Peier et al., 2002), it was safe to assume that these samples stemmed from heat sensitive neurons. Also, these NR nociceptors showed few to no reads mapping to the *Piezo2* gene, which correlated with them being mechanoinensitive. DGE analysis within this subset, comparing juvenile to adult samples, showed several regulated genes. Yet, I found the explanatory power of this list of differentially expressed (DE) genes limited with regard to the decline in hind paw thermosensitivity shown in figure 3.5B, which will be discussed in section 4.1.4. Interestingly, though, one DE gene slightly upregulated in juvenile NR nociceptors was also found to be maturationally regulated in RA-MA samples, but the other way around (see figure 3.12).

scRNA-seq confirms AP categorisation For the third batch of mixed samples, we first compared the mapped reads of three mechanoreceptors and nine nociceptors in the adult group that were unambiguously categorised by the shape of their AP (broad and with bump in the falling phase). The DGE analysis validated a clear upregulation of known nociceptor marker mRNAs in these single-cell

samples. Namely, only the samples electrophysiologically (prospectively) categorised as nociceptors showed elevated transcription of

- calcitonin-related polypeptide alpha (*Calca*, logFC = 8.9, FDR = $6 * 10^{-10}$), classical marker of peptidergic nociceptors (McCoy et al., 2012; Usoskin et al., 2015), alias Cgrp
- neurotrophic tyrosine kinase receptor type 1 (*Ntrk1*, logFC = 8.1, FDR = $9 * 10^{-5}$), crucial player in development of nociceptors and marker of peptidergic nociceptors (Marmigère and Ernfor, 2007; Usoskin et al., 2015), alias tropomyosin-related kinase A, Trka
- voltage-gated sodium channel type X alpha (*Scn10a*, logFC = 5.4, FDR = 0.007), eminent role in human pain disorders (Dib-Hajj et al., 2017; Usoskin et al., 2015), alias Nav1.8

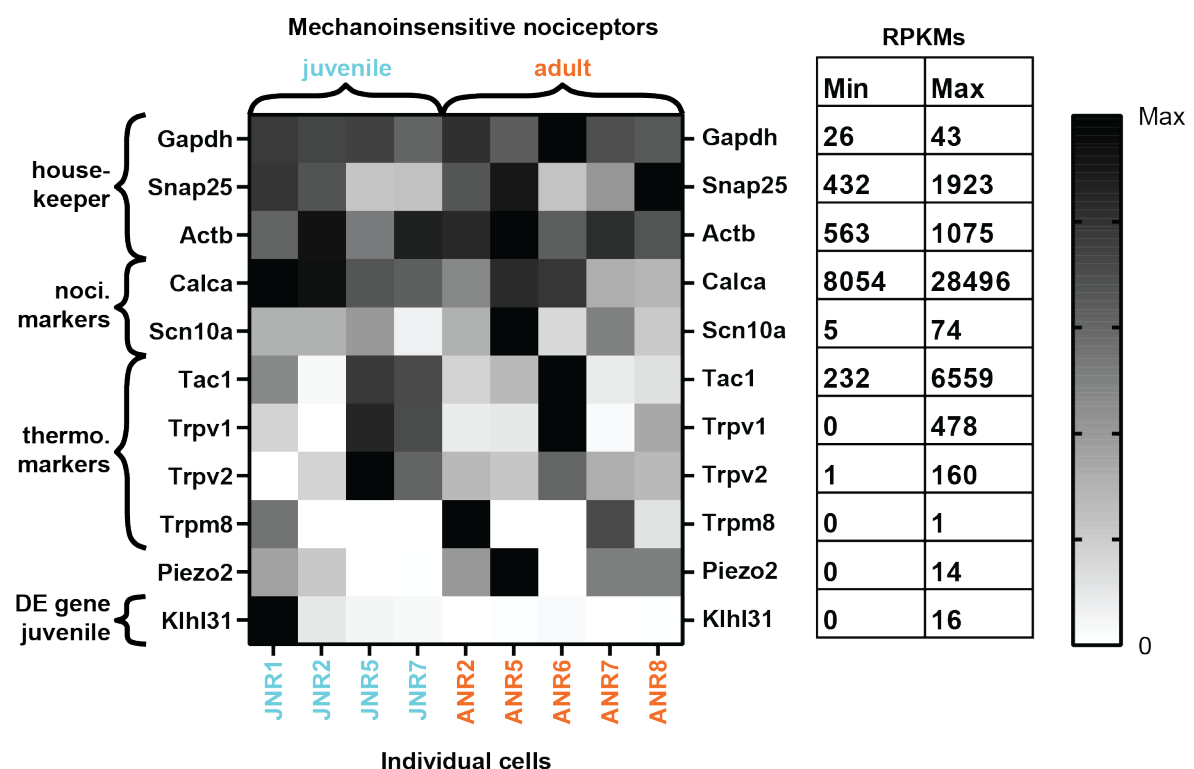


Figure 3.11: Patch-seq of single mechanosensitive sensory DRG neurons

Heatmap of reads per kilobase of transcript, per million mapped reads (RPKM) of selected genes of $n = 9$ electrophysiologically characterised single-cells acquired on a HiSeq4000 with Nextera library preparation ($N_{juvenile} = 4$, $N_{adult} = 4$). Minimum and maximum numerical RPKM values are depicted in the table next to the gene name. Note that the colour code applies to the maximum RPKM per row and gene. Individual NR DRG nociceptors of juvenile and adult WT mice are organised from left to right, no cell showed MA currents following mechanical stimulation of the soma with up to 11 μm membrane indentation. The sensory type of cells was determined by the shape of evoked action potentials and affirmed by elevated mRNA expression of the genes *Calca* and *Scn10a*. All cells presented here show high reads of the genes *Tac1*, *Trpv1* and *Trpv2*, marking them as putative heat sensitive thermoreceptors (thermo.). *Klhl31* is differentially expressed (DE) in juvenile NR nociceptors, $\log_2(\text{fold change}) = 5.1$, $p = 3 * 10^{-5}$, false discovery rate = 0.0098, as calculated using the R package edgeR.

As this mixed sequencing batch contained samples that could not be unmistakably categorised prospectively given the tight AP criteria described in figure 3.8, the sensory type of such samples can be determined retrospectively. Single-cell libraries of ambiguous AP type that showed elevated read counts for both *Calca* and *Scn10a* were categorised as nociceptors, samples with little to no reads of

3. RESULTS

both markers were taken for mechanoreceptors. In this way, differential gene expression analysis was performed again on eight mechanoreceptors and eleven nociceptors, revealing 88 significantly regulated genes.

Besides the already mentioned $Na_V1.8$, there are many regulated mRNAs of ion channels and channel regulators in the lineup. For example, the cluster of *Kcna4*, *Kcna6*, *Kcnn1*, *Kcnp1* and *Kcnmb1* is upregulated in nociceptors, as well as the voltage-gated calcium channel subunits *Cacna1c*, *Cacna1e* and *Cacna2d1*. Such differentially transcribed genes can help explaining the differences seen in patch-clamp experiments, like AP shape and duration and the varying resting membrane potentials observed in nociceptive DRG neurons (figure 3.9). The notion that regulation of membrane excitability and permeability is a hallmark difference between the two sensory neuron types compared here is reflected by functional annotation using Gene Ontology (GO, a major bioinformatic knowledge database). Table 3.1 shows the most significantly enriched GO terms associated to the upregulated genes in nociceptors, as calculated using the topGO R package (Alexa and Rahnenfuhrer, 2018. topGO: Enrichment Analysis for Gene Ontology. R package version 2.35.0.). Many of the other enriched terms listed below confirm the validity of our retrospective categorisation of single sensory neuron samples.

Table 3.1: Gene Ontology annotation verifies categorisation of nociceptors

Listing of the most significantly enriched Gene Ontology terms associated to the genes upregulated in nociceptors versus mechanoreceptors, as revealed by patch-seq of 19 cultured DRG neurons of seven adult WT mice and subsequent differential gene expression analysis using the R package edgeR. Annotated = number of genes annotated to a GO term in the entire background set; Significant = number of genes upregulated in nociceptors and annotated to that GO term. Enrichment analysis and Fisher's statistics done using the topGO R package.

GO.ID	Term	Annotated	Significant	Expected p-value	Fisher's p-value
GO:0034765	regulation of ion transmembrane transport	459	11	1.24	2.1e-07
GO:0001662	behavioral fear response	51	4	0.14	1.1e-05
GO:0045019	negative regulation of nitric oxide biosynthetic process	17	3	0.05	1.2e-05
GO:0050965	detection of temperature stimulus involved in sensory perception of pain	18	3	0.05	1.5e-05
GO:0048266	behavioral response to pain	24	3	0.06	3.6e-05
GO:0006954	inflammatory response	655	9	1.77	7.4e-05

Amongst the genes upregulated in samples categorised as mechanoreceptors was *Calb1* (calbindin 1) that was reported to mark mechanoreceptors (Usoskin et al., 2015). Together with high expression levels of *Ret*, *Ntrk2* and *Ntrk3*, low-threshold mechanoreceptors could be identified within the *Calb1*⁺ population (Usoskin et al., 2015; Li et al., 2018), see figure 3.12.

After all, our small-sample mechano-clamp characterisation patch-seq approach aims at revealing maturational differences in low-threshold mechanoreceptors displaying RA-MA currents and non-nociceptive APs. It is this population of cells that is most likely implicated in the Piezo2-mediated behaviours I showed to be affected by maturation in the first part of this chapter.

scRNA-seq of RA-MA sensory neurons unveils maturationally regulated genes Finally, we compared juvenile and adult DRG neuron samples that displayed a distinct MA current type. Table 3.2 shows all genes that were found to be differentially regulated in RA-MA mechanoreceptors, RA-MA nociceptors and mechanoinensitive NR nociceptors. Figure 3.12 summarises the comparison between RA-MA cells of the different types and ages. In the few cells tested and shown here, there is a trend for higher maximal RA-MA amplitudes in mechanoreceptors, resembling the findings in the harvesting

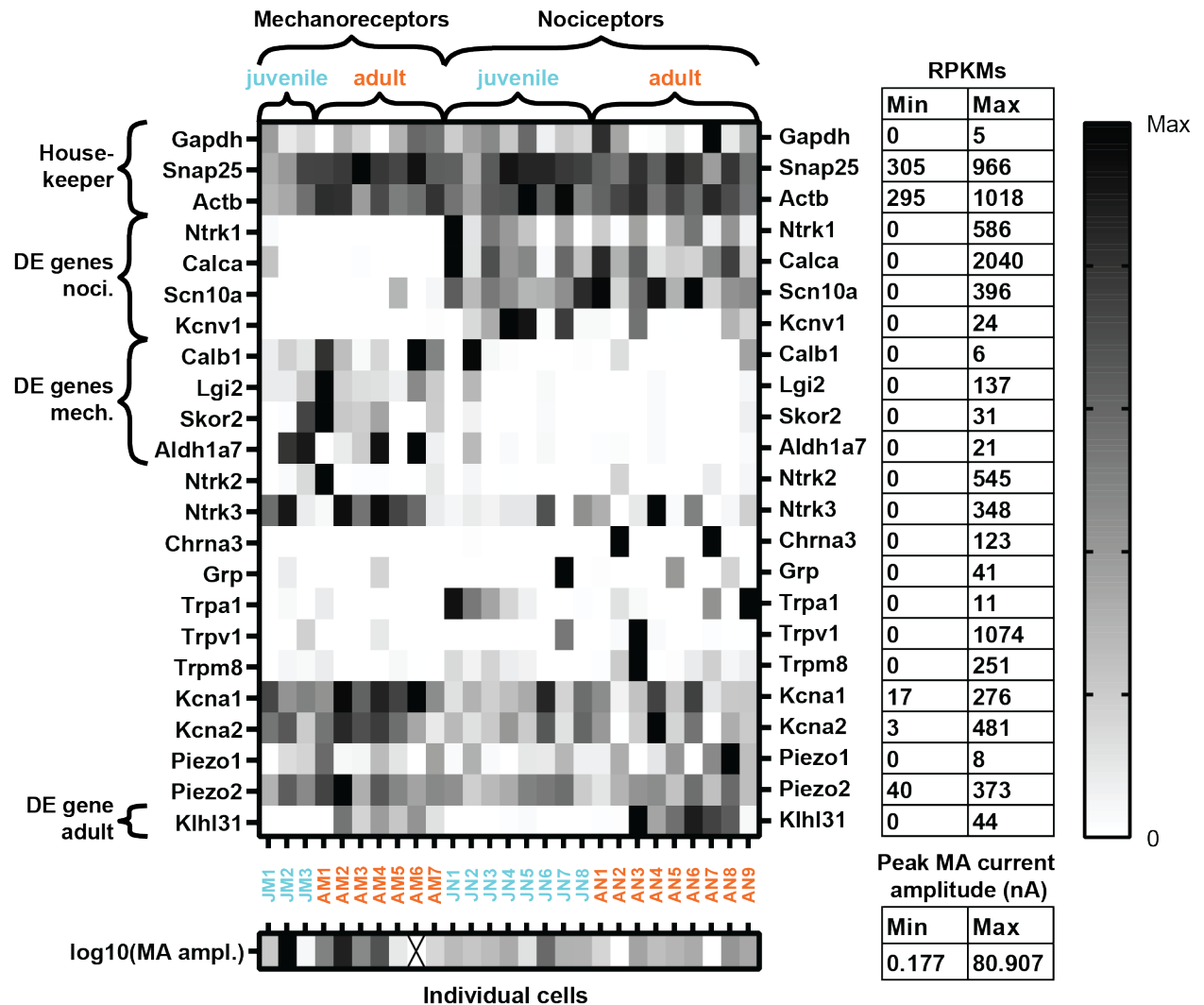


Figure 3.12: Patch-seq of single mechanosensitive sensory DRG neurons

Heatmap of reads per kilobase of transcript, per million mapped reads (RPKM) of $n = 27$ electrophysiologically characterised single-cells acquired on a HiSeq4000 with Nextera library preparation ($N_{juvenile} = 7$, $N_{adult} = 5$). Minimum and maximum numerical RPKM values are depicted in the table next to the gene name. Note that the colour code applies to the maximum RPKM per row and gene. Individual mechanosensitive DRG neurons of juvenile and adult WT mice are organised from left to right, all cells were mechanosensitive (WR or RA-MA). The sensory type of cells was determined by the shape of evoked action potentials; few electrophysiologically ambiguous cells were categorised according to their RPKMs for *Calca* and *Scn10a* (JM2, AM1-3, JN2, AN9). Shown transcribed genes from top to bottom are chosen as follows: Housekeeping genes, differentially expressed (DE) genes in nociceptors and mechanoreceptors, genes of importance to the somatosensory system, Piezo family and a differentially expressed gene as revealed by age group statistics performed with edgeR (significant both for nociceptors and mechanoreceptors). All shown DE genes with $\log_2(\text{fold change}) > 3$ and false discovery rate < 0.02 . Minimum and maximum numerical RPKM values are depicted in the table next to the gene name. Bottom row shows maximal whole-cell MA current amplitude of the cultured neurons following mechanical stimulation of the soma with up to 11 μm membrane indentation; colour coded values are log-transformed to represent the wide numerical range. Cell AM6 could only qualitatively be identified as RA-MA responder.

phase (fig. 3.10). Notably, the maximal MA amplitude measured in mechano-clamp experiments correlated only weakly with the number of reads mapping to the *Piezo2* gene. Some of the strongest RA-MA responders also show high reads of *Piezo2* (see cells JM2, AM2, and AM4 in fig. 3.12), but the opposite is not true. For example, the two adult WR nociceptors AN2 and AN7 displayed the

3. RESULTS

lowest MA amplitude, but not the lowest read count of mRNA of the mechanotransducer. Instead, they show the highest numbers of reads mapping to *Chrna3*. Prato et al., (2017) recently showed that silent nociceptors express the nicotinic acetylcholine receptor subunit alpha-3 encoded by this gene. They demonstrated that nerve growth factor signaling can "un-silence" these neurons to become increasingly mechanosensitive by means of Piezo2-mediated currents. AN2 and AN7 being putative silent nociceptors, slightly un-silenced by nerve growth factor in the culturing medium, could explain them showing weak MA currents, average *Piezo2* and high *Chrna3* transcription. Samples like these show, how the link between mRNA expression and protein-mediated function or phenotype is rather complex than direct.

The RA-MA nociceptor samples JN7 and AN5 showed the highest read count of *Grp*, gastrin releasing peptide, as well as of *Htr2a* encoding the serotonin receptor 2 A, which renders them putative itch sensors or pruritoceptors (Usoskin et al., 2015; Li et al., 2018), all the while being mechanosensitive. The notion that sensory neurons can be polymodal is not new and has been proven before, especially for nociceptors (Li et al., 2016; Li et al., 2018). The adult nociceptor sample AN3 exhibited robust RA-MA currents and showed the highest reads for both the heat sensor *Tprv1* (Caterina et al., 1997) and the cold sensor *Trpm8* (McKemy et al., 2002; Peier et al., 2002), implying this neuron may have been sensitive to at least three different modes.

Strikingly, we found one gene to be significantly regulated in all three age-wise comparisons: *Klhl31*, kelch-like 31. The reads mapping to mRNA transcribed from this gene were found to be elevated in (both mechanoreceptors and nociceptors) adult RA-MA cells and virtually absent from juvenile RA-MA neurons (see bottom row of figure 3.12 and top part of table 3.2). Conversely, transcription of this gene was virtually absent in adult mechanoinensitive NR cells, while juvenile equivalents showed detectable expression levels of the *Klhl31* mRNA (see bottom row of figure 3.11 and lower part of table 3.2).

This gene belongs to the Kelch superfamily, a large and functionally diverse group, all members of which contain an evolutionarily conserved carboxy-terminal Kelch repeat domain (Canning et al., 2013; Dhanoa et al., 2013; Papizan et al., 2017). Some Kelch-like proteins may stabilise substrates (Garg et al., 2014), while many act as substrate-specific adaptors for cullin 3-mediated ubiquitination and substrate degradation (Pintard et al., 2004; Canning et al., 2013; Papizan et al., 2017). Kelch-like protein 31 was reported to attenuate β -catenin-dependent Wnt signaling (Abou-Elhamd et al., 2015), though this was not confirmed in a recent *Klhl31*-KO mouse (Papizan et al., 2017). Instead, Papizan et al., (2017) showed that kelch-like protein 31 interacts with cullin 3 and promotes the degradation of filamin C and possibly other substrates.

Hypothetically, Kelch-like protein 31 could promote the degradation of a Piezo2 regulator, or of the mechanotransducer itself, resulting in decreased Piezo2-mediated function and behaviour in adult mice, where *Klhl31* is expressed, without changing the level of *Piezo2* transcription, as seen in qPCR and patch-seq. For one, *Cul3* mRNA (coding for cullin 3) was present in all tested RA-MA cells (44.29 ± 2.7 RPKM).

3.2.3 Summary of the mechanistic part

In the first part of this chapter I have shown that Piezo2-mediated somatosensory function is decreasing throughout the maturation of male WT C57Bl/6 mice both *in vitro* and *in vivo*. In the second part, I

Table 3.2: Age-dependently differentially transcribed genes in electrophysiologically defined sensory neuron subtypes

Listing of differential gene expression analysis statistics and RPKM values of $n = 40$ electrophysiologically characterised single-cells acquired on a HiSeq4000 with Nextera library preparation ($N_{juvenile} = 8, N_{adult} = 9$). Statistics were calculated using edgeR. $\logFC = \log_2(\text{fold change})$; $\logCPM = \log_2(\text{counts per million})$; LR = likelihood ratio; FDR = false discovery rate

GeneID	Juvenile RA-MA Mechanoreceptors										Adult RA-MA Mechanoreceptors														
	logFC	logCPM	LR	PValue	FDR	JM1	JM2	JM3	JN1	JN2	JN3	JN4	JN5	JN6	JN7	JN8	AN1	AN2	AN3	AN4	AN5	AN6	AN7	AN8	AN9
9130019022Rik	6.8	2.3	19.2	1.20E-05	0.04428	2.72	3.24	0.9	0	0	0	0	0	0	0	0	0	0	0	0	0	0	0	0	0
Ptger4	4.9	4.8	22.0	2.80E-06	0.018099	42.73	2.5	6.28	0.55	0	1.84	0	1.38	0	1.38	0	0.99	0	0	0	0	0	0	0	0.99
Klhl31	-6.5	5.7	23.7	1.13E-06	0.016556	0	0.24	0	0.16	24.16	7.5	16.98	9.8	18.76	5.39										
<i>Piezo2</i>						112.87	238.12	173.03	275.54	373.42	119.20	244.46	179.12	134.07	175.28										

GeneID	Juvenile NR Nociceptors										Adult NR Nociceptors														
	logFC	logCPM	LR	PValue	FDR	JNR1	JNR2	JNR3	JNR4	JNR5	JNR6	JNR7	JNR8	ANR1	ANR2	ANR3	ANR4	ANR5	ANR6	ANR7	ANR8	ANR9			
Lipe	4.9	10.3	25.2	5.13E-07	0.001594	2347.06	274.2	180.16	99.53	51.74	108.46			13.48	5.29	44.49	29.34	52.17	9.37	15.3					
Klhl31	4.2	3.8	15.9	6.83E-05	0.038589	14.45	1.39	1.28	0.74	0.34	0.54			0.14	0.05	0.61	0.24	0.42	0.06	0.13					
Gm20644	4.0	2.0	15.7	7.56E-05	0.040866	6.22	0.81	5.71	1.72	1.61	4.65			0.06	0.01	0.62	0.56	0.32	0.08	0.11					
mt-Tf	2.4	5.2	17.8	2.41E-05	0.017664	1865.82	460.92	914.75	284.53	596.84	529.96			93.84	128.63	154.26	116.76	330.79	223.06	221.31					
Mbp	-3.2	5.4	17.1	3.50E-05	0.023182	2.64	1.38	1.52	0.03	2.03	0.46			13.76	9.73	3.74	8.27	23.43	29.98	20.44					
Sdc4	-4.2	6.0	16.9	3.92E-05	0.023182	1.15	4.73	2.6	1.98	2.06	2.28			23.14	53.04	0.35	0.31	27.11	199.56	60.4					
Sparc	-5.3	8.3	17.0	3.66E-05	0.023182	9.87	11.33	4.71	0	3.57	6.42			711.92	167.79	2.49	1.42	333.68	579.48	271.2					
Angptl4	-5.5	4.5	21.3	3.84E-06	0.00436	0.15	0.11	0	0.94	0.12	0.51			14.88	19.25	0.05	1.66	7.71	49.99	8.11					
Igf1p4	-5.5	3.1	23.4	1.32E-06	0.00234	0.23	0.1	0	0.04	0.01	0.11			7.32	3.8	0.07	4.51	1.8	7.84	4.84					
2610307P16Rik	-5.6	2.1	23.8	1.08E-06	0.00234	0.35	0.03	0	0.29	0	0.06			15.7	7.4	2.23	5.96	2.18	8.01	2.47					
Tmem173	-5.6	4.7	21.8	3.02E-06	0.00436	0.19	0.22	0	0.02	1.48	0.39			21.94	24.03	0.12	52.85	11.63	35.14	4.91					
Mmp14	-5.8	4.8	21.3	3.86E-06	0.00436	0.06	1.45	0	0	0.05	0.5			15.94	9.39	20.6	0.74	13.69	57.15	27.32					
S100a16	-5.8	7.7	17.0	3.73E-05	0.023182	11.78	6.7	9.24	0.09	0	2.02			883.82	279.58	794.52	1.5	36.75	219.06	156.21					
Ndp	-6.0	4.1	20.1	7.16E-06	0.006849	0.85	0.08	0	0	0.23	0.08			62.41	18.52	8.8	6.57	0.2	17.08	8.94					
Ednrb	-6.1	5.7	18.9	1.37E-05	0.011448	0.54	0.11	0	0	0.4	0.65			28.84	14.7	0.21	0.15	48.74	52.02	24.65					
Gpm6b	-6.2	5.9	21.7	3.23E-06	0.00436	0.1	0.11	0	0.82	0.04	1.02			6.63	21.48	1.4	0.19	5.84	95.91	51.91					
Mxra8	-6.2	4.8	15.5	8.17E-05	0.042314	0.68	0.17	0	0	0.09	2.67			42.28	37.04	0.13	0.21	23.28	216.9	35.97					
Prdm5	-6.4	1.2	28.5	9.37E-08	0.000583	0.07	0	0	0	0.03	0.04			1.94	1.56	0.07	2.49	1.96	3.17	2.49					
Selenop	-6.6	4.2	18.3	1.85E-05	0.01434	1.55	0.2	0	0	0.04	0.53			66.47	27.4	0.19	0.4	33.83	98.69	113.56					
Parp14	-6.7	1.2	25.7	4.00E-07	0.001594	0.02	0	0	0	0	0.01			0.54	0.41	0.02	0.47	0.14	1.4	1.29					
Serpine2	-6.8	5.5	23.6	1.18E-06	0.00234	0.47	0.14	0	0	0.2	1.03			37.32	36.94	0.64	0.24	29.19	120.25	60.9					
Hmgcs2	-6.8	5.1	18.9	1.38E-05	0.011448	0.06	0.21	0	0	0.01	1.03			4.42	29.11	0.39	0.24	9.7	117.39	28.06					
Fat3	-7.0	1.8	20.5	6.08E-06	0.006297	0	0	0	0	0.01	0.04			0.99	0.32	1.02	2.47	0	1.34	1.45					
Bbs10	-10.6	1.9	45.6	1.48E-11	1.84E-07	0	0	0	0	0	0			0.64	2.01	2.1	7.99	1.2	1.88	0.67					
<i>Piezo2</i>						5.81	3.43	6.20	19.46	0.07	10.16			8.49	6.43	3.04	9.50	16.05	0.05	8.24					

3. RESULTS

followed up on this unreported decline with studying the age-dependent physiology of DRG sensory neurons on the transcriptional level. In qPCR experiments, a possible implication of changes in the Piezo2 isoform expression pattern was discovered. DRG neurons of adult twelve-week-old mice showed lower mRNA levels of Piezo2 exon 33, than juvenile four-week-olds. This exon is located close to the pore domain (Coste et al., 2015; Ge et al., 2015) and was found to be implicated in increased permeability of calcium and a decreased mechanical activation threshold (Szczoł et al., 2017), correlating well with our findings. The distinct Piezo2 isoform expression pattern in low-threshold mechanoreceptors of both the mentioned age groups will be scrutinised in future analyses of our patch-seq datasets.

Furthermore, our patch-seq approach of combining electrophysiological with transcriptomic characterisation of single DRG neurons of WT mice of different ages proved to be insightful, as a promising candidate for maturational regulation of sensory neuron physiology was identified in a subtype-specific manner: *Klhl31*, kelch-like 31. The protein encoded by this mRNA promotes substrate-specific ubiquitin-mediated degradation (Papizan et al., 2017), qualifying itself as a potential player in influencing maturational changes in a sensory neuron subtype specific manner.

3.3 Summary of the experimental findings

In summary we found that in male WT C57Bl/6J mice between the juvenile age of four weeks and the middle-aged phase of ten to 15 months

- prolonged culturing alters Piezo2 mRNA levels and currents
 - slight differences found between DIV 1 and 2
- maturation decreases Piezo2-mediated currents
 - RA-MA currents decrease in amplitude and sensitivity between four and twelve weeks of age
 - IA-MA and Na_v currents remain constant
 - MA responder type ratio among medium- and large-sized DRG neurons remains constant
- maturation decreases somatosensory mechanosensitivity
 - mechanical hind paw withdrawal thresholds increase between four and eight weeks of age
 - heat-induced withdrawal thresholds increase only between six and twelve weeks of age
 - hairy skin mechanosensitivity decreases profoundly between four and twelve weeks of age
- maturation changes splicing of Piezo2 mRNA in DRG cells
 - relative levels of exon 33 mRNA decrease between four and eight weeks of age
- LTMRs showing RA-MA currents of adult mice transcribe *Klhl31*, juvenile ones do not
 - juvenile mechanoinsensitive (NR) nociceptors transcribe *Klhl31*, adult ones do not

4

Discussion

It is both common knowledge and empirical fact that sensory decline occurs with ageing and senescence (e.g. Thornbury and Mistretta, 1981; Peters et al., 2016). In this dissertation however, we have shown a distinct decline before a mature age which is unprecedented, to our knowledge. I will discuss the differences and commonalities of these weakenings of the senses in section 4.2.1. The described phenomenon raises several questions that I will address: When (see 4.2.2), why (see 4.2.3) and how (see 4.2.4) does Piezo2-mediated function decline and what are the implications of this phenomenon (see 4.2.5)?

First though, I need to address some technical concerns and discuss the methods used in this thesis, such as: patching hard-to-clamp neurons (see 4.1.1), consequences of culturing (see 4.1.2), bias in behavioural paradigms (see 4.1.3) and problems with patch-seq (see 4.1.4).

4.1 Questioning the methods

4.1.1 Draw backs in electrophysiology

Piezo2 was initially described in cultured DRG neurons (Coste et al., 2010) and it was demonstrated how small interfering RNA against Piezo2 mRNA can selectively suppress RA-MA currents in these cells. For mechanical stimulation, besides negative pressure applied to the soma, the authors used a piezo-electrically driven fire-polished glass pipette directed at the soma of a cultured neuron clamped in whole-cell-mode, as they and others had before (Coste et al., 2007). However, indenting the soma membrane several micrometres deep may well be viewed as an artificial way of activating the MA ion channels expressed in these neurons. *in vivo*, the cell bodies of somatosensory neurons are packed in the DRG which lie in the intervertebral foramina, i.e. protected from mechanical harm deep in the body next to bony structures. It is rather the endings of their peripheral processes that are mechanosensitive (Hu and Lewin, 2006). These endings are embedded in tissue of extracellular matrix and other non-neuronal cells, tiny and hard to locate. So far, it was not possible to stimulate and record from these very endings directly. A workaround would be to stimulate the neurites rather than the soma in culture, like Hu and Lewin, (2006) have demonstrated. Yet, because the recording pipette patching the soma would then be

4. DISCUSSION

further away from the site of stimulation, mentioned space clamp issues (see 2.3.2.1; Williams and Mitchell, 2008; Bar-Yehuda and Korngreen, 2008; Cummins et al., 2009) can be expected to be worse. Poole et al., (2014) have demonstrated an alternative to poking as a means of evoking MA currents altogether: deflecting small elastomeric pillars on which cultured neurons are extending their neurites. By comparing deflection-induced currents on pillar arrays of different spring constants, they found that deflection rather than force is physically relevant to gate mechanosensitive currents (Poole et al., 2014). Accessibility, however, is the main concern about this approach. Microfabrication of uniform pillar arrays and reliable culturing of sensory neurons on a discontinuous surface are some of the challenges this method brings about. After all, because of its accessibility, reproducibility and reliability soma indentation mechano-clamp is the method of choice in the field and has been used in numerous studies by various groups (Hu and Lewin, 2006; Wetzel et al., 2007; Lechner et al., 2009; Coste et al., 2010; Hao and Delmas, 2011; Coste et al., 2012; Dubin et al., 2012; Hao et al., 2013; Ranade et al., 2014; Woo et al., 2014; Maksimovic et al., 2014; Woo et al., 2015; Zhao et al., 2016; Narayanan et al., 2016; Szczot et al., 2017; Narayanan et al., 2018; Moroni et al., 2018).

A prerequisite for all the above mentioned methods of studying MA currents is a strong attachment of the cell to a surface, so that the stimulating force deforms the membrane, e.g. rather than pressing the whole cell away. In cell culture this is easily achieved by plating the cells on surfaces coated with purified constituents of the extracellular matrix that would surround the cell of interest *in vivo* (Kleinman et al., 1987). The cells will then take care of adherence themselves and can be measured via mechano-clamp the next day.

However, each step in the process of isolating, plating and culturing the cells is a step further away from the *in vivo* state of physiology, potentially altering the characteristics of the cells (e.g. Song et al., 2018). It can hardly be ruled out that the very feature in the focus of observations is not affected by the experimental conditions. To my knowledge, there have not been any explicit reports of the soma and adjacent, non-peripheral regions of neurites of DRG neurons to actually be mechanosensitive *in vivo* or at least *ex vivo*. For instance, while investigating the tactilely specialised duck bill, Eve Schneider, Ph.D. (University of Kentucky College of Arts and Sciences, USA), recorded from intact trigeminal mechanoreceptors in response to mechanical stimulation of the bill (Schneider et al., 2017). To do these measurements, she had to get to the soma of the mechanoreceptor with a recording pipette and apply negative pressure to suck the soma in a bit. Even though such manipulations exert mechanical forces on the soma of interest, she never detected electrical activity, unlike when mechanical stimulation was delivered to the receptive field of this neuron in the bill (Sviatoslav Bagriantsev, Ph.D., Yale University School of Medicine, USA, personal communication). Thus, it is possible that the MA currents recorded in this thesis using the mechano-clamp method are an artifactual or artificial byproduct of the culturing and plating processes.

Maybe, I speculate, Piezo2 localises to adhesion sites and contact points with extracellular matrix domains. Such locations might be limited to the sites of relevant force transduction *in vivo*, such as the peripheral nerve endings embedded in the layers of the skin. In culture, however, plating on a coated glass surface provides possible adhesion sites over the whole length of the planar neuron, including at the soma membrane. Adhesion of the neuron to the surface would thereby make for mechanosensitivity of parts of the neuron, which would not be mechanosensitive *in vivo*. Hints in the direction of this speculation come from the facts that Piezo1 was shown to interact with collagen IV (Gaub and Müller, 2017), which is primarily found in the skin (Abreu-Velez and Howard, 2012), and that, as our group

showed, Piezo2 natively interacts with the collagen IV binding protein col4a3bp (Narayanan et al., 2016).

Until it is possible to record from the distal ends of peripheral nerve endings directly, the mechano-clamp method remains the most direct way to study Piezo2 function. For investigating Piezo2-mediated currents in somatosensory neurons of mice of different ages, we chose this method of cultured soma indentation, as it was accessible, reproducible and the standard in the field, since it is used repeatedly by numerous research groups (Wetzel et al., 2007; Lechner et al., 2009; Coste et al., 2010; Hao and Delmas, 2011; Coste et al., 2012; Dubin et al., 2012; Hao et al., 2013; Ranade et al., 2014; Woo et al., 2014; Maksimovic et al., 2014; Woo et al., 2015; Zhao et al., 2016; Narayanan et al., 2016; Szczot et al., 2017; Narayanan et al., 2018; Moroni et al., 2018). The coating of culture surfaces was done as constant as possible in terms of chemicals used, procedure and experimenter.

Nevertheless, the studied parameters provide only a glimpse of the physiological profile of DRG neurons, as many more factors would need quantification to draw a more complete picture. For example, capsaicin-induced TRPV1 currents, a hallmark feature of thermo- and nociceptive sensory neurons (Caterina et al., 1997), were not recorded for the sake of streamlining the measuring of as many MA currents as possible.

4.1.1.1 Contrasting ionic recording conditions

The switch from caesium chloride- to potassium chloride-based intracellular solution was necessary to record clean action potentials to reliably characterise single-cell samples for RNA-seq, described in section 3.2.2.1. Subsequently, the observed electrophysiology was more complex than the one reported in sections 3.1.1 and 3.1.2. Inwardly rectifying potassium channels (e.g. $K_{ir}2.1$, Abrams et al., 1996) and cyclic nucleotide-regulated channels (Stieber et al., 2005) are not blocked by internal Cs^+ ions in these conditions. This leads to reduced space clamping efficiency, i.e. difficulty to reliably voltage-clamp the whole irregularly shaped and non-spherical DRG neuron with its processes (Williams and Mitchell, 2008; Bar-Yehuda and Korngreen, 2008). As a symptom, MA depolarising currents would sometimes trigger fast voltage-gated sodium currents, even for MA currents with less than 10 nA maximal amplitude. I adhered to excluding MA currents with maximal amplitudes greater than 10 nA from statistical analysis, as I did for experiments with CsCl-based recording solution, described in section 2.3.2.1. Also, I used recording pipettes with openings as wide as possible to reduce series resistance while reliable whole-cell patch-clamp. Other than that, space clamp issues could not further be compensated for.

Further complicating the situation was the presence of $I_{K_{mech}}$ in variable magnitudes: the mechanosensitive and voltage-dependent K^+ current carried by Kv1.1-Kv1.2 heteromers described by Hao et al., (2013). In their publication, using KCl-based pipette solution, they showed $I_{K_{mech}}$ makes for a variable component of total MA current that can even make for outward currents at -70 mV holding potential due its K^+ preference. The representative traces shown in figure 3.10A closely resemble the $I_{K_{mech}}$ traces in the aforementioned paper. In theory, such currents should alter the observed MA amplitudes and inactivation kinetics by mismatch or by summation of currents. An observed example of such superposition of currents is depicted in figure 3.10B. These considerations and observations might help with explaining, why:

4. DISCUSSION

- only few IA- and SA-MA currents were identified, see figure 3.10G
- RA-MA currents inactivated rather quickly, compare figures 3.10F and 3.2D
- age-dependent differences observed with CsCl-based intracellular solution could not be reproduced.

They could also explain, why the considerable decline in Piezo2 function throughout maturation of this popular model system of C57Bl/6 mice described in chapter three has not been published by others yet. Many groups have pooled data from mice of different ages that might have shown age-dependent variation with CsCl-based pipette solution (e.g. Poole et al., 2014 pooled four- to six-week-old mice, Prato et al., 2017 pooled eight- to twelve-week-old mice, see also section 4.2.5).

The notion that the observed maturational differences in Piezo2-mediated currents are not a mere artefact caused by ionic conditions is supported by the correlation with the decline in Piezo2-mediated behaviours, as shown in chapter three.

4.1.2 DIVs

As described before, it is necessary to isolate and culture DRG neurons in order to study them thoroughly. Of course, these procedures have consequences for the observed physiology. Beside the discussed change of somata being mechanosensitive, while they probably are not *in vivo* (see 4.1.1), and the obvious change of the digestion of the extracellular matrix using collagenase and papain greatly altering the mechanobiology of the system (Holle et al., 2018), there are subtle changes within sensory neurons over prolonged periods *in vitro*. Song et al., (2018) described that acutely dissociated rat DRG neurons show increased AP size, reduced excitability and reduced Na_V and Ca_V currents already after one day *in vitro*. Furthermore, they showed that mRNA levels of the corresponding voltage-gated channels are reduced as well, though the application of NGF in the culturing medium could attenuate some of this reduction (Song et al., 2018). Though the culturing medium used for this thesis contained a variety of growth factors including NGF (see 2.2), comparable differences were found between the first and second day *in vitro*. As shown in figure 3.1, DRG neurons of middle-aged mice showed a reduction in RA-MA currents on the second DIV, and a slight reduction in Piezo2 mRNA normalised to GAPDH was observed in all age groups. As the amplitude of MA currents varies greatly from cell to cell, prolonged culturing bringing about described changes was considered to potentially add to the variability. Pooling of the data of different DIVs could therefore not be approved and only data from the first DIV is presented in thesis.

4.1.3 Limitations of behavioural paradigms

4.1.3.1 Dynamic Plantar Aesthesiometer

Piezo2 was shown to be the main *bona fide* mechanotransducer in light touch (Ranade et al., 2014) and proprioception (Woo et al., 2015) and is also implicated in mechanical pain (Eijkelkamp et al., 2013; Ferrari et al., 2015; Murthy et al., 2018; Szczot et al., 2018; Zhang et al., 2019). As it is very challenging to experimentally show small changes in proprioception, and as Piezo2 has not been shown to be the main mechanotransducer in mechanical pain, this assay of hind paw withdrawal responses to a force ramping filament was used to quantify the sensitivity of WT mice to non-noxious mechanical

stimuli. However, in previous studies this very assay was used to probe mechanical pain thresholds (Minett et al., 2011; Avenali et al., 2014; Sondermann et al., 2019). In fact, I sometimes observed the mice to show pain-related behaviours upon plantar testing, such as shaking or licking of the hind paw. It seems that this sort of stimulus does not always create the necessity for the mouse to react before the stimulus becomes painful. In other words, the filament force does not incentivise display of touch- rather than pain-related behaviours. This method was fully established in our lab, readily accessible, highly reproducible and reliable to quantify mechanical thresholds, but also unfit to grade acuity of fine touch. For that, rather, the responses to varying forces should be recorded with differing (von Frey) filaments, as was done by others (Ranade et al., 2014).

4.1.3.2 Hargreaves test

To our surprise, hind paw sensitivity to radiant heat was found to decrease during the maturation of WT mice by means of this assay. Unfortunately, I did not measure TRPV1 currents in cultured DRG neurons (for the sake of a higher MA current data throughput) and can therefore not correlate the behavioural changes to them. Yet, the overall trend of age-dependently decreasing hind paw heat sensitivity in C57Bl/6 mice has been shown before, though Wang et al., (2006) attributed it to ageing rather than maturation. Maybe, a general decline of the senses or at least somatosensation during maturation can in part be attributed to environmental factors, as I will discuss later in this chapter (see 4.2.3).

Nevertheless and more importantly, behavioural responses to thermal and mechanical stimuli changed differently within the testing period, as described under 3.1.3.1. The asymmetry of the two acquired sensitivity time courses confirms that the abrupt decrease of mechanical sensitivity described before is not a mere effect of the longitudinal testing design. Since the measured heat sensitivities at four and six weeks of age are unchanged in the same group of mice, sheer repetition of the test had no effect on it. Rather, the temporal divergence of the two sensitivity decrements underlines the significance of the previously unreported, marked decrease of somatosensory mechanosensation so precipitously and early in murine life, as chronicled in this thesis.

4.1.3.3 Tape response assay

The tape response assay was used by Ranade et al., (2014) to show that Piezo2 is the main mechanotransducer in non-noxious hairy skin mechanosensation. Originally though, adhesive removal tests were mainly used to quantify sensorimotor deficits following brain or spinal cord injury (E.J. et al., 2002; Bouet et al., 2009; Freret et al., 2009; Ogle et al., 2012). Arguably, the success of tape removal from the hairy back skin depends both on the ability to sense the tape in the first place as well as on the motoric ability to reach and remove it. Here, I did not control for age differences in the latter. In this way, one could argue that the observed age-dependent variations of tape responses, especially the removal success rate and the no-response time (figure 3.6D and E), have a strong motoric component. Hence, changes in motoric capability and activity with age would be quasi indistinguishable from sensory changes by the mere analysis of those parameters. Addressing the development of behavioural phenotype of the house mouse (Fox, 1965) showed that reflexes and motoric capability are fully developed and mature-like by the age of twenty-one postnatal days. Self grooming for example, particularly important for the tape assay, develops rapidly within the first six days and is considered adult-like by postnatal day thirteen (Golani and Fentress, 1985; Brust et al., 2015). Exploratory behaviour in WT mice is believed

4. DISCUSSION

to have peaked before the age of twenty-four days (Blaney et al., 2013; Brust et al., 2015). For a recent video article on gait analysis Rostosky and Milosevic, (2018) showed how different motoric parameters are unchanged in WT mice across the age groups subject to this thesis. Also, all mice tested here were calm and not engaging in exploratory and major grooming behaviour anymore upon test start, as they had been introduced to the test setup and were acclimated in the testing boxes for two full hours before every experiment (see 2.4). Considering all this, it is fair to assume that the behavioural age differences reported by the tape response assay are to be attributed pre-eminently to sensory changes rather than motoric ones.

Bout time tracking poses a considerable improvement of the assay's sensitivity The stark difference in tape responses between Piezo2^{WT} and Piezo2^{cKO} mice were shown by Ranade et al., (2014) by plotting the total number of tape directed bouts that had occurred over a five minute period. Here however, neither the total bouts nor the bouts per minute were significantly different between the tested age groups, see 3.6. Age differences in WT mice were of course expected to be more subtle than changes brought about by genetic modifications such as conditional knockout of Piezo2. Noteworthy, upon resolving the exact time course of bouts and inactivity age differences became apparent and reached robust statistical significance. This minor improvement of the assay makes it a quite sensitive method to quantify non-noxious mechanosensitivity of hairy skin, in which Piezo2 is the main molecular player.

4.1.4 Patch-seq

The combination of microscopy, current-clamp, mechano-clamp and RNA-seq yielded detailed insight into somatosensory physiology on the single-cell level. However, some of the genes statistically upregulated in adult versus juvenile NR nociceptors were not of neuronal origin. Genes like matrix remodelling-associated 8 or myelin basic protein (*Mxra8* and *Mbp*, see table 3.2) are primarily expressed in non-neuronal cells (Yonezawa et al., 2003; Han et al., 2013). Yet, their read counts are selectively elevated in the adult samples only. While it is not uncommon to find low expression levels of such atypic genes in single-cell mRNA libraries (Usoskin et al., 2015), it is alarming that there are significantly lower levels of them in the juvenile sample group. All the single-cell samples mentioned in this thesis stem from several animals and were collected by the same experimenter on different days over months strictly following the same procedure using the same kits and chemicals. For cDNA synthesis, library preparation and sequencing the batch of NR samples was not further subdivided into age groups, as all these samples were processed together (in one batch). The other batch of mixed samples presented in this thesis showed low expression of these genes independent of the age of the mice from which the samples stem. Taking all this into consideration, I attribute the described differences between the NR age groups to chance, rather than systematic contamination or age-dependent regulation. However, these differences urged me to disregard the upregulated genes in adult mechanoinensitive nociceptor samples as revealed by DGE analysis for a biological interpretation of the results. Nevertheless, there were a few genes that were significantly downregulated in adult NR samples. One of these candidates, *Klhl31* (see 3.2), also turned out to be maturationally regulated in the other batch of samples, arguing for a legit and interesting regulation of the transcription of that gene.

There are some means of analysis we have yet to perform on the patch-seq data. For example, it is interesting how little the reads of Piezo2 mRNA correlate with the observed MA current amplitudes, see figure 3.12. I mentioned how this discrepancy can partly be explained by the silent nociceptor marker *Chrna3* (see 3.2.2.2). However, we will perform multiple linear regressions to search for correlations between electrophysiological parameters (e.g. MA amplitude, cell capacitance, AP decay time) and mRNA read counts in an unbiased manner.

4.2 Questioning the findings

4.2.1 Comparison to sensory decline in high age

Tactile perception is known to decrease with age (Beard, 1969; Wickremaratchi and Llewelyn, 2006; Skedung et al., 2018). This decrease is carried by multiple changes involving the central nervous system, the peripheral nervous system and the skin (Heft and Robinson, 2017). For instance, changing mechanical properties of the skin increasingly decrease fine touch acuity with high age in humans (Lévêque et al., 2000; Skedung et al., 2018). Interestingly, spatial discrimination and cutaneous coding properties can be improved by hydrating the skin of the elderly with a moisturiser (Lévêque et al., 2000; Skedung et al., 2018). This illustrates the importance of the local deformability of the stratum corneum for mechanotransduction and the spatial resolution of tactile discrimination. Though I did not find reports of major skin elasticity changes in young mice, it would be interesting and easy to test whether skin hydration can rescue some of the observed decline in glabrous skin mechanosensation.

Normal ageing of the central nervous system, i.e. "ageing changes occurring in individuals free from overt neurological disease" (Katzman and Terry, 1983) can also affect touch. Neuronal loss, an increased tendency to develop neuritic plaques and other accumulations, decreasing concentrations of neurotransmitters and progressive loss of myelin and intracellular enzymes can contribute to the slowing of central processing of sensory stimuli (Wickremaratchi and Llewelyn, 2006).

Ageing also affects epidermal innervation density. In facial areas of high innervation density and tactile acuity Besné et al., (2002) found a continuous decrease of innervation density from mature adult to old humans (35 to 75 years of age). Conversely, innervation density in sun-protected truncal areas was found to slightly increase with age (Besné et al., 2002). Since the maturational decline in mechanosensation I described in the previous chapter is abrupt rather than continuous, I suspect no relevant changes in innervation density on the timescale of interest.

Finally, the specialised mechanosensory end organs undergo changes with age. In aged male humans, Meissner's corpuscles were shown to decrease in size and to dramatically decrease in number with high age (Iwasaki et al., 2006), although the cited study compared tissue of only 10 individuals. However, a very recent study confirmed the progressive decrease of the number of Meissner's corpuscles and found them to become smaller, rounded in morphology and located deeper in the dermis with signs of corpuscular denervation in the oldest human subjects (García-Piqueras et al., 2019). Furthermore, while the authors found clusters of up to four Merkel cells in the epidermal rete pegs of young subjects they found only isolated Merkel cells in old subjects along with a general decline in their number as well (García-Piqueras et al., 2019). Moreover, a reduction in the BDNF-TrkB neurotrophin system was found as immunoreactivity in both sensory end organs and the axons innervating them was found to be reduced in the old age group (García-Piqueras et al., 2019). The authors also tellingly showed that

4. DISCUSSION

Piezo2 levels decrease with age in both Meissner's corpuscles and Merkel cells. Interestingly, levels of Piezo2 immunoreactivity in Meissner's corpuscles were found to remain unchanged in the middle-aged group and to be markedly reduced in the older subjects (García-Piqueras et al., 2019), resembling the findings of this thesis with regard to *in vivo* mechanosensitivity being rather unchanged between adult and middle-aged mice. Also, Kinkelin et al., (1999) showed that the number of Merkel cells in the back skin of WT mice remains constant between four weeks and six months of age, and Airaksinen et al., (1996) reported similar results for hind limb skin.

4.2.2 Timeline of the decline

We started our investigations of WT mice as early as possible, i.e. shortly after they were weaned at four weeks of age. Differences in Piezo2-mediated *in vitro* MA currents only reached significance in comparison of the youngest to the adult twelve-week-old group (fig. 3.2). Hind paw mechanosensitivity was found to be significantly reduced after eight weeks of age (fig. 3.5). So were the DRG mRNA levels of Piezo2 exon 33 (fig. 3.7). The improved tape assay even detected a reduced response at six weeks of age already (see area under the bout time courses in fig. 3.6). All findings agree however that the decline is maturational, happening before the age of twelve weeks, as there were no differences between the adult and middle-aged groups in any experiment. From adulthood until senescence the sense of touch is supposedly rather stable compared to the rapid decline before adulthood shown here. The presented data however neither covers the very early postnatal phase, nor of course the prenatal phase. For a start to investigate function of Piezo2 before the four-week time point, neonatal MA currents in cultured DRG neurons should be quantified.

The question, when exactly the most mechanosensitive age of WT C57Bl/6 mice is, cannot be empirically answered with the present data. Yet, it can be addressed by questioning possible reasons for the decline as well as its role in murine life.

4.2.3 Reasons for the decline

Generally, I would oppose two possible reasons for the observed decline in Piezo2-mediated function: "nature" or "nurture". By "nature" I mean that this decline is physiological, genetically programmed and an evolutionary benefit for the species. By "nurture" I mean that this decline is the acute consequence of environmental factors, such as the housing conditions. There are some points that can be made in favour of the latter.

The fact that the studied parameters of mechanosensitivity reach a plateau upon entering adulthood might argue for this decline to be genetically timed and part of physiological maturation. However, the timeline of the decline might also hint at this decline being an acute consequence of the drastic change in the lives of the mice: the weaning and the separation from the (foster) mother had just taken place before the experimental study of juveniles.

If this decline were of evolutionary relevance, it could be viewed as part of sensory specialisation. The groups around Elena Gracheva, Ph.D. and Sviatoslav Bagriantsev, Ph.D. (Yale University School of Medicine, USA) have demonstrated a molecular basis of tactile specialisation in chickens and several duck species. By studying TG sensory neurons that innervate the bill they could correlate foraging behaviour with the abundance of mechanosensory neuron types, the proportion of Piezo2-expressing neurons and the expression levels of markers of sensory neuron types (Schneider et al.,

2019). The majority of embryonic TG neurons of the Pekin duck, a sophisticated tactile forager, are Piezo2-expressing mechanoreceptors with a significantly reduced mechano-activation threshold and elevated MA current amplitude in contrast to the embryonic TG neurons of chicken, a strictly visually foraging bird (Schneider et al., 2017). When comparing other duck species who rely less on tactile sensing for foraging than the Pekin duck, but more so than chicken, they showed how those parameters correlate with their behaviour in a graded manner (Schneider et al., 2019). These studies suggest that the trade-off between neuronal subtypes, such as the expansion of Piezo2-containing mechanoreceptors at the expense of nociceptors and thermoreceptors, is a general mechanism of tactile specialisation of the somatosensory system (Schneider et al., 2019). Along these lines the maturational decrease in tactile sensitivity could be expected to be accompanied by shifts in the MA current type ratios and a change in the size of the mechanosensitive population among DRG neurons.

Recording mainly from medium- and large-sized DRG neurons the here presented picture of the murine DRG population is incomplete. In upcoming experiments, we will investigate the ratio of small-, medium- and large-sized DRG neurons more fully. Nevertheless, even though observing a profound decrease in Piezo2-mediated currents and behaviours we have not seen any considerable change in MA responder type ratio (see figures 3.3C and 3.10G).

Sensory restriction might explain the observations The early postnatal phase is coined by rapid development and plasticity. House mice are born deaf and blind (as reviewed by Brust et al., 2015). Apart from small whiskers on their muzzle, they are born hairless and unable to thermoregulate (as reviewed by Latham and Mason, 2004). Although they start growing fur within a week, the pups rely on the mother for food, to stimulate defecation and for temperature regulation until an age of up to 28 days (Latham and Mason, 2004). Newborns continuously burrow into the centre of the "dynamic huddle" of pups to stay warm and manage to recognise and orient to the mother and her teats (Latham and Mason, 2004). For these tasks, they probably rely on thermosensation, olfaction, gustation and mechanosensation (Brust et al., 2015; Latham and Mason, 2004). Eventually, pups become able to hear, see and thermoregulate, they become nutritionally independent and begin to briefly venture away from the nest at three to four weeks of age (Latham and Mason, 2004). Throughout their lives, free-living mice become excellent climbers, proficient jumpers, able to squeeze through tight cracks and to run along wires and narrow ropes with ease (Latham and Mason, 2004), relying heavily on tactile perception. However, the laboratory animals studied here do not have much to explore and a lack of tactile variety in standard housing conditions. Considering that different tactile stimuli can easily be counted (themselves, littermates, excrements, bedding, water, bottle, (uniform) food, cage wall, grid, nesting material), their housing conditions can be termed sensorily restricted and tactilely impoverished. Studies involving whisker-trimming in rats have shown that sensory restriction and deprivation have many consequences on the neuronal and cortical level with more pronounced effects during maturation than adulthood (Chen et al., 2014). Therefore, I speculate, the observed maturational decline in somatosensory mechanosensation is a consequence of tactile impoverishment, the effects of which increasingly consolidate throughout early murine life phases of increased plasticity. Note that in human children, who are not raised under sensory restriction touch, haptic ability and proprioception have been shown to improve with age (reviewed by Taylor et al., 2016).

In upcoming experiments, we will test the impact of tactile enrichment (e.g LeMessurier and Feldman, 2018) on somatosensory mechanosensation during maturation.

4. DISCUSSION

4.2.4 Mechanism

In contrast to the sensory decline in senescence, the observed maturational decline in somatosensory mechanosensation is rather unlikely to result from progressive epidermal denervation or gradual degradation of sensory end organs given the short time span of the decline and the assumed health in youth, see 4.2.1. The number of Merkel cells in murine back skin was shown to be constant between one and six months of age, for instance (Kinkelin et al., 1999). However, maybe an initial roughening or drying of the plantar skin following increased activity levels in juveniles could marginally contribute to a decrease in tactile acuity of glabrous hind paw skin during early life phases.

Judging from the data shown in the second part of the previous chapter changes on the protein level in LTMRs are likely to contribute to the observed effects. Yet, considering that the mechanistic findings are solely on the level of transcription one has to be careful to infer mechanistic insight on the protein level. To what extent and with how much variance mRNA levels can predict protein levels in a given tissue or cell is being vividly discussed in recent literature (Wilhelm et al., 2014; Li and Biggin, 2015; Liu et al., 2016; Fortelny et al., 2017; Wilhelm et al., 2017). In general, while the nucleotide sequence of a gene greatly determines the respective mRNA sequence, which in turn determines the resulting polypeptide sequence, there is no trivial relationship between mRNA and protein levels (Liu et al., 2016). Transcription is believed to explain the most of the variance of true protein levels (Wilhelm et al., 2014; Li and Biggin, 2015), however, as reviewed by Liu et al., (2016), great variance stems from

- translation rates
 - mRNA sequence affects those, e.g. through internal ribosome entry sites
- translation rate modulation
 - e.g. by micro-RNAs and mRNA degradation
- protein degradation
 - e.g. via the ubiquitin-proteasome pathway
- protein synthesis delay
- protein transport

Hence, further analyses and experiments tackling the true protein level are needed to fully explain the machinery behind the observations (e.g. ongoing immunohistochemistry investigations could not be completed in time for this thesis).

Nevertheless, both the found Piezo2 splicing pattern shift and the differential expression of *Klhl31* mRNA in adult LTMRs are promising for contributing to the observed decline. Considering that the qPCR experiments were performed on whole-DRG lysates, which contain material of many different sensory neurons and non-neuronal cell types, detecting maturational differences in the mRNA levels of alternatively spliced exon 33 but not exon 35 underlines the significance of that finding. If for example adult LTMRs were indeed to have less exon 33 translated into functional Piezo2 mechanotransducers, the latter are thought to have a reduced calcium permeability subsequently (Szcot et al., 2017), as I described in section 3.2.1. A reduced influx of Ca^{2+} ions following a given mechanical stimulus might make for lesser depolarisation of the plasma membrane and thus lower the probability of AP generation

within the transducing neuron. A DRG mechanoreceptor innervating the hair follicles at the back of an adult mouse expressing Piezo2 with such distinct pore properties would presumably be less likely to transduce hair deflection (by an adhesive red dot, for instance) into robust spike firing, culminating in a decreased behavioural response to the stimulus, theoretically.

Some candidate genes were found to be age-dependently transcribed in a sensory neuron subtype-specific manner by our patch-seq approach, one of them being *Klhl31*. The transcription of this gene was found to be upregulated in twelve-week-old LTMRs showing RA-MA currents. Since *Klhl31* transcription was virtually absent from four-week-old equivalents this difference seems rather qualitative and therefore not as easily disputable by the aforementioned concerns of variance in the central dogma of protein expression. The encoded kelch-like protein 31 was shown to promote substrate-specific ubiquitin-mediated protein degradation via the cullin 3 ubiquitin ligase (Papizan et al., 2017). Though consequences of *Klhl31* knockdown were predominantly found in mouse heart and skeletal muscle (Papizan et al., 2017), it is conceivable that even low expression levels of this gene could tune the protein landscape and physiology of somatosensory neurons without decreasing the mRNA levels of Piezo2 (see figure 3.7A). To try a shot in the dark, kelch-like protein 31 could promote the degradation of trafficking mediators, cytoskeleton regulators, chaperones (Papizan et al., 2017) or extracellular matrix modulators (Genschik et al., 2013), all of which could directly or indirectly influence Piezo2-mediated function.

4.2.5 Relevance

Mutations in the human *PIEZO2* gene have been found to be associated to diseases, e.g. distal arthrogryposis 3/Gordon Syndrome and distal arthrogryposis 5/Marden-Walker Syndrome (McMillin et al., 2014). Symptoms of affected patients include joint and muscle contractures, selective loss of discriminative touch perception and profoundly decreased proprioception (Chesler et al., 2016). In mice, despite its major role in touch and proprioception (Ranade et al., 2014; Woo et al., 2015; Florez-Paz et al., 2016), Piezo2 was found to be implicated in mechanical pain sensitivity (Dubin et al., 2012; Eijkelkamp et al., 2013; Ferrari et al., 2015; Murthy et al., 2018; Zhang et al., 2019). Tactile hypersensitivity also plays a role in various human pain conditions (e.g. inflammatory pain, Ma and Woolf, 1996). Furthermore, Riquelme et al., (2016) recently showed that children with autism spectrum disorder show increased mechanical pain sensitivity, touch sensitivity (see also Blakemore et al., 2006) and abnormal proprioception.

The Piezo protein family is a conserved one with orthologs in many plants and animals (Coste et al., 2010). Sharing 47 % gene sequence identity among each other, Piezo1 and Piezo2 lack sequence homology to any other known protein or ion channel (Coste et al., 2010, 2012). Human and mouse Piezo2 share 85 % sequence identity at the mRNA level and 88 % at amino acid level (National Center for Biotechnology Information, Basic Local Alignment Search Tool, 04/26/19). Genetic and physiological similarities between mice and humans together with many other advantages make the house mouse a formidable model system for basic and preclinical research.

It has been almost a century since Clarence C. Little created the C57 strain of mice in 1921 (Jackson and Little, 1933). The C57Bl/6J substrain is the most widely used and studied and has even gone on spaceflights (e.g. Mao et al., 2014). In general, development, ageing and senescence were extensively studied. With regard to the somatosensory cortex and whisker-mediated mechanosensation

4. DISCUSSION

development, maturation, plasticity and critical periods are being studied intensively (e.g. Briner et al., 2010; Erzurumlu and Gaspar, 2012; Lo et al., 2017). Yet, maturation of somatosensation and the peripheral nervous system has not received much attention. As a result, many research groups have assumed that mature physiology is present at six or eight weeks of age. Below some examples from the somatosensation research field are listed:

- Minett et al., (2011): for "behavioural measures of pain thresholds" mice are of "optimal age" at six to eight weeks
- Heidenreich et al., (2012): *in vitro* skin-nerve-recordings from "adult" mice, no age stated for mice in tactile acuity test
- Eijkelkamp et al., (2013): behavioural testing of eight- to twelve-week-old mice
- Ranade et al., (2014): immunofluorescence experiments with tissue from seven-week-old mice
- Murthy et al., (2018): behavioural testing of mice "at least 4 weeks" of age

More specifically, below are some age statements from studies involving murine (mostly C57Bl/6) DRG neuron MA current recordings similar to the ones presented under 3.1.1 and 3.2.2.1, using different intracellular solutions:

- Eijkelkamp et al., (2013): "Adult mice DRG neurons", CH₃COOK-based ICS
- Poole et al., (2014): four to six weeks old, KCl-based ICS
- Ranade et al., (2014): no age stated, K-gluconate-based ICS
- Schrenk-Siemens et al., (2015): six weeks old, KCl-based ICS
- Zhang et al., (2019): four to eight weeks old, CsCl-based ICS

A lot of the Piezo2 research done with age groups rendered immature by this thesis comprised mechano-clamp recordings with potassium-based pipette solutions. Maybe that is why nobody reported the age-dependent differences we saw in this widely studied strain yet. In our lab, both the differences in *in vitro* RA-MA DRG currents and the hind paw mechanical thresholds were observed by two different experimenters each (Pratibha Narayanan, Ph.D, and me, and Elena Ciirdaeva (MPI of Brain Research, Germany, formerly Schmidt Group) and me, respectively).

In this thesis, it was shown that maturational plasticity of somatosensory mechanosensation in WT C57Bl/6J mice can last as far as twelve weeks of age. I hope my research accomplishes the recognition of mice being of mature adult physiology only at an age of greater than or equal to twelve weeks.

References

- Abou-Elhamd, A., A. F. Alrefaei, G. F. Mok, C. Garcia-Morales, M. Abu-Elmagd, G. N. Wheeler, and A. E. Münsterberg (2015). “Khl31 attenuates β -catenin dependent Wnt signaling and regulates embryo myogenesis”. In: *Developmental Biology* 402.1, pp. 61–71. doi: 10.1016/j.ydbio.2015.02.024.
- Abrams, C. J., N. W. Davies, P. A. Shelton, and P. R. Stanfield (1996). “The role of a single aspartate residue in ionic selectivity and block of a murine inward rectifier K⁺ channel Kir2.1.” eng. In: *The Journal of physiology* 493 (Pt 3, pp. 643–649.
- Abreu-Velez, A. M. and M. S. Howard (2012). “Collagen IV in Normal Skin and in Pathological Processes”. eng. In: *North American journal of medical sciences* 4.1, pp. 1–8. doi: 10.4103/1947-2714.92892.
- Airaksinen, M. S., M. Koltzenburg, G. R. Lewin, Y. Masu, C. Helbig, E. Wolf, G. Brem, K. V. Toyka, H. Thoenen, and M. Meyer (1996). “Specific subtypes of cutaneous mechanoreceptors require neurotrophin-3 following peripheral target innervation”. In: *Neuron* 16.2, pp. 287–295. doi: 10.1016/S0896-6273(00)80047-1.
- Alisch, F., A. Weichert, K. Kalache, V. Paradiso, A. C. Longardt, C. Dame, K. Hoffmann, and D. Horn (2017). “Familial Gordon syndrome associated with a PIEZO2 mutation”. In: *American Journal of Medical Genetics, Part A* 173.1, pp. 254–259. doi: 10.1002/ajmg.a.37997.
- Anderson, E. O., E. R. Schneider, and S. N. Bagriantsev (2017). *Piezo2 in Cutaneous and Proprioceptive Mechanotransduction in Vertebrates*. Vol. 79. Elsevier Ltd, pp. 197–217. doi: 10.1016/bs.ctm.2016.11.002.
- Andres, K. (1961). “[Research on the fine-structure of spinal ganglia]”. In: *Zellforsch. Mikrosk. Anat.* 55, pp. 1–48.
- Avenali, L., P. Narayanan, T. Rouwette, I. Cervellini, M. Sereda, D. Gomez-Varela, and M. Schmidt (2014). “Annexin A2 Regulates TRPA1-Dependent Nociception”. In: *Journal of Neuroscience* 34.44, pp. 14506–14516. doi: 10.1523/JNEUROSCI.1801-14.2014.
- Bar-Yehuda, D. and A. Korngreen (2008). “Space-Clamp Problems When Voltage Clamping Neurons Expressing Voltage-Gated Conductances”. In: *Journal of Neurophysiology* 99.3, pp. 1127–1136. doi: 10.1152/jn.01232.2007.
- Beard, B. B. (1969). “Sensory Decline in Very Old Age”. In: *Gerontologia Clinica* 11.3, pp. 149–158.
- Besné, I., C. Descombes, and L. Breton (2002). “Effect of Age and Anatomical Site on Density of Sensory Innervation in Human Epidermis”. In: *Archives of dermatology* 138.11, pp. 1445–50. doi: 10.1001/archderm.138.11.1445.

REFERENCES

- Blakemore, S. J., T. Tavassoli, S. Calò, R. M. Thomas, C. Catmur, U. Frith, and P. Haggard (2006). “Tactile sensitivity in Asperger syndrome”. In: *Brain and Cognition* 61.1, pp. 5–13. doi: 10.1016/j.bandc.2005.12.013.
- Blaney, C. E., R. K. Gunn, K. R. Stover, and R. E. Brown (2013). “Maternal genotype influences behavioral development of 3xTg-AD mouse pups.” eng. In: *Behavioural brain research* 252, pp. 40–48. doi: 10.1016/j.bbr.2013.05.033.
- Bouet, V., M. Boulouard, J. Toutain, D. Divoux, M. Bernaudin, P. Schumann-Bard, and T. Freret (2009). “The adhesive removal test: A sensitive method to assess sensorimotor deficits in mice”. In: *Nature Protocols* 4.10, pp. 1560–1564. doi: 10.1038/nprot.2009.125.
- Briner, A., M. De Roo, A. Dayer, D. Muller, J. Z. Kiss, and L. Vutskits (2010). “Bilateral whisker trimming during early postnatal life impairs dendritic spine development in the mouse somatosensory barrel cortex”. In: *Journal of Comparative Neurology* 518.10, pp. 1711–1723. doi: 10.1002/cne.22297.
- Brust, V., P. M. Schindler, and L. Lewejohann (2015). “Lifetime development of behavioural phenotype in the house mouse (*Mus musculus*)”. eng. In: *Frontiers in zoology* 12 Suppl 1.Suppl 1, S17–S17. doi: 10.1186/1742-9994-12-S1-S17.
- Cadwell, C. R., R. Sandberg, X. Jiang, and A. S. Tolias (2017a). “Q&A: Using Patch-seq to profile single cells”. In: *BMC Biology* 15.1, pp. 1–7. doi: 10.1186/s12915-017-0396-0.
- Cadwell, C. R., F. Scala, S. Li, G. Livrizzi, S. Shen, R. Sandberg, X. Jiang, and A. S. Tolias (2017b). “Multimodal profiling of single-cell morphology, electrophysiology, and gene expression using Patch-seq”. In: *Nature Protocols* 12.12, pp. 2531–2553. doi: 10.1038/nprot.2017.120.
- Canning, P., C. D. O. Cooper, T. Krojer, J. W. Murray, A. C. W. Pike, A. Chaikuad, T. Keates, C. Thangaratnarajah, V. Hojzan, B. D. Marsden, O. Gileadi, S. Knapp, F. von Delft, and A. N. Bullock (2013). “Structural Basis for Cul3 Protein Assembly with the BTB-Kelch Family of E3 Ubiquitin Ligases”. In: *Journal of Biological Chemistry* 288.11, pp. 7803–7814. doi: 10.1074/jbc.M112.437996.
- Caterina, M. J., M. A. Schumacher, M. Tominaga, T. A. Rosen, J. D. Levine, and D. Julius (1997). “The capsaicin receptor: A heat-activated ion channel in the pain pathway”. In: *Nature* 389.6653, pp. 816–824. doi: 10.1038/39807.
- Chalfie, M. (2009). “Neurosensory mechanotransduction”. In: *Nature Reviews Molecular Cell Biology* 10.1, pp. 44–52. doi: 10.1038/nrm2595.
- Chen, C.-C., J. C. Brumberg, and A. Bajnath (2014). “The Impact of Development and Sensory Deprivation on Dendritic Protrusions in the Mouse Barrel Cortex”. In: *Cerebral Cortex* 25.6, pp. 1638–1653. doi: 10.1093/cercor/bht415.
- Chesler, A. T., M. Szczot, D. Bharucha-Goebel, M. Ceko, S. Donkervoort, C. Laubacher, L. H. Hayes, K. Alter, C. Zampieri, C. Stanley, A. M. Innes, J. K. Mah, C. M. Grosmann, N. Bradley, D. Nguyen, A. R. Foley, C. E. Le Pichon, and C. G. Bonnemann (2016). “The Role of PIEZO2 in Human Mechanosensation.” eng. In: *The New England journal of medicine* 375.14, pp. 1355–1364. doi: 10.1056/NEJMoa1602812.
- Cohen, J. (1989). *Statistical Power Analysis for the Behavioural Sciences*. Vol. 15. 6. doi: 10.1007/BF00544941.
- Coste, B., M. Crest, and P. Delmas (2007). “Pharmacological Dissection and Distribution of Na^v1.9, T-type Ca²⁺ Currents, and Mechanically Activated Cation Currents in Different Populations of DRG Neurons”. In: *The Journal of General Physiology* 129.1, pp. 57–77. doi: 10.1085/jgp.200609665.

- Coste, B., J. Mathur, M. Schmidt, T. J. Earley, S. Ranade, M. J. Petrus, A. E. Dubin, and A. Patapoutian (2010). “Piezo1 and Piezo2 Are Essential Components of Distinct Mechanically Activated Cation Channels”. In: *Science (New York, N.Y.)* 330.October, pp. 7–12. DOI: 10.1126/science.1193270.
- Coste, B., S. E. Murthy, J. Mathur, M. Schmidt, Y. Mechoukhi, P. Delmas, and A. Patapoutian (2015). “Piezo1 ion channel pore properties are dictated by C-terminal region”. In: *Nature Communications* 6.May, pp. 1–11. DOI: 10.1038/ncomms8223.
- Coste, B., B. Xiao, J. S. Santos, R. Syeda, J. Grandl, K. S. Spencer, S. E. Kim, M. Schmidt, J. Mathur, A. E. Dubin, M. Montal, and A. Patapoutian (2012). “Piezo proteins are pore-forming subunits of mechanically activated channels”. In: *Nature* 483.7388, pp. 176–181. DOI: 10.1038/nature10812.
- Cummins, T. R., A. M. Rush, M. Estacion, S. D. Dib-Hajj, and S. G. Waxman (2009). “Voltage-clamp and current-clamp recordings from mammalian DRG neurons”. In: *Nature Protocols* 4.8, pp. 1103–1112. DOI: 10.1038/nprot.2009.91.
- D’Agostino, R. B. and A. Belanger (1990). “A Suggestion for Using Powerful and Informative Tests of Normality”. In: *The American Statistician* 44.4, pp. 316–321. DOI: 10.2307/2684359.
- Dai, S., K. Dieterich, M. Jaeger, B. Wuyam, P.-S. Jouk, and D. Pérennou (2018). “Disability in adults with arthrogyriposis is severe, partly invisible, and varies by genotype”. In: *Neurology* 90.18, e1596–e1604. DOI: 10.1212/WNL.0000000000005418.
- Delle Vedove, A., M. Storbeck, R. Heller, I. Hölker, M. Hebbbar, A. Shukla, O. Magnusson, S. Cirak, K. M. Girisha, M. O’Driscoll, B. Loeys, and B. Wirth (2016). “Biallelic Loss of Proprioception-Related PIEZO2 Causes Muscular Atrophy with Perinatal Respiratory Distress, Arthrogyriposis, and Scoliosis”. In: *American Journal of Human Genetics* 99.5, pp. 1206–1216. DOI: 10.1016/j.ajhg.2016.09.019.
- Dhanao, B. S., T. Cogliati, A. G. Satish, E. A. Bruford, and J. S. Friedman (2013). “Update on the Kelch-like (KLHL) gene family”. In: *Human Genomics* 7.1, p. 13. DOI: 10.1186/1479-7364-7-13.
- Dib-Hajj, S. D., P. Geha, and S. G. Waxman (2017). “Sodium channels in pain disorders: pathophysiology and prospects for treatment.” eng. In: *Pain* 158 Suppl, S97–S107. DOI: 10.1097/j.pain.0000000000000854.
- Djoughri, L., L. Bleazard, and S. N. Lawson (1998). “Association of somatic action potential shape with sensory receptive properties in guinea-pig dorsal root ganglion neurones”. In: *Journal of Physiology* 513.3, pp. 857–872. DOI: 10.1111/j.1469-7793.1998.857ba.x.
- Djoughri, L. and S. N. Lawson (2001). “Differences in the size of the somatic action potential overshoot between nociceptive and non-nociceptive dorsal root ganglion neurones in the guinea-pig”. In: *Neuroscience* 108.3, pp. 479–491. DOI: 10.1016/S0306-4522(01)00423-7.
- Dobin, A., C. A. Davis, F. Schlesinger, J. Drenkow, C. Zaleski, S. Jha, P. Batut, M. Chaisson, and T. R. Gingeras (2013). “STAR: ultrafast universal RNA-seq aligner”. eng. In: *Bioinformatics (Oxford, England)* 29.1, pp. 15–21. DOI: 10.1093/bioinformatics/bts635.
- Dubin, A. E., M. Schmidt, J. Mathur, M. J. Petrus, B. Xiao, B. Coste, and A. Patapoutian (2012). “Inflammatory Signals Enhance Piezo2-Mediated Mechanosensitive Currents”. In: *Cell Reports* 2.3, pp. 511–517. DOI: 10.1016/j.celrep.2012.07.014.
- Durinck, S., P. T. Spellman, E. Birney, and W. Huber (2009). “Mapping identifiers for the integration of genomic datasets with the R/Bioconductor package biomaRt”. eng. In: *Nature protocols* 4.8, pp. 1184–1191. DOI: 10.1038/nprot.2009.97.

REFERENCES

- Eijkelkamp, N., J. E. Linley, J. M. Torres, L. Bee, A. H. Dickenson, M. Gringhuis, M. S. Minett, G. S. Hong, E. Lee, U. Oh, Y. Ishikawa, F. J. Zwartkuis, J. J. Cox, and J. N. Wood (2013). “A role for Piezo2 in EPAC1-dependent mechanical allodynia”. In: *Nature Communications* 4. DOI: 10.1038/ncomms2673.
- E.J., B., M. L.D.F., P. R.J., K. V.R., B. G.S., P. P.N., and F. J.W. (2002). “Chondroitinase ABC promotes functional recovery after spinal cord injury”. In: *Nature* 416.6881, pp. 636–640. DOI: 10.1038/416636a.
- English, R. B. (1915). “Democritus’ Theory of Sense Perception”. In: *Transactions and Proceedings of the American Philological Association* 46, pp. 217–227. DOI: 10.2307/282943.
- Erzurumlu, R. S. and P. Gaspar (2012). “Development and critical period plasticity of the barrel cortex”. In: *European Journal of Neuroscience* 35.10, pp. 1540–1553. DOI: 10.1111/j.1460-9568.2012.08075.x.
- Fang, X., S. McMullan, S. N. Lawson, and L. Djouhri (2005). “Electrophysiological differences between nociceptive and non-nociceptive dorsal root ganglion neurones in the rat in vivo”. In: *Journal of Physiology* 565.3, pp. 927–943. DOI: 10.1113/jphysiol.2005.086199.
- Ferrari, L. F., O. Bogen, P. Green, and J. D. Levine (2015). “Contribution of Piezo2 to endothelium-dependent pain”. In: *Molecular Pain* 11.1, pp. 1–8. DOI: 10.1186/s12990-015-0068-4.
- Florez-Paz, D., K. K. Bali, R. Kuner, and A. Gomis (2016). “A critical role for Piezo2 channels in the mechanotransduction of mouse proprioceptive neurons”. In: *Scientific Reports* 6, pp. 1–9. DOI: 10.1038/srep25923.
- Fortelny, N., C. M. Overall, P. Pavlidis, and G. V. C. Freue (2017). “Can we predict protein from mRNA levels?” In: *Nature* 547.7664, E19–E20. DOI: 10.1038/nature22293.
- Fox, W. M. (1965). “Reflex-ontogeny and behavioural development of the mouse”. In: *Animal behaviour* 13.2, pp. 234–41.
- Freret, T., V. Bouet, C. Leconte, S. Roussel, L. Chazalviel, P. Schumann-bard, and M. Boulouard (2009). “Behavioral Deficits After Distal Focal Cerebral Ischemia in Mice : Usefulness of Adhesive Removal Test”. In: 123.1, pp. 224–230. DOI: 10.1037/a0014157.
- Fuzik, J., A. Zeisel, Z. Mate, D. Calvigioni, Y. Yanagawa, G. Szabo, S. Linnarsson, and T. Harkany (2016). “Integration of electrophysiological recordings with single-cell RNA-seq data identifies neuronal subtypes”. In: *Nature Biotechnology* 34.2, pp. 175–183. DOI: 10.1038/nbt.3443.
- Gagnon, R. C. and J. J. Peterson (1998). “Estimation of Confidence Intervals for Area Under the Curve from Destructively Obtained Pharmacokinetic Data”. In: *Journal of Pharmacokinetics and Biopharmaceutics* 26.1, pp. 87–102. DOI: 10.1023/A:1023228925137.
- García-Piqueras, J., Y. García-Mesa, L. Cárcaba, J. Feito, I. Torres-Parejo, B. Martín-Biedma, J. Cobo, O. García-Suárez, and J. A. Vega (2019). “Ageing of the somatosensory system at the periphery: age-related changes in cutaneous mechanoreceptors”. In: *Journal of Anatomy*, joa.12983. DOI: 10.1111/joa.12983.
- Garg, A., J. O’Rourke, C. Long, J. Doering, G. Ravenscroft, S. Bezprozvannaya, B. R. Nelson, N. Beetz, L. Li, S. Chen, N. G. Laing, R. W. Grange, R. Bassel-Duby, and E. N. Olson (2014). “KLHL40 deficiency destabilizes thin filament proteins and promotes Nemaline myopathy”. In: *Journal of Clinical Investigation* 124.8, pp. 3529–3539. DOI: 10.1172/JCI74994.

- Gaub, B. M. and D. J. Müller (2017). “Mechanical Stimulation of Piezo1 Receptors Depends on Extracellular Matrix Proteins and Directionality of Force”. In: *Nano Letters* 17.3, pp. 2064–2072. DOI: 10.1021/acs.nanolett.7b00177.
- Ge, J., W. Li, Q. Zhao, N. Li, M. Chen, P. Zhi, R. Li, N. Gao, B. Xiao, and M. Yang (2015). “Architecture of the mammalian mechanosensitive Piezo1 channel”. In: *Nature* 527.7576, pp. 64–69. DOI: 10.1038/nature15247.
- Genschik, P., I. Sumara, and E. Lechner (2013). “The emerging family of CULLIN3-RING ubiquitin ligases (CRL3s): cellular functions and disease implications.” eng. In: *The EMBO journal* 32.17, pp. 2307–2320. DOI: 10.1038/emboj.2013.173.
- Golani, I. and J. C. Fentress (1985). “Early ontogeny of face grooming in mice”. In: *Developmental Psychobiology* 18.6, pp. 529–544. DOI: 10.1002/dev.420180609.
- Haliloglu, G., K. Becker, C. Temucin, B. Talim, N. Küçüksahin, M. Pergande, S. Motameny, P. Nürnberg, U. Aydingoz, H. Topaloglu, and S. Cirak (2017). “Recessive PIEZO2 stop mutation causes distal arthrogryposis with distal muscle weakness, scoliosis and proprioception defects”. In: *Journal of Human Genetics* 62.4, pp. 497–501. DOI: 10.1038/jhg.2016.153.
- Han, H., M. Myllykoski, S. Ruskamo, C. Wang, and P. Kursula (2013). “Myelin-specific proteins: A structurally diverse group of membrane-interacting molecules”. eng. In: *BioFactors* 39.3, pp. 233–241. DOI: 10.1002/biof.1076.
- Hao, J. and P. Delmas (2011). “Recording of mechanosensitive currents using piezoelectrically driven mechanostimulator”. In: *Nature Protocols* 6.7, pp. 979–990. DOI: 10.1038/nprot.2011.343.
- Hao, J., F. Padilla, M. Dandonneau, C. Lavebratt, F. Lesage, J. Noël, and P. Delmas (2013). “Kv1.1 channels act as mechanical brake in the senses of touch and pain”. In: *Neuron* 77.5, pp. 899–914. DOI: 10.1016/j.neuron.2012.12.035.
- Hargreaves, K., R. Dubner, F. Brown, C. Flores, and J. Joris (1988). “A new and sensitive method for measuring thermal nociception in cutaneous hyperalgesia.” eng. In: *Pain* 32.1, pp. 77–88.
- Heft, M. W. and M. E. Robinson (2017). “Somatosensory function in old age”. In: *Journal of Oral Rehabilitation* 44.4, pp. 327–332. DOI: 10.1111/joor.12488.
- Heidenreich, M., S. G. Lechner, V. Vardanyan, C. Wetzel, C. W. Cremers, E. M. De Leenheer, G. Aránguez, M. Á. Moreno-Pelayo, T. J. Jentsch, and G. R. Lewin (2012). “KCNQ4 K⁺ channels tune mechanoreceptors for normal touch sensation in mouse and man”. In: *Nature Neuroscience* 15.1, pp. 138–145. DOI: 10.1038/nn.2985.
- Holle, A. W., J. L. Young, K. J. Van Vliet, R. D. Kamm, D. Discher, P. Janmey, J. P. Spatz, and T. Saif (2018). “Cell-Extracellular Matrix Mechanobiology: Forceful Tools and Emerging Needs for Basic and Translational Research”. In: *Nano Letters* 18.1, pp. 1–8. DOI: 10.1021/acs.nanolett.7b04982.
- Hong, G. S., B. Lee, J. Wee, H. Chun, H. Kim, J. Jung, J. Y. Cha, T. R. Riew, G. H. Kim, I. B. Kim, and U. Oh (2016). “Tentonin 3/TMEM150c Confers Distinct Mechanosensitive Currents in Dorsal-Root Ganglion Neurons with Proprioceptive Function”. In: *Neuron* 91.1, pp. 107–118. DOI: 10.1016/j.neuron.2016.05.029.
- Hu, J. and G. R. Lewin (2006). “Mechanosensitive currents in the neurites of cultured mouse sensory neurones”. In: *Journal of Physiology* 577.3, pp. 815–828. DOI: 10.1113/jphysiol.2006.117648.

REFERENCES

- Huang, X.-t., X. Li, P.-z. Qin, Y. Zhu, S.-n. Xu, and J.-p. Chen (2018). “Technical Advances in Single-Cell RNA Sequencing and Applications in Normal and Malignant Hematopoiesis”. In: *Frontiers in Oncology* 8.December, pp. 1–15. doi: 10.3389/fonc.2018.00582.
- Iftinca, M., R. Flynn, L. Basso, H. Melo, R. Aboushousha, L. Taylor, and C. Altier (2016). “The stress protein heat shock cognate 70 (Hsc70) inhibits the Transient Receptor Potential Vanilloid type 1 (TRPV1) channel”. In: *Molecular Pain* 12, pp. 1–15. doi: 10.1177/1744806916663945.
- Iwasaki, T., N. Goto, J. Goto, H. Ezure, and H. Moriyama (2006). “The Aging of Human Meissner’s Corpuscles as Evidenced by Parallel Sectioning”. In: *Okajimas Folia Anatomica Japonica* 79.6, pp. 185–189. doi: 10.2535/ofaj.79.185.
- Jackson, R. B. and C. C. Little (1933). “THE EXISTENCE OF NON-CHROMOSOMAL INFLUENCE IN THE INCIDENCE OF MAMMARY TUMORS IN MICE”. In: *Science* 78.2029, 465 LP –466. doi: 10.1126/science.78.2029.465.
- Jia, Z., R. Ikeda, J. Ling, V. Viatchenko-Karpinski, and J. G. Gu (2016). “Regulation of Piezo2 mechanotransduction by static plasma membrane tension in primary afferent neurons”. In: *Journal of Biological Chemistry* 291.17, pp. 9087–9104. doi: 10.1074/jbc.M115.692384.
- Katzman, R. and R. D. Terry (1983). *The Neurology of Aging*. Philadelphia : F.A. Davis Co., p. 249.
- Kinkelin, I., C. L. Stucky, and M. Koltzenburg (1999). “Postnatal loss of Merkel cells, but not of slowly adapting mechanoreceptors in mice lacking the neurotrophin receptor p75”. In: *European Journal of Neuroscience* 11.11, pp. 3963–3969. doi: 10.1046/j.1460-9568.1999.00822.x.
- Kleinman, H. K., L. Luckenbill-Edds, F. W. Cannon, and G. C. Sephel (1987). “Use of extracellular matrix components for cell culture.” eng. In: *Analytical biochemistry* 166.1, pp. 1–13.
- Koerber, H. R., R. E. Druzinsky, and L. M. Mendell (1988). “Properties of somata of spinal dorsal root ganglion cells differ according to peripheral receptor innervated.” In: *Journal of neurophysiology* 60.5, pp. 1584–1596. doi: 10.1152/jn.1988.60.5.1584.
- Lambolez, B., E. Audinat, P. Bochet, and J. Rossier (1995). “Patch-clamp recording and RT-PCR on single cells”. In: *Neuromethods: Patch-clamp applications and protocols* 26, pp. 193–231. doi: 10.1385/0-89603-311-2:193.
- Latham, N. and G. Mason (2004). “From house mouse to mouse house : the behavioural biology of free-living *Mus musculus* and its implications in the laboratory”. In: 86, pp. 261–289. doi: 10.1016/j.applanim.2004.02.006.
- Lay, K., T. Kume, and E. Fuchs (2016). “FOXC1 maintains the hair follicle stem cell niche and governs stem cell quiescence to preserve long-term tissue-regenerating potential”. In: doi: 10.1073/pnas.1601569113.
- Lechner, S. G., H. Frenzel, R. Wang, and G. R. Lewin (2009). “Developmental waves of mechanosensitivity acquisition in sensory neuron subtypes during embryonic development”. In: *EMBO Journal* 28.10, pp. 1479–1491. doi: 10.1038/emboj.2009.73.
- LeMessurier, A. M. and D. E. Feldman (2018). “Tactile enrichment drives emergence of functional columns and improves sensory coding in L2/3 of mouse S1”. In: *bioRxiv*, p. 447508. doi: 10.1101/447508.
- Lévêque, J. L., J. Dresler, E. Ribot-Ciscar, J. P. Roll, and C. Poelman (2000). “Changes in tactile spatial discrimination and cutaneous coding properties by skin hydration in the elderly”. In: *Journal of Investigative Dermatology* 115.3, pp. 454–458. doi: 10.1046/j.1523-1747.2000.00055.x.

- Li, C. L., K. C. Li, D. Wu, Y. Chen, H. Luo, J. R. Zhao, S. S. Wang, M. M. Sun, Y. J. Lu, Y. Q. Zhong, X. Y. Hu, R. Hou, B. B. Zhou, L. Bao, H. S. Xiao, and X. Zhang (2016). “Somatosensory neuron types identified by high-coverage single-cell RNA-sequencing and functional heterogeneity”. In: *Cell Research* 26.1, pp. 83–102. DOI: 10.1038/cr.2015.149.
- Li, C., S. Wang, Y. Chen, and X. Zhang (2018). “Somatosensory Neuron Typing with High-Coverage Single-Cell RNA Sequencing and Functional Analysis”. In: *Neuroscience Bulletin* 34.1, pp. 200–207. DOI: 10.1007/s12264-017-0147-9.
- Li, J. J. and M. D. Biggin (2015). “Statistics requantitates the central dogma”. In: *Science* 347.6226, pp. 1066–1067. DOI: 10.1126/science.aaa8332.
- Liao, Y., G. K. Smyth, and W. Shi (2014). “featureCounts: an efficient general purpose program for assigning sequence reads to genomic features.” eng. In: *Bioinformatics (Oxford, England)* 30.7, pp. 923–930. DOI: 10.1093/bioinformatics/btt656.
- Linford, N. J., T.-H. Kuo, T. P. Chan, and S. D. Pletcher (2011). “Sensory perception and aging in model systems: from the outside in”. eng. In: *Annual review of cell and developmental biology* 27, pp. 759–785. DOI: 10.1146/annurev-cellbio-092910-154240.
- Liu, Y., A. Beyer, and R. Aebersold (2016). “On the Dependency of Cellular Protein Levels on mRNA Abundance”. In: *Cell* 165.3, pp. 535–550. DOI: 10.1016/j.cell.2016.03.014.
- Livak, K. J. and T. D. Schmittgen (2001). “Analysis of relative gene expression data using real-time quantitative PCR and the 2- $\Delta\Delta$ CT method”. In: *Methods* 25.4, pp. 402–408. DOI: 10.1006/meth.2001.1262.
- Lo, S. Q., J. C. Sng, and G. J. Augustine (2017). “Defining a critical period for inhibitory circuits within the somatosensory cortex”. In: *Scientific Reports* 7.1, pp. 1–13. DOI: 10.1038/s41598-017-07400-8.
- Loos, M., B. Koopmans, E. Aarts, G. Maroteaux, S. van der Sluis, M. Verhage, A. B. Smit, A. B. Brussaard, J. G. Borst, Y. Elgersma, N. Galjart, G. T. van der Horst, C. N. Levelt, C. M. Pennartz, B. M. Spruijt, and C. I. de Zeeuw (2015). “Within-strain variation in behavior differs consistently between common inbred strains of mice”. In: *Mammalian Genome* 26.7-8, pp. 348–354. DOI: 10.1007/s00335-015-9578-7.
- Luu-The, V., N. Paquet, E. Calvo, and J. Cumps (2005). “<Van Luu-The et al 2005_Improved real-time RT-PCR method for high-throughput measurements.pdf>”. In: 38.2, pp. 287–293.
- Ma, Q. P. and C. J. Woolf (1996). “Progressive tactile hypersensitivity: an inflammation-induced incremental increase in the excitability of the spinal cord.” eng. In: *Pain* 67.1, pp. 97–106.
- Mahmud, A. A., N. A. Nahid, C. Nassif, M. S. Sayeed, M. U. Ahmed, M. Parveen, M. I. Khalil, M. M. Islam, Z. Nahar, F. Rypens, F. F. Hamdan, G. A. Rouleau, A. Hasnat, and J. L. Michaud (2017). “Loss of the proprioception and touch sensation channel PIEZO2 in siblings with a progressive form of contractures”. In: *Clinical Genetics* 91.3, pp. 470–475. DOI: 10.1111/cge.12850.
- Maksimovic, S., M. Nakatani, Y. Baba, A. M. Nelson, K. L. Marshall, S. A. Wellnitz, P. Firozi, S. H. Woo, S. Ranade, A. Patapoutian, and E. A. Lumpkin (2014). “Epidermal Merkel cells are mechanosensory cells that tune mammalian touch receptors”. In: *Nature* 509.7502, pp. 617–621. DOI: 10.1038/nature13250.
- Mao, X. W., M. J. Pecaut, L. S. Stodieck, V. L. Ferguson, T. A. Bateman, M. L. Bouxsein, and D. S. Gridley (2014). “Biological and metabolic response in STS-135 space-flown mouse skin.” eng. In: *Free radical research* 48.8, pp. 890–897. DOI: 10.3109/10715762.2014.920086.

REFERENCES

- Marmigère, F. and P. Ernfors (2007). “Specification and connectivity of neuronal subtypes in the sensory lineage.” eng. In: *Nature reviews. Neuroscience* 8.2, pp. 114–127. DOI: 10.1038/nrn2057.
- Martinac, B. and K. Poole (2018). “Mechanically activated ion channels”. In: *International Journal of Biochemistry and Cell Biology* 97.November 2017, pp. 104–107. DOI: 10.1016/j.biocel.2018.02.011.
- Massie, P. (2013). “Touching, thinking, being: The sense of touch in Aristotle’s De Anima and its implications”. In: *Minerva - An Internet Journal of Philosophy* 17.1.
- Matías-Pérez, D., L. A. García-Montaña, M. Cruz-Aguilar, I. A. García-Montalvo, J. Nava-Valdéz, T. Barragán-Arevalo, C. Villanueva-Mendoza, C. E. Villarroel, C. Guadarrama-Vallejo, R. V. de la Cruz, O. Chacón-Camacho, and J. C. Zenteno (2018). “Identification of novel pathogenic variants and novel gene-phenotype correlations in Mexican subjects with microphthalmia and/or anophthalmia by next-generation sequencing”. In: *Journal of Human Genetics* 63.11, pp. 1169–1180. DOI: 10.1038/s10038-018-0504-1.
- McCoy, E. S., B. Taylor-Blake, and M. J. Zylka (2012). “CGRP α -expressing sensory neurons respond to stimuli that evoke sensations of pain and itch”. eng. In: *PloS one* 7.5, e36355–e36355. DOI: 10.1371/journal.pone.0036355.
- McKemy, D. D., W. M. Neuhausser, and D. Julius (2002). “Identification of a cold receptor reveals a general role for TRP channels in thermosensation.” eng. In: *Nature* 416.6876, pp. 52–58. DOI: 10.1038/nature719.
- McMahon, S. B., M. P. Armanini, L. H. Ling, and H. S. Phillips (1994). “Expression and coexpression of Trk receptors in subpopulations of adult primary sensory neurons projecting to identified peripheral targets.” eng. In: *Neuron* 12.5, pp. 1161–1171.
- McMillin, M. J., A. E. Beck, J. X. Chong, K. M. Shively, K. J. Buckingham, H. I. Gildersleeve, M. I. Aracena, A. S. Aylsworth, P. Bitoun, J. C. Carey, C. L. Clericuzio, Y. J. Crow, C. J. Curry, K. Devriendt, D. B. Everman, A. Fryer, K. Gibson, M. L. Giovannucci Uzielli, J. M. Graham, J. G. Hall, J. T. Hecht, R. A. Heidenreich, J. A. Hurst, S. Irani, I. P. Krapels, J. G. Leroy, D. Mowat, G. T. Plant, S. P. Robertson, E. K. Schorry, R. H. Scott, L. H. Seaver, E. Sherr, M. Splitt, H. Stewart, C. Stumpel, S. G. Temel, D. D. Weaver, M. Whiteford, M. S. Williams, H. K. Tabor, J. D. Smith, J. Shendure, D. A. Nickerson, and M. J. Bamshad (2014). “Mutations in PIEZO2 cause Gordon syndrome, Marden-Walker Syndrome, and distal arthrogyrosis type 5”. In: *American Journal of Human Genetics* 94.5, pp. 734–744. DOI: 10.1016/j.ajhg.2014.03.015.
- Minett, M. S., K. Quick, and J. N. Wood (2011). “Behavioral Measures of Pain Thresholds”. In: *Current Protocols in Mouse Biology*. DOI: 10.1002/9780470942390.mo110116.
- Moehring, F., M. Waas, T. R. Keppel, D. Rathore, A. M. Cowie, C. L. Stucky, and R. L. Gundry (2018). “Quantitative Top-Down Mass Spectrometry Identifies Proteoforms Differentially Released during Mechanical Stimulation of Mouse Skin”. In: *Journal of Proteome Research* 17.8, pp. 2635–2648. DOI: 10.1021/acs.jproteome.8b00109.
- Moroni, M., M. R. Servin-Vences, R. Fleischer, O. Sánchez-Carranza, and G. R. Lewin (2018). “Voltage gating of mechanosensitive PIEZO channels”. In: *Nature Communications* 9.1, pp. 1–15. DOI: 10.1038/s41467-018-03502-7.
- Motulsky, H. J. and R. E. Brown (2006). “Detecting outliers when fitting data with nonlinear regression—a new method based on robust nonlinear regression and the false discovery rate”. In: DOI: 10.1186/1471-2105-7-123.

- Murthy, S. E., M. C. Loud, I. Daou, K. L. Marshall, F. Schwaller, J. Kühnemund, A. G. Francisco, W. T. Keenan, A. E. Dubin, G. R. Lewin, and A. Patapoutian (2018). “The mechanosensitive ion channel Piezo2 mediates sensitivity to mechanical pain in mice”. In: *Science Translational Medicine* 10.462. DOI: 10.1126/scitranslmed.aat9897.
- Narayanan, P., M. Hütte, G. Kudryasheva, F. J. Taberner, S. G. Lechner, F. Rehfeldt, D. Gomez-Varela, and M. Schmidt (2018). “Myotubularin related protein-2 and its phospholipid substrate PIP2 control Piezo2-mediated mechanotransduction in peripheral sensory neurons”. In: *eLife* 7.4, pp. 1–28. DOI: 10.7554/eLife.32346.
- Narayanan, P., J. Sondermann, T. Rouwette, S. Karaca, H. Urlaub, M. Mitkovski, D. Gomez-Varela, and M. Schmidt (2016). “Native Piezo2 interactomics identifies pericentrin as a novel regulator of Piezo2 in somatosensory neurons”. In: *Journal of Proteome Research* 15.8, pp. 2676–2687. DOI: 10.1021/acs.jproteome.6b00235.
- Nonomura, K., S. H. Woo, R. B. Chang, A. Gillich, Z. Qiu, A. G. Francisco, S. S. Ranade, S. D. Liberles, and A. Patapoutian (2017). “Piezo2 senses airway stretch and mediates lung inflation-induced apnoea”. In: *Nature* 541.7636, pp. 176–181. DOI: 10.1038/nature20793.
- Ogle, M. E., X. Gu, A. R. Espinera, and L. Wei (2012). “Inhibition of prolyl hydroxylases by dimethylxaloylglycine after stroke reduces ischemic brain injury and requires hypoxia inducible factor-1 α ”. In: *Neurobiology of Disease* 45.2, pp. 733–742. DOI: 10.1016/j.nbd.2011.10.020.
- Olson, W., P. Dong, M. Fleming, and W. Luo (2016). “The specification and wiring of mammalian cutaneous low-threshold mechanoreceptors”. In: *Wiley Interdisciplinary Reviews: Developmental Biology* 5.3, pp. 389–404. DOI: 10.1002/wdev.229.
- Papizan, J. B., G. A. Garry, S. Brezprozvannaya, J. R. McAnally, R. Bassel-Duby, N. Liu, and E. N. Olson (2017). “Deficiency in Kelch protein Khlh31 causes congenital myopathy in mice”. In: *Journal of Clinical Investigation*. Vol. 127. 10, pp. 3730–3740. DOI: 10.1172/JCI93445.
- Peier, A. M., A. Moqrich, A. C. Hergarden, A. J. Reeve, D. A. Andersson, G. M. Story, T. J. Earley, I. Dragoni, P. McIntyre, S. Bevan, and A. Patapoutian (2002). “A TRP channel that senses cold stimuli and menthol.” eng. In: *Cell* 108.5, pp. 705–715.
- Peters, R. M., M. D. McKeown, M. G. Carpenter, and J. T. Inglis (2016). “Losing touch: age-related changes in plantar skin sensitivity, lower limb cutaneous reflex strength, and postural stability in older adults”. In: *Journal of Neurophysiology* 116.4, pp. 1848–1858. DOI: 10.1152/jn.00339.2016.
- Pintard, L., A. Willems, and M. Peter (2004). “Cullin-based ubiquitin ligases: Cul3-BTB complexes join the family”. In: *EMBO Journal* 23.8, pp. 1681–1687. DOI: 10.1038/sj.emboj.7600186.
- Poole, K., R. Herget, L. Lapatsina, H. D. Ngo, and G. R. Lewin (2014). “Tuning Piezo ion channels to detect molecular-scale movements relevant for fine touch”. In: *Nature Communications* 5, pp. 1–14. DOI: 10.1038/ncomms4520.
- Prato, V., F. J. Taberner, J. R. Hockley, G. Callejo, A. Arcourt, B. Tazir, L. Hammer, P. Schad, P. A. Heppenstall, E. S. Smith, and S. G. Lechner (2017). “Functional and Molecular Characterization of Mechanoinsensitive “Silent” Nociceptors”. In: *Cell Reports* 21.11, pp. 3102–3115. DOI: 10.1016/j.celrep.2017.11.066.
- Ranade, S. S., R. Syeda, and A. Patapoutian (2015). “Mechanically Activated Ion Channels”. In: *Neuron* 87.6, pp. 1162–1179. DOI: 10.1016/j.neuron.2015.08.032.
- Ranade, S. S., S. H. Woo, A. E. Dubin, R. A. Moshourab, C. Wetzel, M. Petrus, J. Mathur, V. Bégay, B. Coste, J. Mainquist, A. J. Wilson, A. G. Francisco, K. Reddy, Z. Qiu, J. N. Wood, G. R. Lewin,

REFERENCES

- and A. Papatoutian (2014). “Piezo2 is the major transducer of mechanical forces for touch sensation in mice”. In: *Nature* 516.729, pp. 121–125. doi: 10.1038/nature13980.
- Rasmussen, R. (2011). “Quantification on the LightCycler”. In: *Rapid Cycle Real-Time PCR*. Ed. by S. Meuer, C. Wittwer, and K.-I. Nakagawara. Berlin, Heidelberg: Springer Berlin Heidelberg, pp. 21–34. doi: 10.1007/978-3-642-59524-0_3.
- Riquelme, I., S. M. Hatem, and P. Montoya (2016). “Abnormal Pressure Pain , Touch Sensitivity , Proprioception , and Manual Dexterity in Children with Autism Spectrum Disorders”. In: 2016. doi: 10.1155/2016/1723401.
- Roberson, D. P., S. Gudes, J. M. Sprague, H. A. Patoski, V. K. Robson, F. Blasl, B. Duan, S. B. Oh, B. P. Bean, Q. Ma, A. M. Binshtok, and C. J. Woolf (2013). “Activity-dependent silencing reveals functionally distinct itch-generating sensory neurons”. In: *Nature Neuroscience* 16.7, pp. 910–918. doi: 10.1038/nn.3404.
- Robinson, M. D., D. J. McCarthy, and G. K. Smyth (2010). “edgeR: a Bioconductor package for differential expression analysis of digital gene expression data”. eng. In: *Bioinformatics (Oxford, England)* 26.1, pp. 139–140. doi: 10.1093/bioinformatics/btp616.
- Rostovsky, C. M. and I. Milosevic (2018). “Gait Analysis of Age-dependent Motor Impairments in Mice with Neurodegeneration”. In: *Journal of Visualized Experiments* 136. doi: 10.3791/57752.
- Rouvette, T., J. Sondermann, L. Avenali, D. Gomez-Varela, and M. Schmidt (2016). “Standardized Profiling of The Membrane-Enriched Proteome of Mouse Dorsal Root Ganglia (DRG) Provides Novel Insights Into Chronic Pain”. In: *Molecular & Cellular Proteomics* 15.6, pp. 2152–2168. doi: 10.1074/mcp.M116.058966.
- Schneider, E. R., E. O. Anderson, V. V. Feketa, M. Mastrotto, Y. A. Nikolaev, E. O. Gracheva, and S. N. Bagriantsev (2019). “A Cross-Species Analysis Reveals a General Role for Piezo2 in Mechanosensory Specialization of Trigeminal Ganglia from Tactile Specialist Birds”. In: *Cell Reports* 26.8, 1979–1987.e3. doi: 10.1016/j.celrep.2019.01.100.
- Schneider, E. R., E. O. Anderson, M. Mastrotto, J. D. Matson, V. P. Schulz, P. G. Gallagher, R. H. LaMotte, E. O. Gracheva, and S. N. Bagriantsev (2017). “Molecular basis of tactile specialization in the duck bill”. In: *Proceedings of the National Academy of Sciences*, p. 201708793. doi: 10.1073/pnas.1708793114.
- Schrenk-Siemens, K., H. Wende, V. Prato, K. Song, C. Rostock, A. Loewer, J. Utikal, G. R. Lewin, S. G. Lechner, and J. Siemens (2015). “PIEZO2 is required for mechanotransduction in human stem cell-derived touch receptors”. In: *Nature Neuroscience* 18.1, pp. 10–16. doi: 10.1038/nn.3894.
- Skedung, L., C. E. Rawadi, M. Arvidsson, C. Farcet, G. S. Luengo, L. Breton, and M. W. Rutland (2018). “Mechanisms of tactile sensory deterioration amongst the elderly”. In: December 2017, pp. 1–10. doi: 10.1038/s41598-018-23688-6.
- Sondermann, J. R., A. M. Barry, O. Jahn, N. Michel, R. Abdelaziz, S. Kügler, D. Gomez-Varela, and M. Schmidt (2019). “Vti1b promotes TRPV1 sensitization during inflammatory pain”. In: *Pain* 160.2, pp. 508–527. doi: 10.1097/j.pain.0000000000001418.
- Song, Y., M. Zhang, X. Tao, Z. Xu, Y. Zheng, M. Zhu, L. Zhang, J. Qiao, and L. Gao (2018). “Difference of acute dissociation and 1-day culture on the electrophysiological properties of rat dorsal root ganglion neurons”. In: *Journal of Physiology and Biochemistry* 74.2, pp. 207–221. doi: 10.1007/s13105-017-0606-9.

- Stieber, J., G. Stockl, S. Herrmann, B. Hassfurth, and F. Hofmann (2005). “Functional expression of the human HCN3 channel.” eng. In: *The Journal of biological chemistry* 280.41, pp. 34635–34643. DOI: 10.1074/jbc.M502508200.
- Sucher, N. J. and D. L. Deitcher (1995). “PCR and patch-clamp analysis of single neurons”. In: *Neuron* 14.6, pp. 1095–1100. DOI: 10.1016/0896-6273(95)90257-0.
- Sucher, N. J., D. L. Deitcher, D. J. Baro, R. M. Harris Warrick, and E. Guenther (2000). “Genes and channels: Patch/voltage-clamp analysis and single-cell RT-PCR”. In: *Cell and Tissue Research* 302.3, pp. 295–307. DOI: 10.1007/s004410000289.
- Szczot, M., J. Liljencrantz, N. Ghitani, A. Barik, R. Lam, J. H. Thompson, D. Bharucha-Goebel, D. Saade, A. Necaie, S. Donkervoort, A. R. Foley, T. Gordon, L. Case, M. C. Bushnell, C. G. Bönnemann, and A. T. Chesler (2018). “PIEZO2 mediates injury-induced tactile pain in mice and humans”. In: *Science Translational Medicine* 10.462, pp. 1–10. DOI: 10.1126/scitranslmed.aat9892.
- Szczot, M., L. A. Pogorzala, H. J. Solinski, L. Young, P. Yee, C. E. Le Pichon, A. T. Chesler, and M. A. Hoon (2017). “Cell-Type-Specific Splicing of Piezo2 Regulates Mechanotransduction”. In: *Cell Reports* 21.10, pp. 2760–2771. DOI: 10.1016/j.celrep.2017.11.035.
- Taylor, S., B. McLean, T. Falkmer, L. Carey, S. Girdler, C. Elliott, and E. Blair (2016). “Does somatosensation change with age in children and adolescents? A systematic review”. In: *Child: Care, Health and Development* 42.6, pp. 809–824. DOI: 10.1111/cch.12375.
- The Harrison Lab (2007). *Life span as a biomarker* (<https://www.jax.org/research-and-faculty/research-labs/the-harrison-lab/gerontology/life-span-as-a-biomarker>).
- Thornbury, J. M. and C. M. Mistretta (1981). “Tactile sensitivity as a function of age”. In: *Journals of Gerontology* 36.1, pp. 34–39. DOI: 10.1093/geronj/36.1.34.
- Tukey, J. W. (1949). “Comparing Individual Means in the Analysis of Variance”. In: *Biometrics* 5.2, p. 99. DOI: 10.2307/3001913.
- Usoskin, D., A. Furlan, S. Islam, H. Abdo, P. Lönnerberg, D. Lou, J. Hjerling-Leffler, J. Haeggström, O. Kharchenko, P. V. Kharchenko, S. Linnarsson, and P. Ernfors (2015). “Unbiased classification of sensory neuron types by large-scale single-cell RNA sequencing”. In: *Nature Neuroscience* 18.1, pp. 145–153. DOI: 10.1038/nn.3881.
- Viatchenko-Karpinski, V. and J. G. Gu (2016). “Mechanical sensitivity and electrophysiological properties of acutely dissociated dorsal root ganglion neurons of rats”. In: *Neuroscience Letters* 634, pp. 70–75. DOI: 10.1016/j.neulet.2016.10.011.
- Wang, S., B. M. Davis, M. Zwick, S. G. Waxman, and K. M. Albers (2006). “Reduced thermal sensitivity and Nav1.8 and TRPV1 channel expression in sensory neurons of aged mice”. In: *Neurobiology of Aging* 27.6, pp. 895–903. DOI: 10.1016/j.neurobiolaging.2005.04.009.
- Wetzel, C., J. Hu, D. Riethmacher, A. Benckendorff, L. Harder, A. Eilers, R. Moshourab, A. Kozlenkov, D. Labuz, O. Caspani, B. Erdmann, H. Macheltska, P. A. Heppenstall, and G. R. Lewin (2007). “A stomatin-domain protein essential for touch sensation in the mouse”. In: *Nature* 445.7124, pp. 206–209. DOI: 10.1038/nature05394.
- Wetzel, C., S. Pifferi, C. Picci, C. Gök, D. Hoffmann, K. K. Bali, A. Lampe, L. Lapatsina, R. Fleischer, E. S. J. Smith, V. Bégay, M. Moroni, L. Estebanez, J. Kühnemund, J. Walcher, E. Specker, M. Neuenschwander, J. P. Von Kries, V. Haucke, R. Kuner, J. F. Poulet, J. Schmoranzler, K. Poole, and G. R. Lewin (2017). “Small-molecule inhibition of STOML3 oligomerization reverses pathological mechanical hypersensitivity”. In: *Nature Neuroscience* 20.2, pp. 209–218. DOI: 10.1038/nn.4454.

REFERENCES

- Wickremaratchi, M. M. and J. G. Llewelyn (2006). “Effects of ageing on touch”. In: *Postgraduate Medical Journal* 82.967, pp. 301–304. DOI: 10.1136/pgmj.2005.039651.
- Wilhelm, M., H. Hahne, M. Savitski, H. Marx, S. Lemeer, M. Bantscheff, and B. Kuster (2017). “Wilhelm et al. reply”. In: *Nature* 547, E23.
- Wilhelm, M., J. Schlegl, H. Hahne, A. M. Gholami, M. Lieberenz, M. M. Savitski, E. Ziegler, L. Butzmann, S. Gessulat, H. Marx, T. Mathieson, S. Lemeer, K. Schnatbaum, U. Reimer, H. Wenschuh, M. Mollenhauer, J. Slotta-Huspenina, J.-H. Boese, M. Bantscheff, A. Gerstmair, F. Faerber, and B. Kuster (2014). “Mass-spectrometry-based draft of the human proteome.” In: *Nature* 509.7502, pp. 582–7. DOI: 10.1038/nature13319.
- Williams, S. R. and S. J. Mitchell (2008). “Direct measurement of somatic voltage clamp errors in central neurons.” eng. In: *Nature neuroscience* 11.7, pp. 790–798. DOI: 10.1038/nn.2137.
- Woo, S. H., V. Lukacs, J. C. De Nooij, D. Zaytseva, C. R. Criddle, A. Francisco, T. M. Jessell, K. A. Wilkinson, and A. Patapoutian (2015). “Piezo2 is the principal mechanotransduction channel for proprioception”. In: *Nature Neuroscience* 18.12, pp. 1756–1762. DOI: 10.1038/nn.4162.
- Woo, S. H., S. Ranade, A. D. Weyer, A. E. Dubin, Y. Baba, Z. Qiu, M. Petrus, T. Miyamoto, K. Reddy, E. A. Lumpkin, C. L. Stucky, and A. Patapoutian (2014). “Piezo2 is required for Merkel-cell mechanotransduction”. In: *Nature* 509.7502, pp. 622–626. DOI: 10.1038/nature13251.
- Wu, J., A. H. Lewis, and J. Grandl (2017). “Touch, Tension, and Transduction – The Function and Regulation of Piezo Ion Channels”. In: *Trends in Biochemical Sciences* 42.1, pp. 57–71. DOI: 10.1016/j.tibs.2016.09.004.
- Yamaguchi, S. and K. ichi Otsuguro (2017). “A mechanically activated ion channel is functionally expressed in the MrgprB4 positive sensory neurons, which detect stroking of hairy skin in mice”. In: *Neuroscience Letters* 653, pp. 139–145. DOI: 10.1016/j.neulet.2017.05.036.
- Yamaguchi, T., K. Takano, Y. Inaba, M. Morikawa, M. Motobayashi, R. Kawamura, K. Wakui, E. Nishi, S. Hirabayashi, Y. Fukushima, H. Kato, J. Takahashi, and T. Kosho (2019). “PIEZO2 deficiency is a recognizable arthrogryposis syndrome: A new case and literature review”. In: *American Journal of Medical Genetics Part A* March, ajmg.a.61142. DOI: 10.1002/ajmg.a.61142.
- Yang, X., E. E. Schadt, S. Wang, H. Wang, A. P. Arnold, L. Ingram-Drake, T. A. Drake, and A. J. Lusis (2006). “Tissue-specific expression and regulation of sexually dimorphic genes in mice”. In: *Genome Research* 16.8, pp. 995–1004. DOI: 10.1101/gr.5217506.
- Yonezawa, T., A. Ohtsuka, T. Yoshitaka, S. Hirano, H. Nomoto, K. Yamamoto, and Y. Ninomiya (2003). “Limitrin, a novel immunoglobulin superfamily protein localized to glia limitans formed by astrocyte endfeet.” eng. In: *Glia* 44.3, pp. 190–204. DOI: 10.1002/glia.10279.
- Zapata-Aldana, E., S. B. Al-Mobarak, N. Karp, and C. Campbell (2019). “Distal arthrogryposis type 5 and *PIEZO2* novel variant in a Canadian family”. In: *American Journal of Medical Genetics Part A* February, ajmg.a.61143. DOI: 10.1002/ajmg.a.61143.
- Zhang, M., Y. Wang, J. Geng, S. Zhou, and B. Xiao (2019). “Mechanically Activated Piezo Channels Mediate Touch and Suppress Acute Mechanical Pain Response in Mice”. In: *Cell Reports* 26.6, 1419–1431.e4. DOI: 10.1016/j.celrep.2019.01.056.
- Zhao, Q., K. Wu, J. Geng, S. Chi, Y. Wang, P. Zhi, M. Zhang, and B. Xiao (2016). “Ion Permeation and Mechanotransduction Mechanisms of Mechanosensitive Piezo Channels”. In: *Neuron* 89.6, pp. 1248–1263. DOI: 10.1016/j.neuron.2016.01.046.



Appendix A

A.1 Declaration

Herewith I declare that I prepared the dissertation “Touch comes of Age - Maturational Plasticity in Somatosensory Mechanosensation” on my own and with no other sources and aids than quoted.

Göttingen, 30th of April 2019

Niklas Michel

A.2 Curriculum Vitae

See next page.